REPORT DOCUMENTATION PAGE

AFRL-SR-BL-TR-02-

0033

1. AGENCY USE ONLY (Leave blank)	2. REPORT DATE	3. REPORT TYPE AND DATES COVERED
	1 September 2001	Final Technical Report 5 Nov 97 – 4 Feb 01

4. TITLE AND SUBTITLE

Refractive Turbulence – Measurements and Analysis

5. FUNDING NUMBERS

G: F49620-98-1-0114

6. AUTHOR(S)

Jörg M. Hacker

7. PERFORMING ORGANIZATION NAME(S) AND ADDRESS(ES)

ARA - Airborne Research Australia
PO Box 2100
Flinders University
Adelaide, 5001
Australia

8. PERFORMING ORGANIZATION REPORT NUMBER

ARA-TR-01/2001

9. SPONSORING / MONITORING AGENCY NAME(S) AND ADDRESS(ES)

AOARD
7-23-17 Roppongi
Tokyo 106
Japan

10. SPONSORING / MONITORING AGENCY REPORT NUMBER

11. SUPPLEMENTARY NOTES

12a. DISTRIBUTION / AVAILABILITY STATEMENT

12b. DISTRIBUTION CODE

13. ABSTRACT ***(Maximum 200 Words)***

Airborne military microwave radar surveillance systems (AWACS & JSTAR) and long-range communication systems have sensitivities to atmospheric refraction that can adversely affect their expected performance. Couple that with the fact that airborne platforms operate in all seasons; are continually in motion during operations; have extended operational ranges; and operate in varying geographical locations and the problem of measurement and generalization (modeling) both the mean and turbulent structure of atmospheric refraction is a formidable task. In the context of this project, a series of globally distributed airborne measurement campaigns of turbulent structure in the upper troposphere and lower stratosphere were conducted using a unique high altitude research aircraft, the Grob G520T Egrett of ARA - Airborne Research Australia. Three independent turbulence probes that measure temperature and the three components of atmospheric velocity were mounted on the Egrett. The specific aim of these measurements was to generate datasets which help to set bounds on the magnitude of refractive turbulence, particularly the index-of-refraction structure parameter, which is important in model studies of laser scintillation that support ABL design, and will allow investigation of the spatial and temporal variation of that parameter with the large-scale variation of meteorological structure. Measurement campaigns were carried out in the jetstream over Southern Australia, Japan and the UK.

14. SUBJECT TERMS			15. NUMBER OF PAGES
Atmospheric refraction, refractive turbulence, airborne measurements			16. PRICE CODE
17. SECURITY CLASSIFICATION OF REPORT	**18. SECURITY CLASSIFICATION OF THIS PAGE**	**19. SECURITY CLASSIFICATION OF ABSTRACT**	**20. LIMITATION OF ABSTRACT**

20020206 102

REFRACTIVE TURBULENCE MEASUREMENTS AND ANALYSIS

FINAL TECHNICAL REPORT

J.M. Hacker and C. Kargl

26 December 2001

Contract No. F49620-98-1-0114

Airborne Research Australia / Flinders University
PO Box 335
Salisbury South, 5106
Australia

ARA Technical Report No. 13-2001

Airborne Research Australia

The Flinders University of South Australia

Flinders Institute for Atmospheric and Marine Sciences

12 Feb 99	Successful mission 5300m, 6470m, 7690m, 8930m, 11850m, 9230m
13 Feb 99	Successful mission 7898m, 9315m, 10595m, 11580m, 12540m
20 Feb 99	Successful mission
21 Feb 99	Successful mission
22 Feb 99	Successful mission
23 Feb 99	Successful mission

February off the south coast of Japan was chosen to provide measurement opportunity in the strongest winter jet stream winds that occur in the northern hemisphere. During the 28 days of February that the ARA EGRETT aircraft was at Yokota Air Base to the west of Tokyo, eight full measurement missions were flown and one partial. The altitude range over which these measurements were made was 12,537 km to 5,294 km. Flight operations were from Yokota AB because that was the base that United States Forces Japan (USFJ) obtained permission from the Japanese Foreign Ministry for EGRETT operations. It was also the only USAF base in Korea-Japan region which would guarantee EGRETT hanger space during the month of February. This was essential to keep the pressure probes from getting wet (rain, snow, condensation etc) and freezing up at high altitudes.

Yokota AB was a good operating location related to the airspace congestion in Japan. To make measurements at multiple levels on each mission, EGRETT needed to be in restricted airspace. Yokota AB is the location of the 5th Air Force to which there was a Japanese Self Defense Force (JSDF) liaison office. Through the collaboration of 5AF/DOO and the JSDF liaison office, EGRETT obtained permission to operate in three restricted air space regions, two managed by JSDF and one managed by the US Navy. One JASDF area (G-1) was at 38N and 138E; the other area (K-1) was at 34N and 137.5E (approximately 440 km separation). The US Navy area was at 34.3N and 141E.

Allowing 28 days to obtain about fifty hours of measurements was just sufficient. The weather was very cooperative. Only three days were lost to flying because of snow or rain. Seven flying days were lost to flu as all six members of the mission crew came down with it at the same time.

The turbulence instrumentation on the aircraft was identical to the one used during the Australian study in mid-1998, but had been improved again in terms of response time and reliability. Only very few failures occurred, mainly caused by insufficient GPS satellite coverage.

Flight and altitude tracks of these flights are shown in Appendix B.

2.3 Southern Australia (14 Jul 1999 – 15 Aug 1999, Adelaide)

Eight research missions were flown with a total of 36 hours.

Date	**Comments**
16 Jul 99	Instrumentation test flight
28 Jul 99	Instrumentation test flight
29 Jul 99	Instrumentation test flight
3 Aug 99	Instrumentation test flight
5 Aug 99	Calibration flight
6 Aug 99	Successful mission FL290, FL300, FL310, FL320, FL270, FL330, FL390, FL365
11 Aug 99	Successful mission

	FL310, FL450, FL440, FL360
12 Aug 99	Successful mission FL320, FL305

Flight and altitude tracks of these flights are shown in Appendix B.

2.4 United Kingdom (1 May 2000 – 7 June 2000, Boscombe Downs)

The campaign in the UK was funded by a research grant from the UK National Environmental Research Council (NERC) to the University of Wales (UWA, Principal Investigators: Drs. Jim Whiteway and Geraint Vaughan/University of Wales). Data from this campaign was available to the current AFOSR/AOARD project. The campaign was conducted under the acronym AberEgrett, short for Aberystwyth – Egrett – Experiment. The main aim of AberEgrett was to investigate atmospheric processes around the Tropopause (around 9-12km altitude at that time of the year) which influence the transport of trace gases harmful to the Ozone Layer from low level up into the Ozone Layer. Such processes include gravity waves, as well as turbulence which may be caused by breaking waves in the lee of the Welsh mountains or vertical wind shear, especially around the high wind layers (jet streams) which occur frequently at that altitude.

In addition to the standard turbulence instrumentation (BAT-Probes), the Egrett carried sensors for humidity and trace gases. Amongst these was a GC (gas-chromatograph) developed at Imperial College at Cambridge University, a TDL (tunable diode laser) developed by UK/NPL (National Physics Laboratory), a fast Ozone analyser developed at the German Aerospace Agency (DLR), a frost point mirror also from DLR, and an ultra-fast temperature (UFT) sensor developed at the University of Warsaw in Poland.

Apart from the aircraft measurements, there were also measurements using radars, lidars and balloons.

A total of 90 hours were flown during 18 flight missions.

Date	**Comments**
4 May 00	Instrumentation test flight to 13km altitude
5 May 00	Chemistry flight (aborted)
10 May 00	Gravity wave flight
11 May 00	Gravity wave flight
12 May 00	Gravity wave flight
13 May 00	Chemistry flight
15 May 00	Chemistry flight
16 May 00	Chemistry flight
17 May 00	Gravity wave flight
18 May 00	Chemistry flight
19 May 00	Gravity wave flight (aborted)
22 May 00	Gravity wave flight (aborted)
24 May 00	Gravity wave flight
25 May 00	Gravity wave flight
31 May 00	Gravity wave flight
2 Jun 00	Chemistry flight

5 Jun 00	Calibration and chemistry flight
6 Jun 00	Gravity wave flight

The flight patterns were designed with regard to the scientific objectives and the meteorological conditions. The most basic mode was to fly the Egrett at successive levels from below the tropopause and up to 15 km. These flights passed over Aberystwyth in a convenient pattern (eg. race-track or figure-eight). A number of flight paths sampled the wave field above the ocean, making them very useful for identifying wave sources other than mountains. When possible, flight paths were designed to observe the distribution of gravity wave activity and tracer filamentation with respect to the jet stream. Another basic mode was to focus more directly on the tropopause: flying slightly above and below, in order to concentrate on stratosphere-troposphere exchange by gravity wave breaking and turbulent mixing. Measurements of ozone and water vapour indicated how the wave breaking and turbulence is affecting vertical transport. In this regard, upwind measurements by the Egrett were be indispensable in the interpretation of vertical profiles measured above Aberystwyth; and also the converse.

Apart from the aircraft measurements, the following observations were taken:

Radar: The NERC MST radar located just East of Aberystwyth provided measurements of the three dimensional motion field and turbulence up to an altitude of 20 km. The basic technique is to detect the backscatter of VHF (46.6 MHz) radar signals from small-scale temperature and humidity fluctuations. Wind velocity is derived from the Doppler shift and the intensity of turbulence is determined from the broadening of the radar backscatter spectra. The MST radar is also of utility for studies of filamentation and layering: the radar backscatter power profiles can monitor the progression of long lived static stability anomalies in the lower stratosphere.

Balloons: Temperature and wind radiosondes were launched four times each day from the weather station at Aberporth (40 km from Aberystwyth) providing regular profiles of temperature and horizontal wind. Radiosondes launched at Aberystwyth provided temperature profiles (wind is measured by the radar). and profiles of ozone

Lidar measurements: The UWA differential absorption lidar (DIAL) was used for continuous measurements of ozone vertical profiles in the tropopause region with temporal and vertical resolutions of 30 min. and 500 m. This lidar is based on a Nd:YAG laser (fourth harmonic output at 266 nm) with Raman shifting in D2 and H2 to generate the transmitted wavelengths of 289 nm, 299 nm, and 316 nm. The resolution of these measurements is sufficient to observe the perturbations induced by gravity waves and also the consequences of irreversible mixing during gravity wave breaking. This lidar also indicated the presence of cirrus clouds.

Flight and altitude tracks of these flights are shown in Appendix B.

3 INSTRUMENTATION

3.1 BAT-Probe:

Measuring turbulence from aircraft is a technologically demanding task. It involves, in general, the measurements of air temperature, pressures and the 3D-wind vector with high accuracy and at sampling rates of tens of Hertz. Fast sensors for air temperature and pressures are available, are light-weight and do not require much space and electrical power. Until recently, the main problem was to measure the 3D-wind vector accurately.

Wind measurements from an aircraft require observation of the wind velocity relative to the sensors and the velocity of the sensors relative to the Earth. The 3D-wind vector is then found as the small resultant vector sum of these two large vector velocities.

None of the two large vector velocities can be measured directly, but require the measurement of a number of other parameters, amongst them, the angles of attack and sideslip of the aircraft, the aircraft's heading and its pitch and roll angles, 3D-accelerations of the aircraft, its angular rates and more. All measurements have to be combined in a very careful manner, without phase shifts or other inconsistencies between them, to derive the two large vector quantities. For most applications, it is also essential to know the position of the aircraft accurately at all times.

Traditionally, combinations of a number of different sensor systems were used to measure turbulence, amongst them Inertial Navigation Systems (INS), Doppler systems, smaller gyro systems, GPS attitude systems, differential pressure port systems at the nose section of research aircraft or moveable or rigid vanes mounted to nose booms. Most of these systems involved one or several very complex, heavy, power-hungry and expensive components and were usually only 'one-off' dedicated installations.

The BAT-Probe (it got its name from its shape - it looks like a baseball bat- but it also could mean "Best" Aircraft Turbulence Probe) was developed as a means to overcome most of the above mentioned complexity of installation. It is an attempt to make the complex measurements basically independent of the platform by combining the latest sensor technology with powerful electronics and computing hard- and software into a small package.

The BAT-Probe combines (low-cost) sensors for pressure, air speed, angles of attack and sideslip, 3D-acceleration and air temperature with differential GPS systems for high precision position, ground speed and attitude (aircraft pitch and roll angles and heading) measurements packaged together in a small stand-alone package. The probe contains its own 16-bit A/D-unit which converts the measurements to digital values directly at the sensor location and transmits the data in a serial data stream to a PC-based real-time processing computer.

Combining the sensors at one location in close proximity of the A/D-unit minimises possible attenuation of the small signal voltages. The small size of the probe with its very short pressure lines between the pressure ports and the pressure transducers also virtually eliminates problems with time lags or resonance effects in pressure lines.

The sensor package itself was mainly developed under NOAA/ATDD responsibility, while ARA and FIAMS (the predecessor of ARA) developed the A/D-unit and associated digital electronics. Both organisations have joint responsibility for the low- and high-level software development.

The probe weighs about 4kg and requires about 50 W of 10 to 30 VDC power. Like a sonic anemometer, data is received serially at 50 Hz.

The housing consists of a 15-cm diameter hemisphere supported by a truncated circular cone. Its carbon-fiber construction is light but very strong. Further, carbon-fibers attenuate any potential electromagnetic interference.

Mechanical and electrical installation on any aircraft is simplified by placing electronics and sensors within the housing. Relative winds are computed from the pressure distribution observed at nine pressure taps on the sphere. Two unique features of the BAT probe are the method of measuring static pressure and atmospheric temperature.

Static pressure is difficult to measure on an aircraft because the sensed pressure is easily contaminated by flow distortion about the static ports and airframe. The BAT probe mitigates static error by its unique 9-hole design. With the BAT probe, static pressure is obtained from a pneumatic average of the four pressure taps placed 41.8° aft of the Design Stagnation Point (DSP) and 45° off vertical. At zero angle of attack (when the instantaneous stagnation point is coincident with the DSP), the BAT probe

correctly senses static pressure. However, like a conventional Pitot probe, static pressure is increasingly underestimated with increasing angles of attack. With this approach, the static error is less with the BAT design and an analytical model exists to remove the error.

Solid state precision compensated, low pressure sensors form SenSym (for example model SCXL004) or Data Instruments (Model series XCX) are used. Such pressure sensors have a frequency response approaching 1kHz with an accuracy of around 0.2% of their full scale reading. Furthermore, the sensors are heated to reduce temperature related drift.

The actual sensor choice is optimized for the design flight speed. As a result, sensors with unnecessarily large ranges are not used and accuracy within the desired sensing range is high. For example, a ±12hPa sensor is usually used on angle of attack and sideslip pressure ports. This yields an accuracy of ±0.05hPa. Such accuracy is not possible with more conventional aircraft sensors.

At aircraft flight speeds, the observed temperature is contaminated by compressibility effects. Correction of the sensed temperature is functionally dependent on dynamic and static pressure. The BAT probe places a micro-bead sensing element within the DSP where both dynamic and static pressure are known accurately and at high frequency. The DSP port is designed to ventilate the micro bead at 10m/s with small thermal housing influence. The resulting housing sensor combination has a 0.07s time response that is much faster than more conventional housings/sensor combinations.

For fast temperature measurement, a Victory Engineering Corp's 0.005" micro-bead thermistor is used. Within the BAT housing, they have a time response of 0.07s that is ten times faster than a fast Rosemount sensor housing combination. On the other hand, the BAT probe temperature sensor is more fragile. Although the housing design is great for fast response and observing the micro-beads pressure environment for use in temperature recovery computations, it offers the micro-bead little protection from foreign object damage (bugs, rain drops etc.). Regardless, this has not been a serious problem as micro-beads are infrequently damaged. To further mitigate this concern, the BAT probe electronics allow installation of twin micro-beads.

The BAT probe relies strongly on DGPS technology and does not require any gyro-based systems. In the past few years, Differential GPS (DGPS) techniques have developed into a powerful measurement utility. Currently DGPS measurement techniques allow dynamic observation of position, velocity and attitude at 10Hz and with accuracy of ±0.5m, ±2cm/s and ±0.05° respectively. If necessary, accelerometers can be used to extend these observations to higher frequencies.

Position is required to document aircraft location and is not needed for wind computation. Regardless, simple DGPS allows documentation of position to ±3m. Where necessary, extension to high accuracy sub-meter techniques is not difficult.

Using Doppler DGPS techniques, observation of probe velocity to 20Hz and at an accuracy of ±2cm/s is simple. A main advantage of DGPS approaches is that one obtains the velocity of the probe in Earth coordinates. Again, accelerometers within the BAT probe can be used to extend velocity frequency response to 50Hz.

Attitude is important since winds relative to the BAT probe must be rotated to Earth coordinates. Attitude, at 10Hz and with an accuracy of ±0.05°, is obtained from a Trimble TANS VECTOR GPS attitude receiver. Although 10Hz may be fast enough for large aircraft, it is not for smaller aircraft with less inertia. For smaller craft, GPS attitude output is low-passed then mixed with high-passed twice integrated differential acceleration observations. The result is attitude, at 50Hz and with an accuracy of ±0.05°. Four small GPS patch antennas must be installed for use of a TANS VECTOR system.

The A/D system for the BAT-Probe was developed by FIAMS/ARA to provide high speed, high resolution, multi-channel data logging. The system consists of two boards with an 8 pole low pass (anti-aliasing) filter for each of eight channels combined with an 8 channel multiplexer and an intelligent 16 bit A/D board. The three boards together comprise a signal conditioned, 16 channel, 16 bit A/D system with serial output. A custom ISA serial board provides an intelligent interface to a PC.

The system is unique in its combination of high speed, high resolution, high channel count, and on board intelligence. Software filters and other operations may be implemented on the A/D board, relieving the PC processor from such simple, but time consuming tasks. Additionally, multiple systems may reside on one PC, allowing for very high channel count systems.

The hardware and firmware are configured to provide 50Hz data output from the 16 channels. Each of the 16 channel is first conditioned by the 8 pole 30Hz low pass (anti-aliasing) filter. Then it is

interrogated or over sampled 32 times by the 16 bit A/D. The resulting data is averaged and then serially transmitted and timed tagged to ±1ms based on the 1sec pulse available from the GPS receiver.

3.2 Global Positioning System

Two GPS receivers are installed in the aircraft's mission bay, a 12-channel NovAtel system for position and velocity measurements using differential technology and a Trimble TANS Vector system for aircraft attitude (pitch, roll and heading).

3.3 Data acquisition and real-time monitoring system

The data system installed in the Egrett consisted of

- a 19" rack EMI-proof Pentium PC with dedicated EISA interface cards for communication with the REM-Boxes (remote analogue/digital converter units), MUX-box (digital multiplexer unit for REM-boxes), the BAT-Probes and the two GPSs
- a 166MHz Pentium CPU, 64Mb of memory, a 2Gb hard disk, an Ethernet networking card
- a TFT touch screen in the rear cockpit
- a small keyboard with a built-in trackball
- a built-in IOMEGA ZIP-drive for data exchange

The PC runs under the Windows '95 operating system. The FIAMS/ARA real-time data acquisition program DAMS and the testing program REMTEST are installed and used to collect the data and to test the installation. The system connects directly to the pre-installed wiring in the aircraft.

4 DATA PROCESSING

Most of the data processing was carried out using the ARA/FIAMS software package RAMF/ARAMF.

The original version of *RAMF* (*Routinen zur Auswertung Meteorologischer Forschungsflüge, Routines for the Processing of Meteorological Research Flights*) was developed by J.M. Hacker at the Meteorological Institute of the University of Bonn/Germany, to process data from research flights with three motor-gliders owned by the *DLR*'s (German AeroSpace Agency) Institute for Atmospheric Physics. Today it is used at a number of sites to process data from meteorological research aircraft as well as a multitude of other more general time series applications. The core site for *RAMF* is ARA. ARAMF is an enhanced version of RAMF, meaning "Advanced RAMF". More details about ARAMF can be found at website http://www.AirborneResearch.com.au.

5 SOME DETAILED RESULTS

The strongest turbulence of all measurement campaigns was found during the flight on 6 August 1999. The results shown relate mainly to this case. The data obtained on the flights on 25 and 26 August 1998 are also discussed in more detail. For all other flights, a summary is presented only.

5.1 Flight 25 August 1998

5.1.1 Synoptic situation

On the days before 25 August 1998, a jet stream with its maximum located immediately above Perth/Western Australia was observed with a maximum wind speed of approximately 80m/s. The jet stream core moved east along the south coast of Australia and passed to the north of Adelaide. A low pressure system formed south east of Australia but did not fully develop. A ridge of high pressure was situated over the Great Australian Bight.

The 500hPa analysis for 25 August (*Figure 1*) shows a low pressure trough over South Australia and a strong low pressure cell over Tasmania.

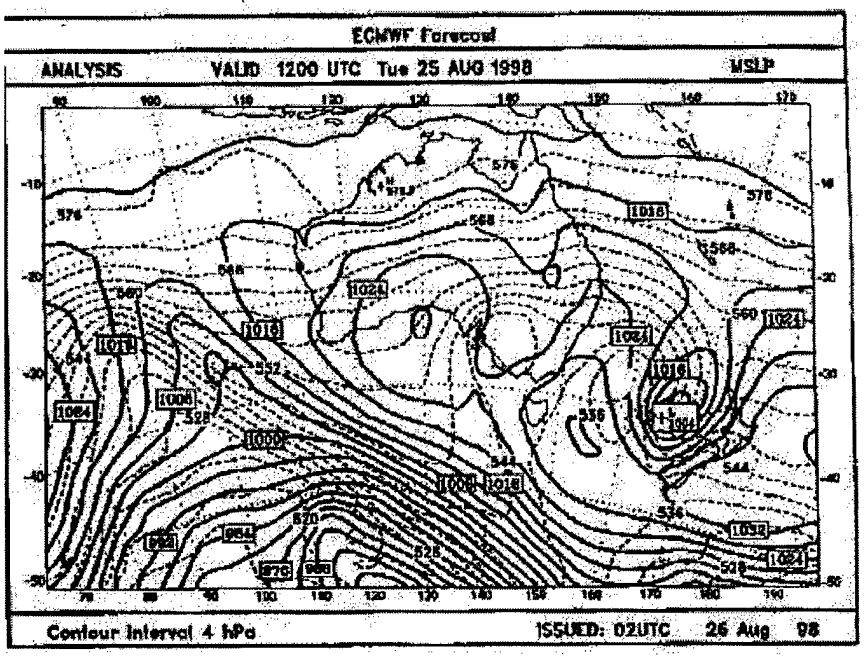

Figure 1: *ECMWF analysis of the surface and 500hPa isobars (Bureau of Meteorology, website).*

The amplitude of the planetary wave in the polar front was forecast to intensify and a new low pressure system formed on 26 August. The aviation weather forecast published on 25 August at 07:31 UTC indicated a weak front approaching Adelaide at 04:00 UTC.

Broken altocumulus and altostratus were expected between FL100 (~3km) and FL200 (~6km) with broken stratus between 1,500ft (~0.5km) and 2,500ft (0.8km) with rain east of the front and with showers west of the front. To the west of the front scattered cumulus was expected between 2,500ft (0.8km) and 10,000ft (~3km).

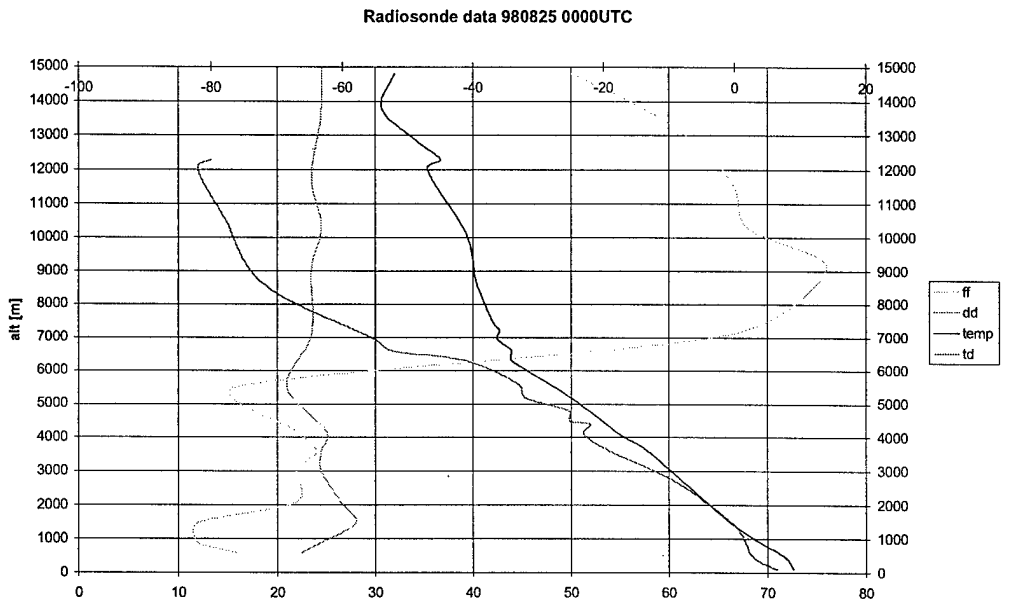

Figure 2: *Radiosonde sounding at Adelaide Airport on 25 August 1998 at 00:00UTC. Shown are: wind speed in m/s (yellow); wind direction in °true (scaled by dividing by ten, cyan); air temperature in °C (blue); and dewpoint in °C (magenta).*

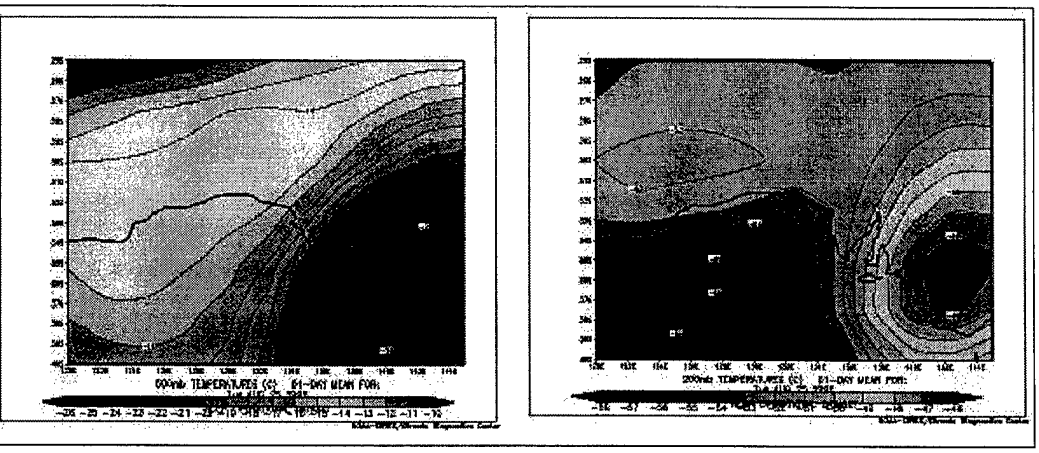

Figure 3: *Longitudinal cross-section of the temperature field at 500hPa (left) and 200hPa (right). Data shown is 1-day mean for 25 August 1998. (from NOAA website http://www.noaa.gov)*

At the time of the flight, the edge of the jet stream was overhead Adelaide. As is shown in the Adelaide Airport sounding in *Figure 2*, wind speed increased from just 15m/s at 5,500m to 75m/s at 9,000m with a moderate decrease above. The wind profile was linked to the large temperature gradient of

approximately 2K/100km between cold air to the south, east of Adelaide, and a warm continental air mass north west of Adelaide. *Figure 3* shows a longitudinal cross-section of the temperature field. Note the reversal of the temperature gradient overhead Adelaide.

5.1.2 Measurements

The flight on 25 August 1998 commenced at 18:11LT and ended at 20:51LT. Turbulence was found at around 7,000m, 10,000m and 11,800m altitude. The mean wind direction was 215°true. Seven horizontal legs were flown between FL360 (~11km) and FL460 (~14km), see *Figure 4*.

After climbing up to FL360 (~11km), the Egrett headed into the wind and flew legs at FL360, FL380, FL400, FL420, FL460, FL400, FL360, ie. 11.0km, 11.6km, 12.2km, 12.8km, 14.0km, 12.2km, 11km altitude).

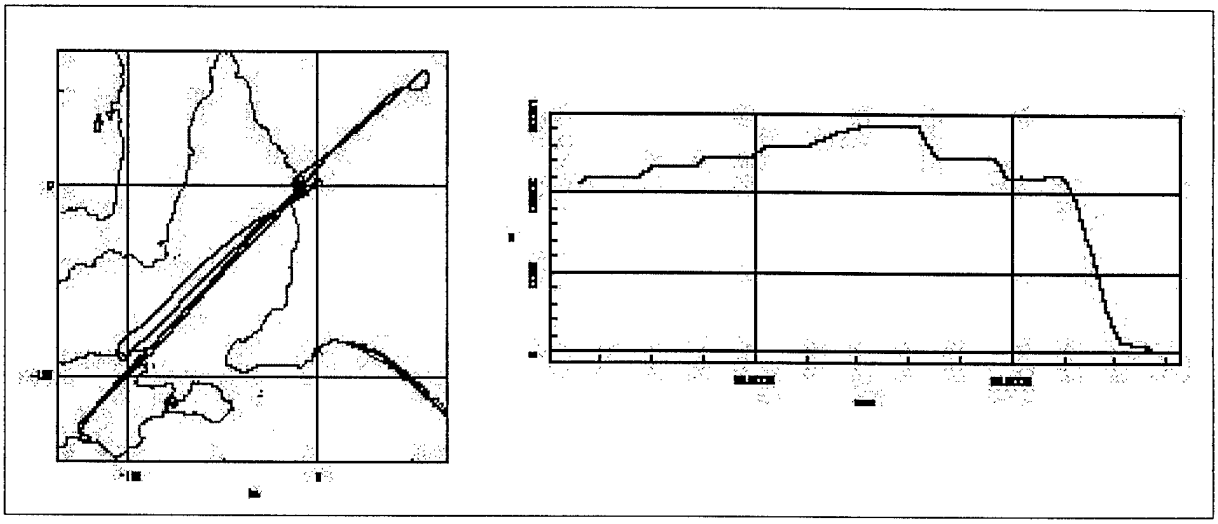

Figure 4: *Horizontal and vertical flight path for flight on 25 August 1998*

The flight legs relative to the temperature and wind speed field are shown in ***Figure 5*** which was constructed from routine soundings at Woomera, Ceduna, Adelaide and Mt. Gambier (note the reversed abscissa with East left and West right). The jet core was located at 12km altitude just below the tropopause to the north west of Adelaide with wind speeds of approximately 50m/s. The largest temperature gradient can be found just south of Adelaide.

Vertical profiles of temperature, dewpoint, wind speed, wind direction and potential temperature as measured during the descent of the Egrett are shown in *Figure 6*. Turbulence was computed as the RMS of the 3D-accelerations. The jet stream was approximately 2,500m thick with a maximum shear of 17kt per 1,000ft (2.8m/s per 100m). A significant change of wind direction together with strong wind shear lead to a thin layer of turbulent air at 7km altitude. The temperature in this layer was constant with an inversion at the top of the turbulent layer of the order of +1K. More turbulence was found at 11km and 14km altitude.

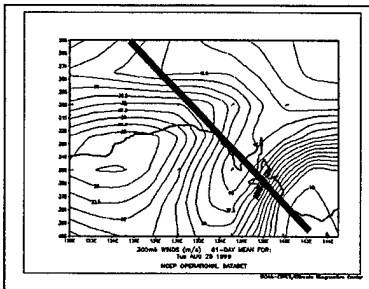

Figure 5: The large diagram shows vertical cross sections of air temperature in °C (solid lines) and wind speed in m/s (broken lines) as constructed from radiosonde soundings at Woomera, Ceduna, Adelaide and Mt. Gambier at 00UTC on 25 August 1998. Also shown is the location of Adelaide (green) and the altitudes of the horizontal flight legs (blue). Note the reversed abscissa with East left and West right.

The small diagram shows the location of the cross-section (red), the flight track (green) and coastline, as well as the 1-day mean of the 300hPa wind field.

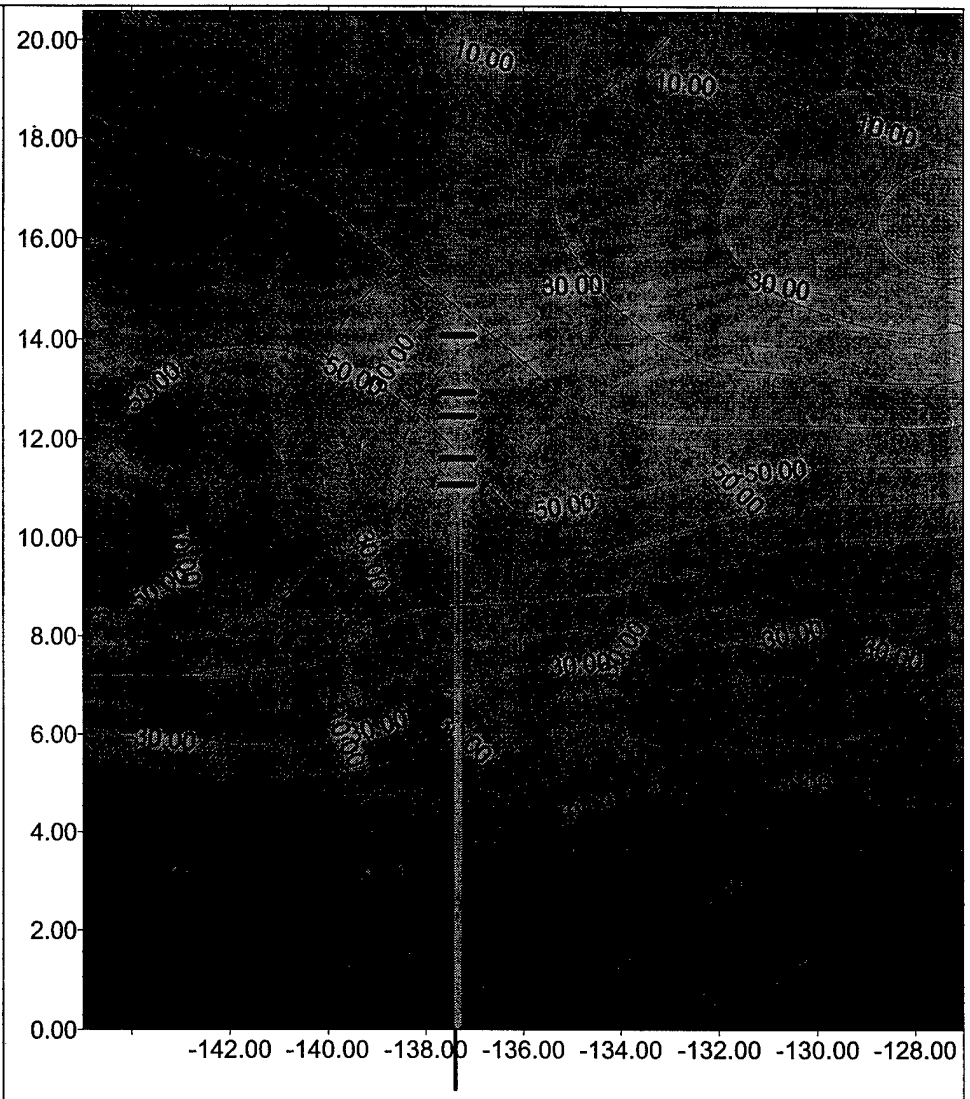

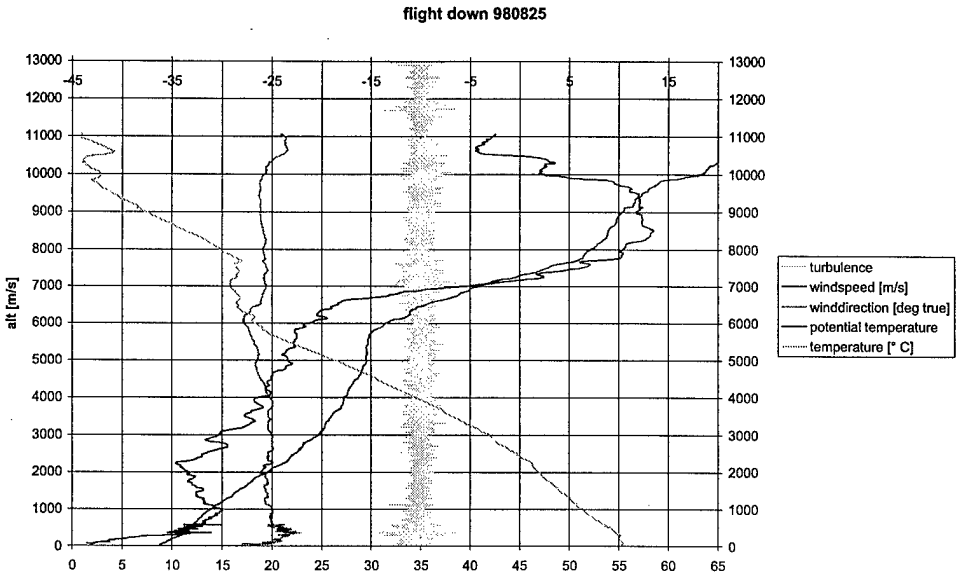

Figure 6: *Vertical profiles of atmospheric parameters as measured by the Egrett during the descent of the flight on 25 August 1998. Shown are: Turbulence (see text) in arbitrary units (yellow); wind speed in m/s (grey); wind direction in °true (scaled by a factor of 10, magenta); potential temperature in °C (brown); and air temperature in °C (light blue).*

5.2 Flight 26 August 1998

5.2.1 Synoptic Situation

As the jet core of 25 August 1998 moved east, a pool of cold air remained near Adelaide. Another jet stream approached from Western Australia but was too far away to influence the upper airflow in South Australia. The approaching front weakened and a new low pressure cell formed south west of Perth. The high pressure cell moved south to Tasmania. The 500hPa chart (not shown) for 26 August 1998 showed a high pressure ridge over Perth and a trough over New South Wales. The wind speed in the jet stream was expected to increase to approximately 45m/s in the early hours of 26 August 1998 with a maximum increase of wind speed of about 20m/s between 5.6km and 7.3km (~1.2m/s per 100m). A wide horizontal band of more or less constant wind speed was then forcast for the next six hours. The radiosonde data indicate 33m/s wind speed at the 400hPa level, the bottom of the jet stream, and 34m/s at the 150hPa level, the top of the jet stream.

A front passed Adelaide the day before and brought a few showers and the temperature decreased by about 4K. As this system passed, the strong temperature gradient in the area above Adelaide weakened in the upper troposphere. The cold air moved east and warmed, as can be seen in *Figure 7* when comparing it to *Figure 3*.

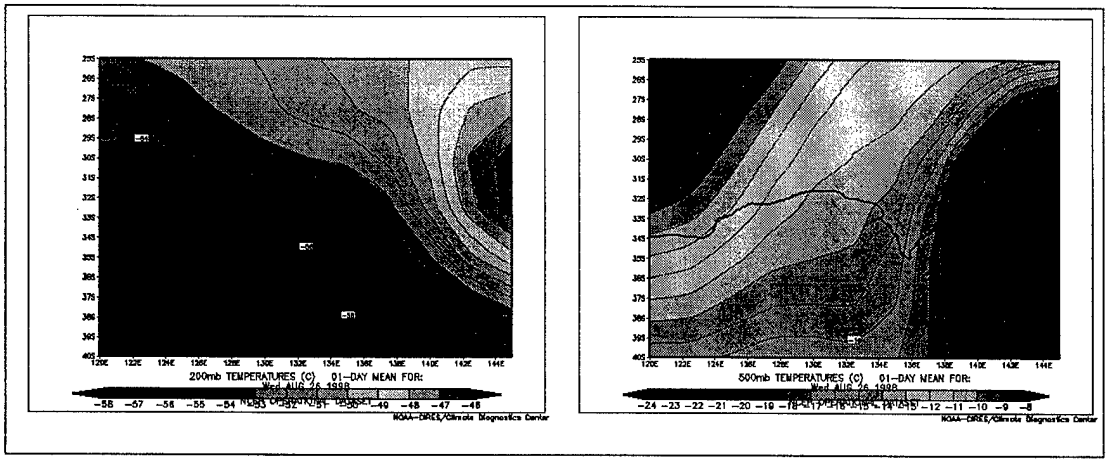

Figure 7: *Longitudinal cross-section of the temperature field at 500hPa (left) and 200hPa (right). Data shown is 1-day mean for 26 August 1998. (from NOAA website http://www.noaa.gov)*

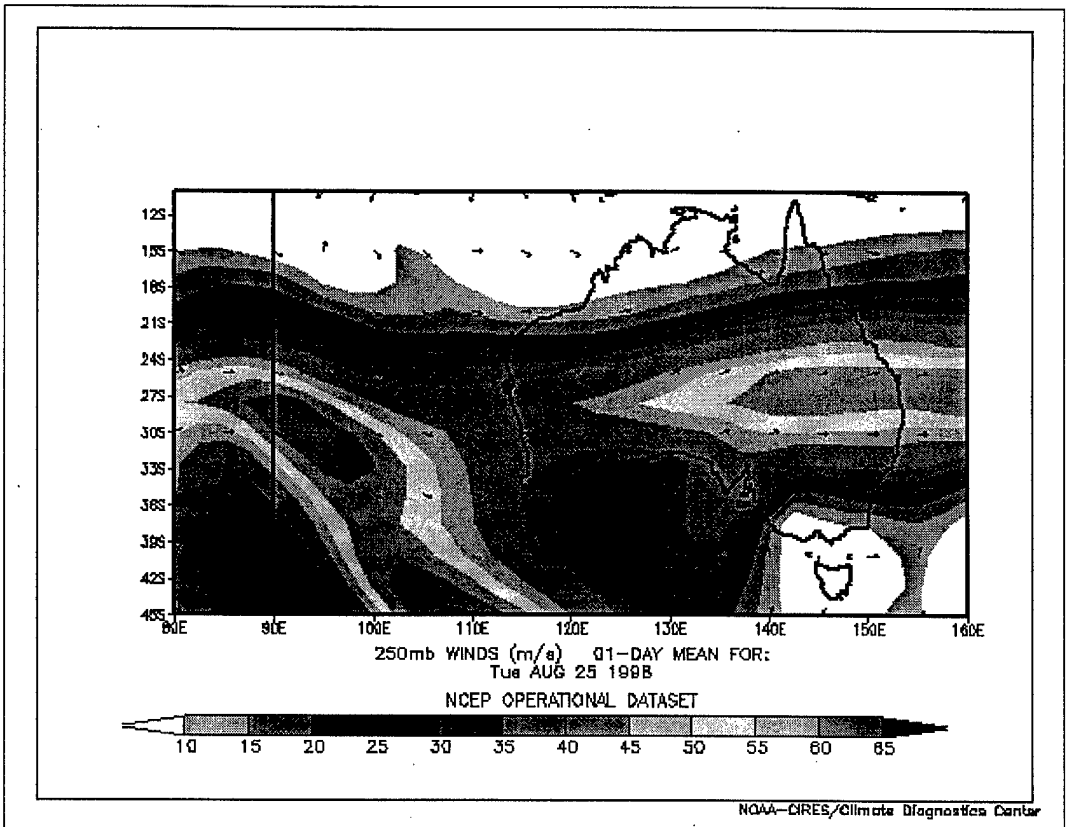

Figure 8: *1-day mean of 250hPa winds for 25 August 1998 (NOAA, website http://www.noaa.gov)*

Figure 8 shows the 250hPa winds. Note the confluence zone near Adelaide.

5.2.2 Measurements

The flight on 26 August 1998 commenced at 17:42LT and ended at 21:37LT. Nine horizontal legs were flown between FL210 (~6.4km) and FL435 (~13.3km), see*Figure 9*.

After climbing up to FL360 (~11km), the Egrett headed into the wind and flew several legs at FL210, FL360, FL380, FL400, FL420 and FL435, ie. 6.4km, 11.0km, 11.6km, 12.2km, 12.8km and 13.3km altitude).

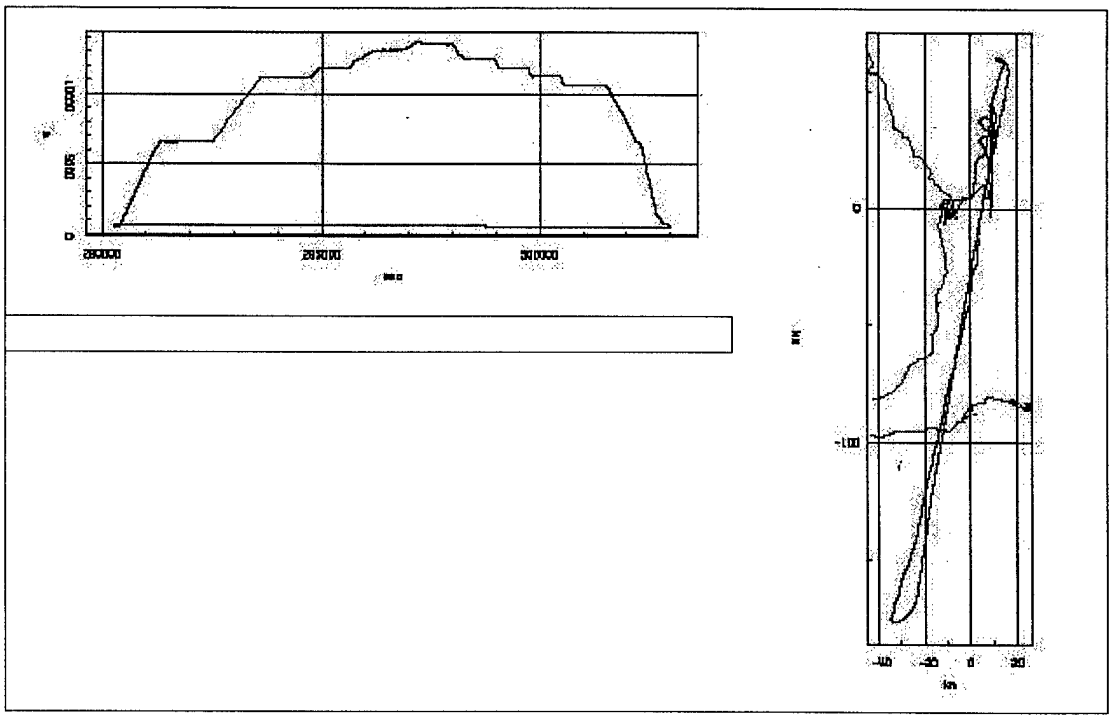

Figure 9: *Horizontal and vertical flight path for flight on 26 August 1998*

The flight legs relative to the temperature and wind speed field are shown in *Figure 10* which was constructed from routine soundings at Esperance, Forrest, Ceduna, Adelaide and Wagga Wagga (note the reversed abscissa with East left and West right).

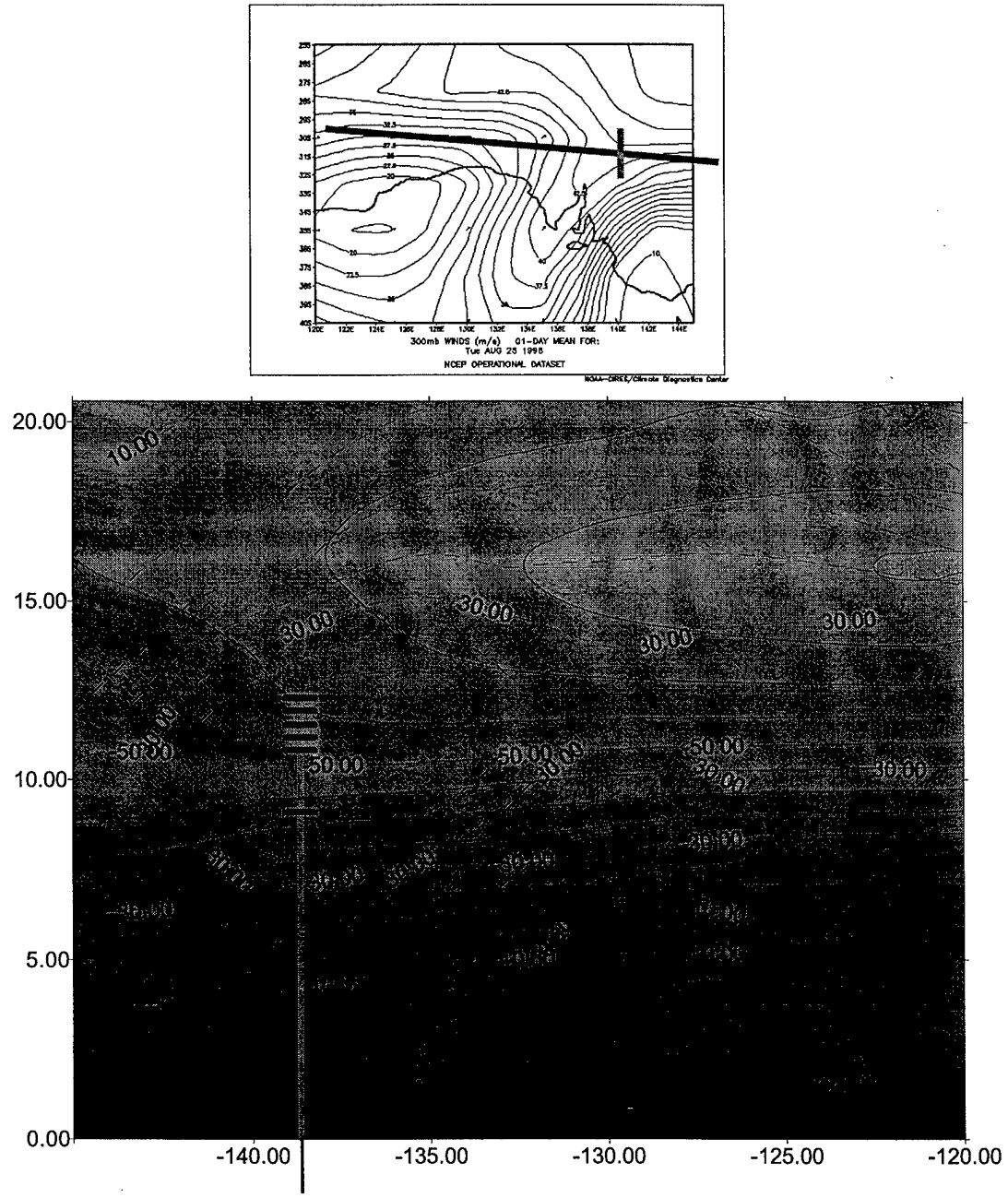

Figure 10: *The large diagram shows vertical cross sections of air temperature in °C (solid lines) and wind speed in m/s (broken lines) as constructed from radiosonde soundings at Esperance, Forrest, , Ceduna, Adelaide and Wagga Wagga at 00UTC on 25 August 1998. Also shown is the location of Adelaide (green) and the altitudes of the horizontal flight legs (blue). Note the reversed abscissa with East left and West right. The small diagram shows the location of the cross-section (red), the flight track (green) and coastline, as well as the 1-day mean of the 300hPa wind field*

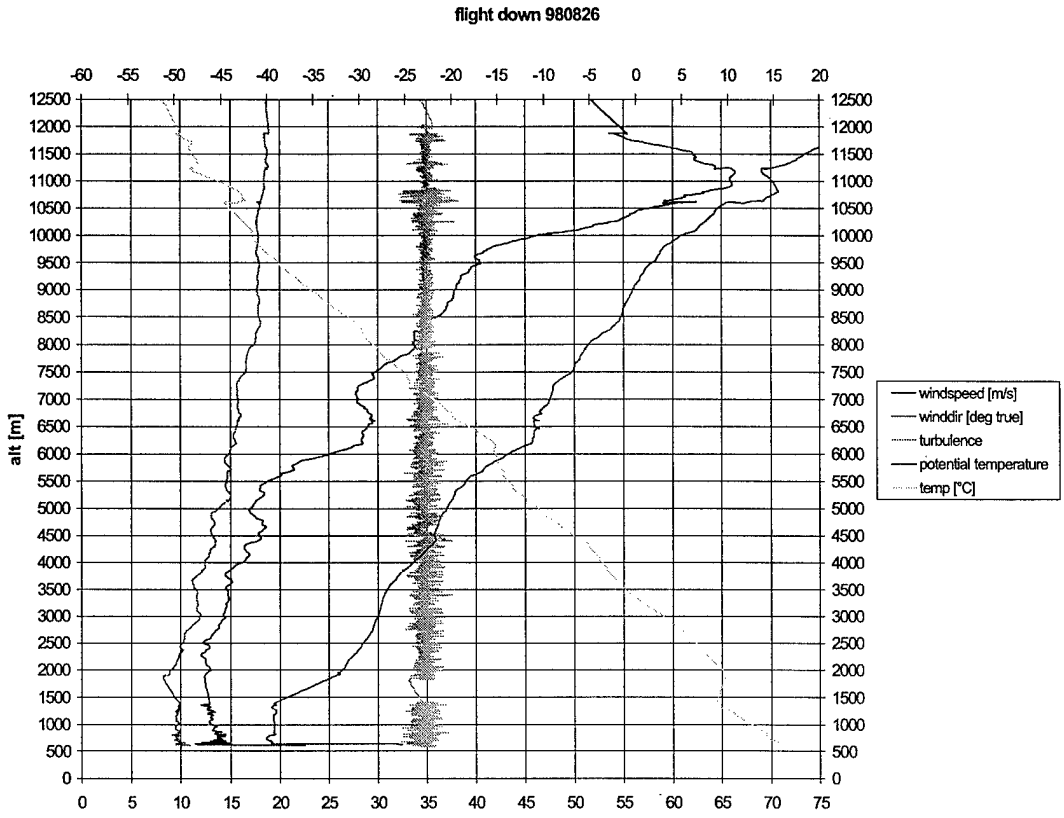

Figure 11: *Vertical sounding with the Egrett aircraft on 26 August 1998*

For 26 August 1998, there was no data available from a routine sounding at Adelaide airport.

Figure 11 shows the Egrett data for the descent at 21:37LT. The thick layer of wind speed greater then 30m/s as forecast by the Bureau of Meteorology was not confirmed by the aircraft measurements.

The jet stream had a narrow maximum at 11km altitude with wind speeds up to 34m/s and a turbulent layer about 250m below this maximum. The wind direction stayed constant throughout the upper troposphere at around 170° to 180°true.

5.3 Flight 6 August 1999

5.3.1 Synoptic Situation

The situation in the preceding days indicated a strong jet stream extending from Western Australia towards the Great Australian Bight, heading east. The 24 hour forecast of NCEP indicated wind speeds of between 90 and 100m/s for 8 August. The wind speed was forecast to decrease during the day to between 80 and 90m/s whilst it passed the Great Australian Bight. Adelaide was at the diffluent exit area of the jet with decreased wind speeds of between 70 and 80m/s.The grid point forecast from the Bureau of Meteorology indicated a similar situation. It positioned the jet maximum at about 500km south of the Great Australian Bight with a maximum speed of 155kt (75m/s) at the 200hPa level and with a cyclonic curvature to the north in the vicinity of Eyre Peninsula.

As observed in the preceding weeks, the jet was expected to pass Adelaide to the north and out of range of the aircraft. An inspection of the mean sea level chart from the Bureau of Meteorology indicated a partially occluded but weak cold front system centered south of Perth, with a large meridional extent from latitude 45°S to 23°S. Adelaide remained cloud free with some advective cumulus clouds up to 1,000m and excellent visibility. Wave-like cirrus clouds were observed in narrow ranges. The tropopause height, as given by the Bureau of Meteorology, was 119hPa (15,200m) with a temperature of –63.1°C.

Figure 12 shows the two closest aerological diagrams of the flight track in terms of time. The data was taken from the radiosonde soundings at Adelaide Airport. The green and cyan lines are the temperature and dewpoint temperature respectively, with the scale on the top axis, whilst the blue line is the wind speed. The wind direction is indicated by the magenta line and scaled by division of 10 around north (0 on bottom axis). The radiosonde released at 23:00UTC (08:30LT) indicated very dry conditions above the boundary layer up to 1,000m due to a nocturnal inversion. The temperature increase in the inversion was approximately 2.3°C in a layer approximately 140m thick. A second inversion at 9,500m and a strong change of wind direction between 7,500 and 8,500m was also evident.

The first significant change was at the height of 1,000m, with an inversion on top of the boundary layer due to radiative cooling during the night. A few clouds were observed just below the inversion. The temperature then followed the temperature gradient of the standard atmosphere with dry to very dry conditions throughout the middle troposphere. The average wind speed up to 7,000m was 10m/s decreasing to 5m/s at 8,000m combined with a rapid change of direction from 40°true to 240°true which was the direction of the jet stream.

The boundary layer height increased to 1,500 m during the day due to heating of the Earth's surface. Very dry conditions were found above. A layer of much moister air was advected from the west. This layer was about 2,000m thick topped by an inversion of aproximately +2K. The overlying airmass was very dry. The wind speed increased during the day because of the jet stream maximum which passed Adelaide to the north during the day.

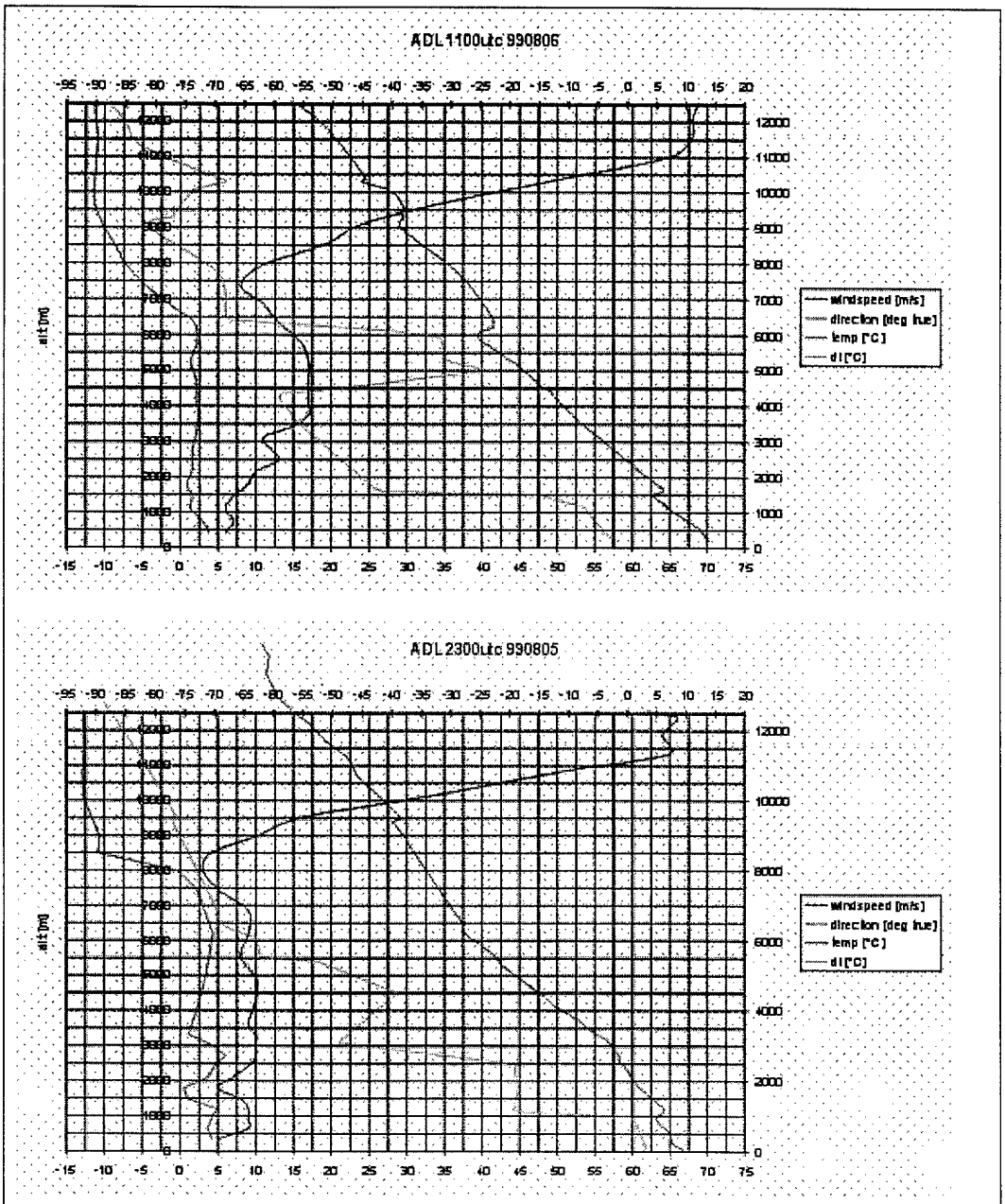

Figure 12: *Radiosonde ascents from Adelaide Airport on 5 August 1999 11UTC and 23UTC. Shown are: wind speed in m/s (dark blue); wind direction in °true (scaled by dividing by ten, magenta); air temperature in °C (green); and dewpoint in °C (light blue).*

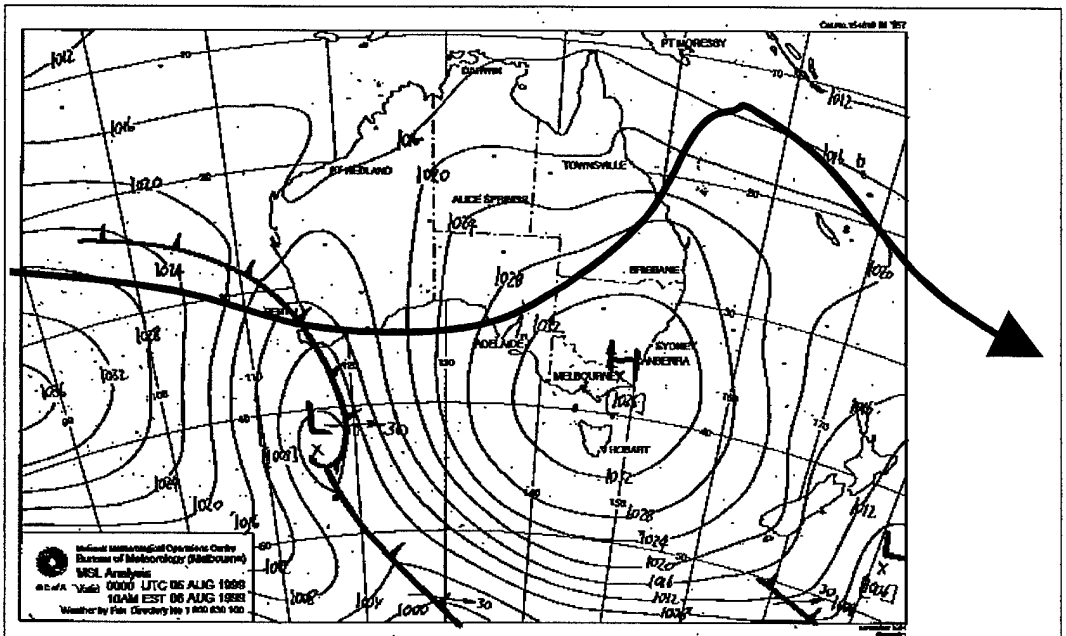

Figure 13: *Surface analysis chart valid for 6 August 1999 00UTC.*

The mean sea level analysis at 09:3LT (*Figure 13*) indicated that the cold front was particularly weak with the center of the low pressure system to the south of Albany moving east at approximately 15m/s. The jet axis is shown as a blue line. The maximum wind speed was 85m/s directly above the cold front. The system was becoming occluded on the next day with the wind speed decreasing to 10m/s (see *Figure 14).* The 24 hour isallobaric analysis (*Figure 15*) supported the indications about the weakness of the cold front with a maximum pressure change of –2.7hPa per day. The next fast moving low pressure system was approaching from the south so that the high pressure area was forced to move north east.

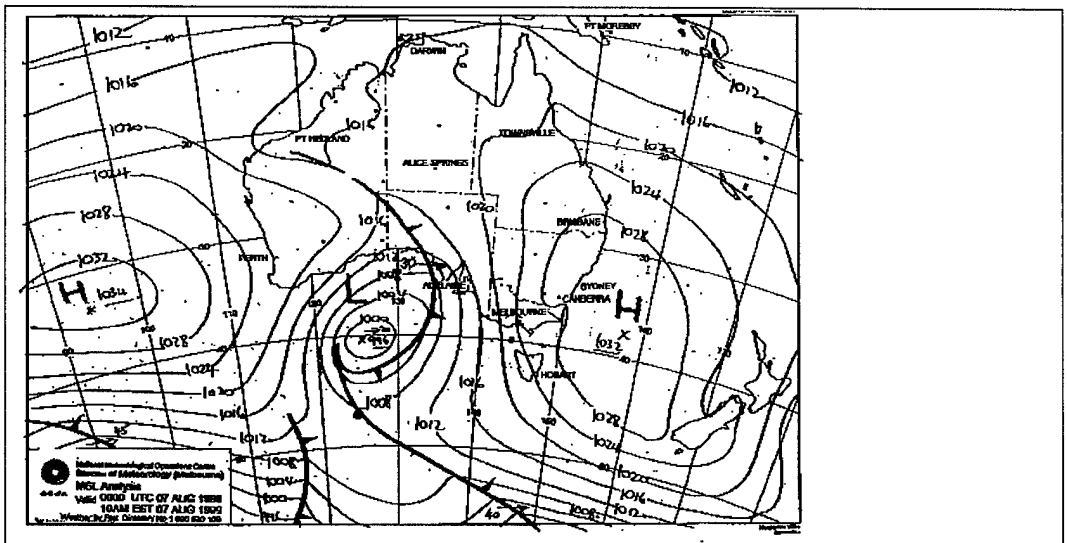

Figure 14: *Surface analysis chart valid for 7 August 1999 00UTC.*

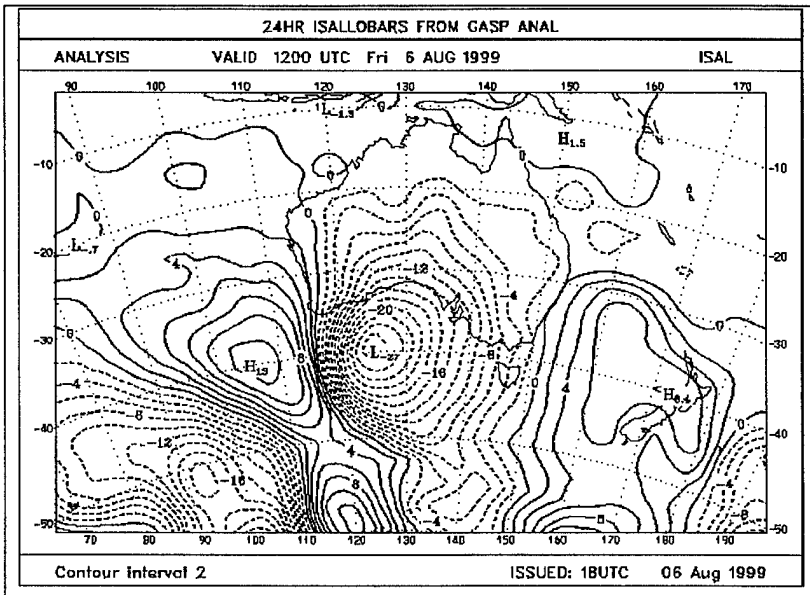

Figure 15: *Isallobaric analysis 6 August 1999 12UTC*

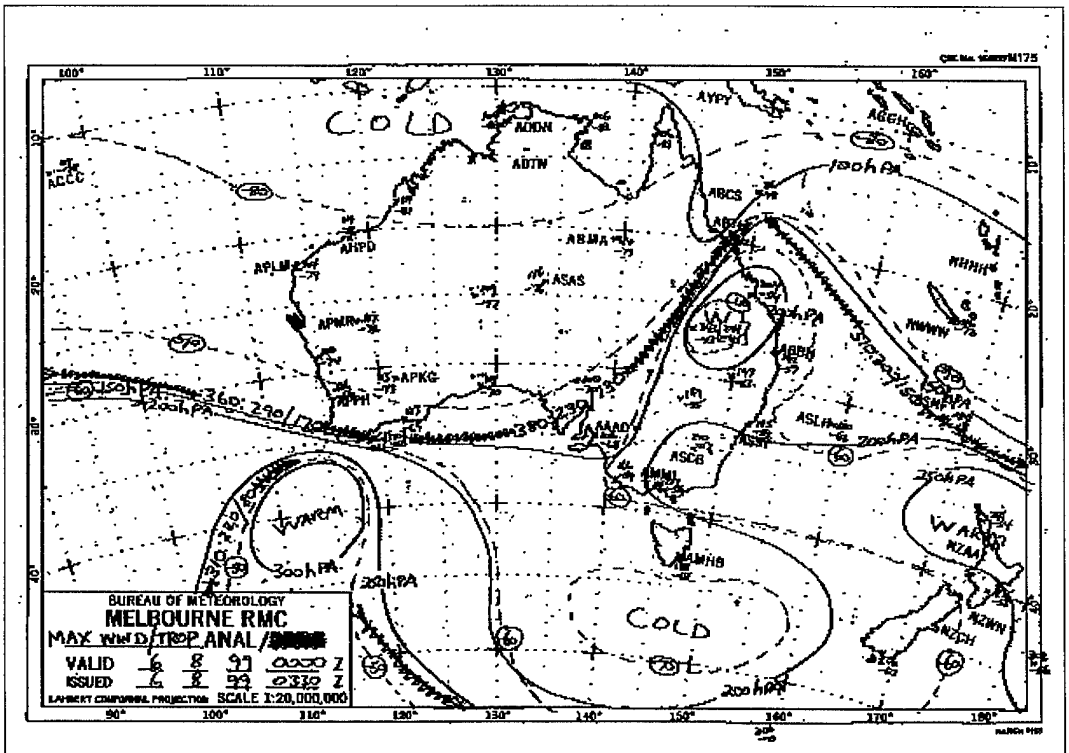

Figure 16: *Max wind and Tropopause analysis 6 August 1999 00UTC*

The Bureau of Meteorology's maximum wind and tropopause analysis from 6 August 1999 shows the wave-like axis of the jet stream and upper atmospheric temperature conditions (*Figure 16*). Further information about the synoptic conditions can be taken from *Figure 17* and *Figure 18*.

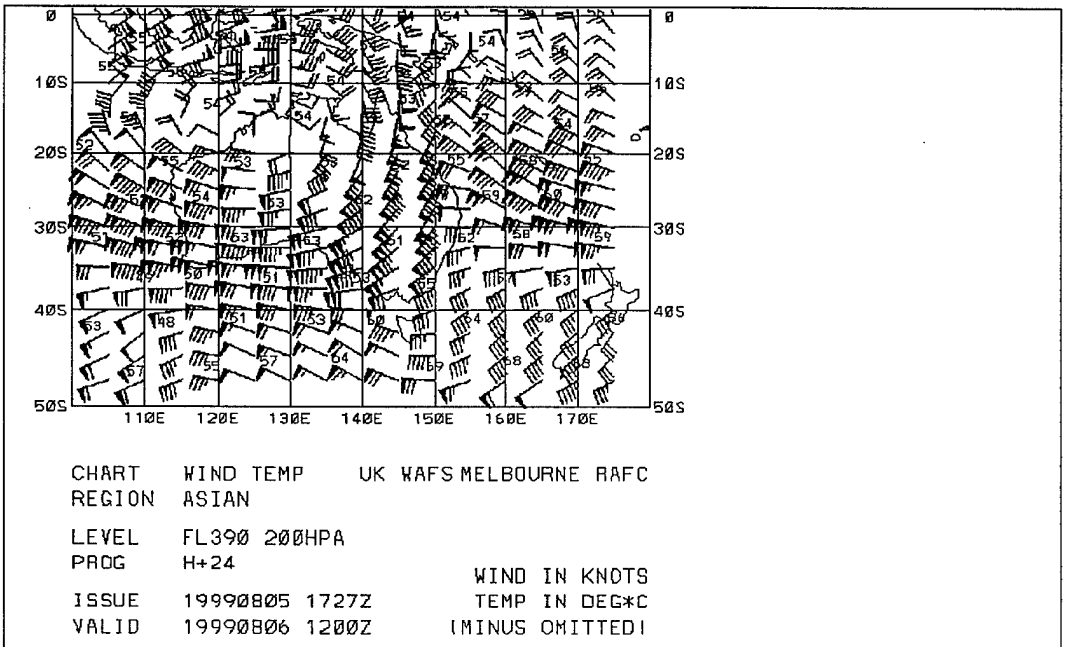

Figure 17: *Wind and temperature chart of the Australian region valid for 6 August 1999.*

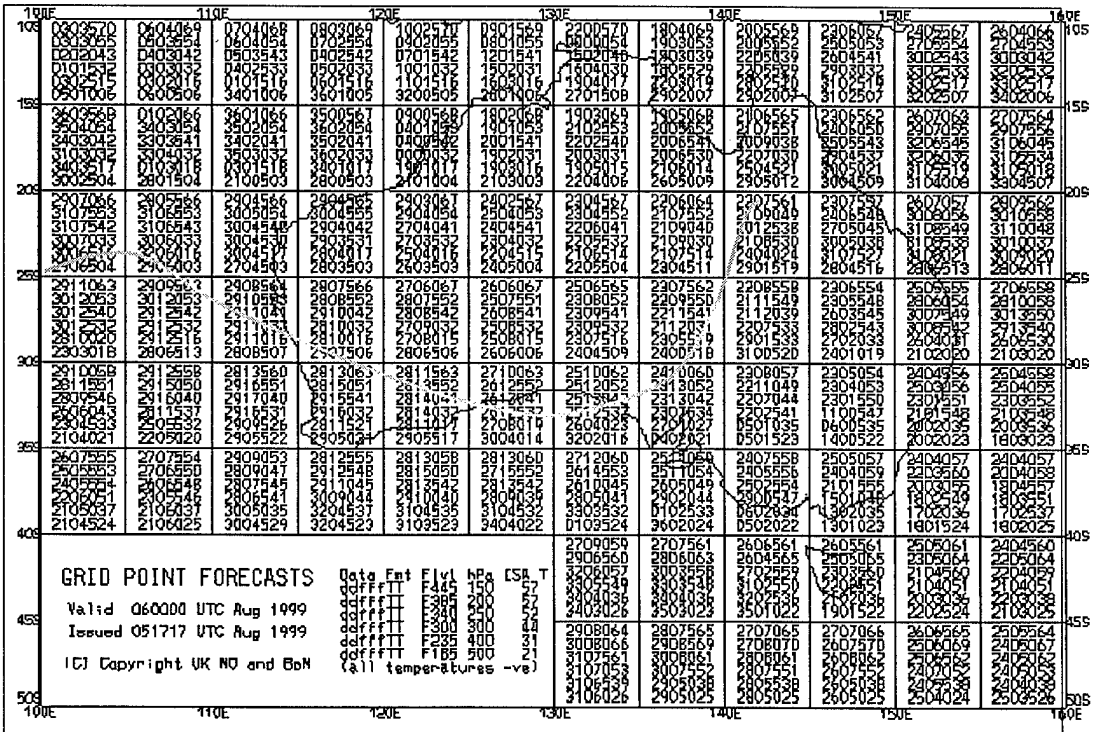

Figure 18: *Grid point forecast for the Australian region valid for 6 August 1999 06UTC.*

5.3.2 Measurements

The flight on 6 August was one of the most successful flights in this project. Very strong turbulence was found in a thick layer between 8,000m and 9,200m with total acceleration sometimes exceeding 1.5g.

The flight commenced at 13:39LT and ended at 18:44LT (*Figure 19*). After climbing to 29,000ft (8.8km), the aircraft was heading straight into the wind, flying quasi horizontal levels at FL290, FL300, FL310, FL320, FL365 and FL390, ie. 8.8km, 9.1km, 9.5km, 9.8km, 11.1km and 11.9km. Each leg was approximately 30min. In between there were two legs flown from FL320 (11.1km) down to FL270 (8.2km) and back up to FL330 (10.0km).

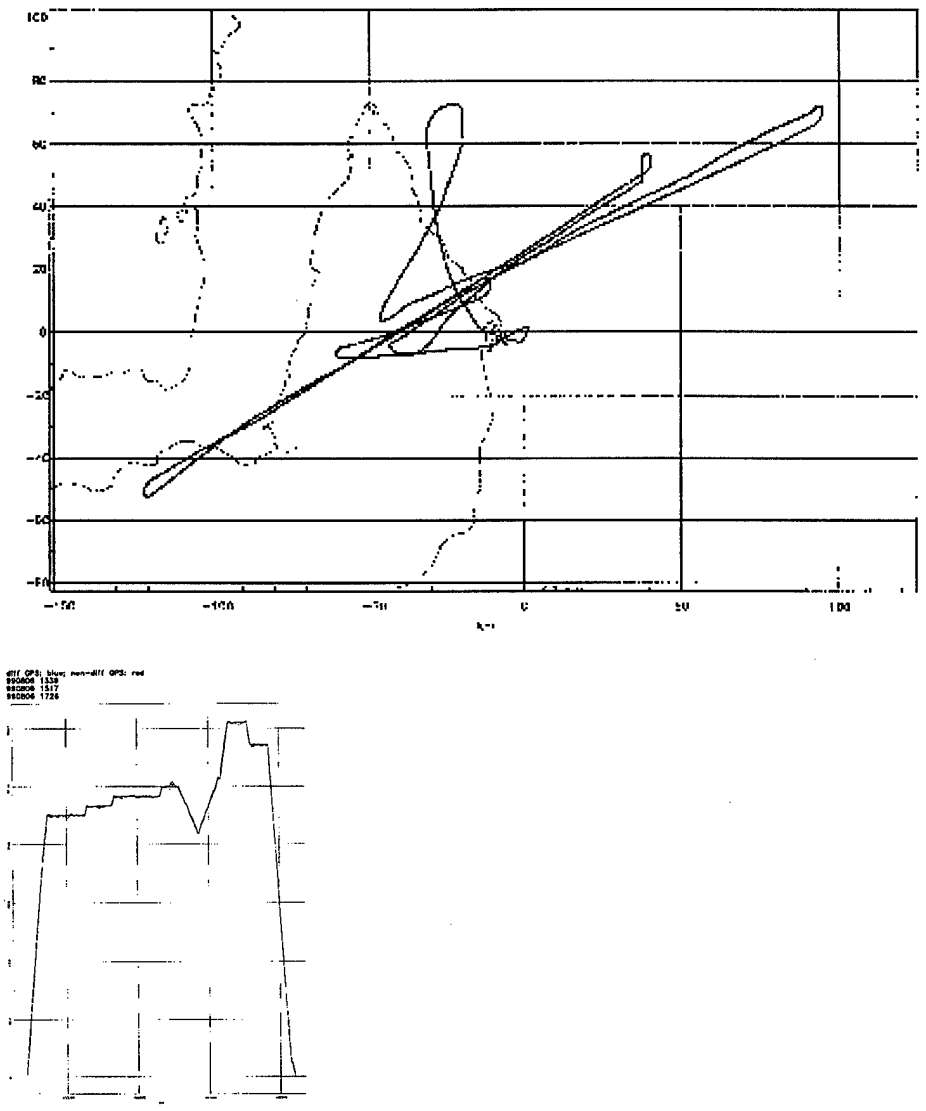

***Figure 19**: Flight track on 6 August 1999.*

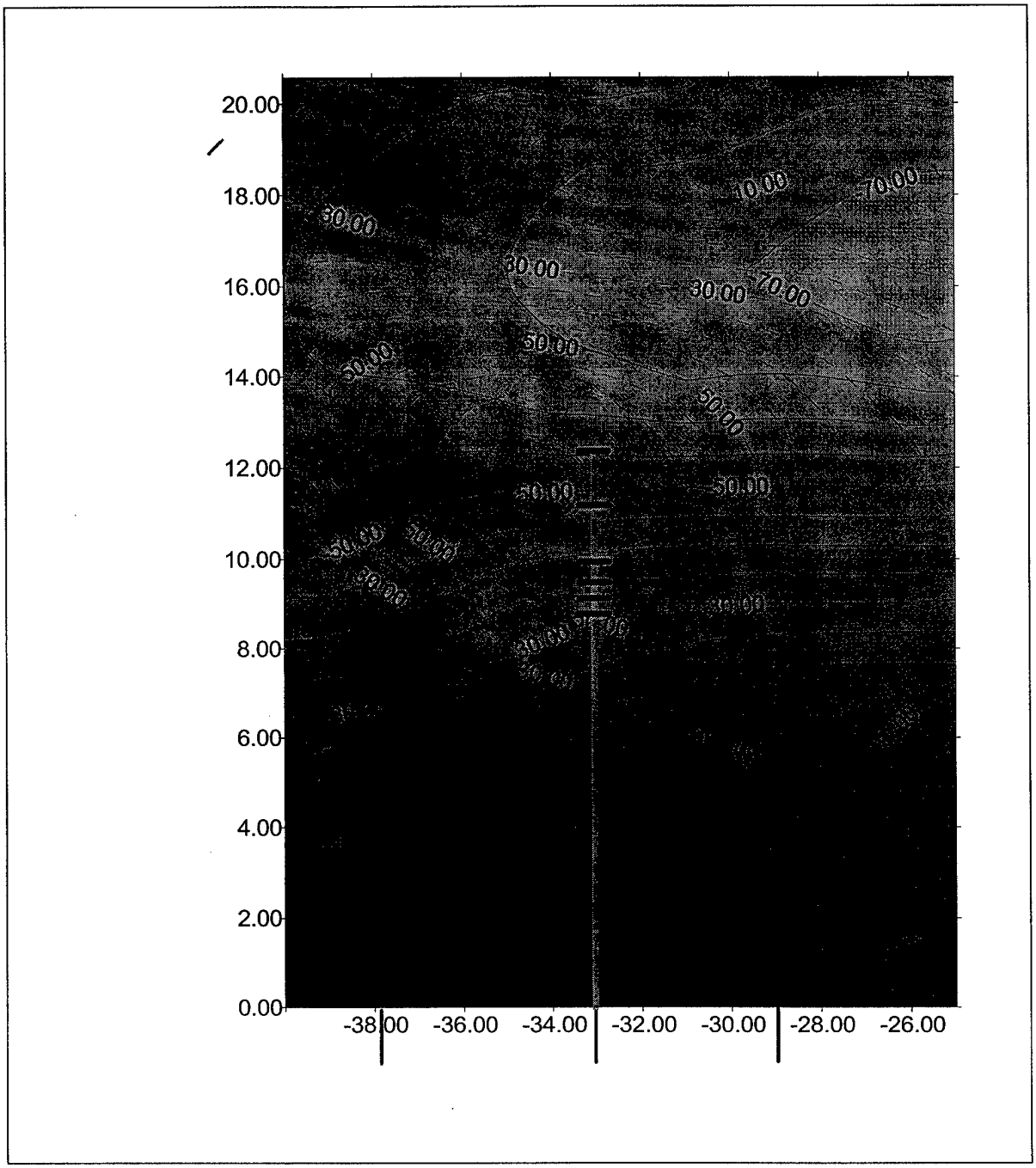

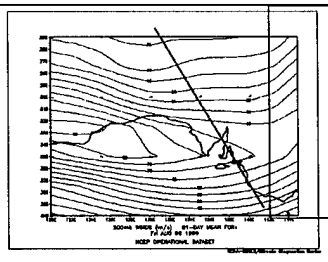

Figure 20: As Figure 10, but for the soundings at Mount Gambier, Adelaide and Coober Pedy, at 00UTC on 6 August 1999.

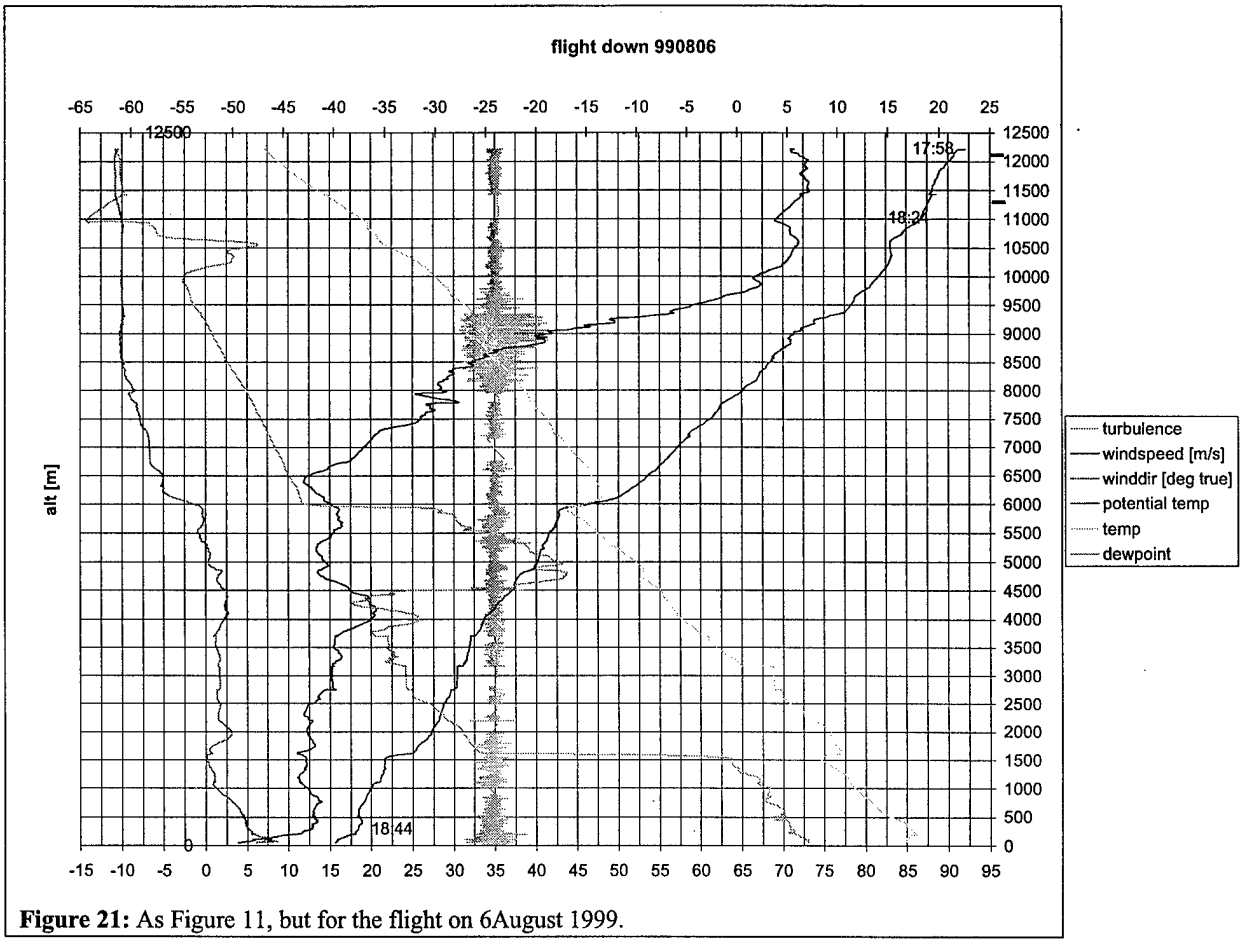

Figure 21: As Figure 11, but for the flight on 6August 1999.

APPENDIX A: Conference Paper

CLEAR AIR TURBULENCE AND REFRACTIVE TURBULENCE IN UPPER TROPOSPHERE AND LOWER STRATOSPHERE

Owen R. Coté*, Air Force Research Laboratory, Space Vehicles Directorate, Hanscom AFB,

Jorg M.Hacker, Airborne Research Australia, Flinders University, 5016 Salisbury

South, Australia, Timothy L. Crawford, NOAA/ERL/ARL, Idaho Falls, and

Ronald J. Dobosy, NOAA/ERL/ARL, Oak Ridge.

1. Introduction.

Refractive Turbulence, the local fluctuations of the propagation speed of electromagnetic waves relative to speed in a vacuum, is associated with atmospheric density fluctuations and is a main contributor to fast scintillation of laser communication, wide-area microwave and infra-red surveillance, and directed energy weapon systems. Slow fading and the phenomena of radar or radio "holes" defined by periods of anomalous low signal strength are associated with strong and persistent mean vertical gradients of refraction that occur with humidity layering and temperature inversion layers. The goal of direct airborne measurement of refractive turbulence is to understand and hopefully predict the evolution of both mean and turbulent atmospheric structure that causes adverse performance of systems such as an airborne early warning radar or an airborne laser communication system. In the upper atmosphere the refractive turbulence parameter of primary concern is the temperature structure constant, C_T^2

Because the US Air Force concern is with global operation of such systems the need is to know in what geographic regions, in what season, and in what part of a large-scale meteorological pattern, their operations could be most severely degraded by refractive turbulence. To answer the question on just how severe refractive turbulence can be a collaborative research program to directly measure refractive turbulence above and below the core of the winter sub-tropical jet stream between the altitudes of 8 and 15 km was developed. The GROB 520T EGRETT, owned and operated by Airborne Research Australia (ARA) was chosen to be the airborne platform with the NOAA/FRD BAT probe chosen as a turbulence sensor. The BAT probe is a 13 cm diameter pressure hemisphere with nine pressure ports. A micro-bead thermistor for temperature measurement is mounted in the central pressure port. The BAT probe is designed to be flown on aircraft without inertial navigation systems. Each probe contains a GPS receiver and three component accelerometers. For a more complete description of the BAT probe see Crawford and Dobosy (1992). A more recent description is available on the web site: http://www.noaa.inel.gov/frd/Capabilities/BAT/.

Three of the BAT probes were mounted on EGRETT, one under each wing and one at the top of the tail. The use of three probes was a response to several problems relative to high altitude turbulence measurements. The first is the averaging time problem discussed by Lumley and Panofsky (1964), and Wyngaard (1973). The second problem is flow distortion. It is hoped that the multiple probes will help in the identification of flow distortion affects on spectra. The final problem is to obtain measurements of vertical gradients of mean horizontal wind and mean potential temperature with comparable accuracy to the turbulence estimates. Both measurements are used to evaluate budgets of kinetic energy, temperature variance, and heat flux.

2. Where and When to Measure for Turbulence.

Because funding was limited it was important that any measurement campaign should provide information relevant to the range of maximum temperature structure parameter, C_T^2, that occurs above 9 km. The determination of where to measure, in what season, and at what altitudes to measure was greatly helped

by use of climate data available on the NOAA web site (http://www.cdc.noaa.gov/HistData/). Using this data base it was concluded that in the winter subtropical jet stream, which is found near 30 degrees latitude in both hemispheres, some of the strongest winds are found near the south coast of Japan in the northern hemisphere and in the Perth to Adelaide corridor in the southern hemisphere. Associated with the jet

* *Corresponding author address*: Owen R. Coté,
AFRL/VSBL, 29 Randolph Rd., Hanscom AFB,
MA 01731-3010; owen.cote@hanscom.af.mil

core is a change in tropopause heights. On the pole-ward edge it was about 9 to 10 km and 300 mb pressure. On the equator-ward edge it was varied from 15 to 16 km and about 120 mb pressure. The

daily plot of the spatial distribution of the tropopause pressure jump clearly identifies a narrow ribbon four or five degrees of latitude wide which migrates toward the pole in spring, and retreats toward the equator in the fall season. Some estimate of relative turbulence intensity can be obtained from the temperature plots for the standard pressure levels. The magnitude of horizontal temperature gradients on a constant pressure surface indicates the strength of the vertical gradient of the geostrophic wind. A narrow ribbon of the maximum temperature gradient at each pressure coincided with the location jet core and the tropopause jump with the greatest geostrophic shear found above and below the jet core at the 150 mb and 300 mb pressure levels. Examining several years of this led to the choice of February in Japan and August in Australia.

Having made the turbulence measurements in these months in 1999, the NOAA database is still useful in estimating the order of magnitude of the horizontal shear and stratification production terms in the energy, flux, and temperature variance budgets. The upper troposphere and lower stratosphere are not homogeneous. The measurement flights where accordingly in the direction in which the atmosphere is most homogeneous, either upwind or downwind. The length of a constant altitude measurement was 1200 seconds, which is about 100 kilometers at EGRETT airspeed. In Japan the smallest separation of measurement levels was 660 meters and in Australia it was 330 meters.

3. Measurements

In Table 1 are summarized the structure function parameters for temperature for temperature and the three velocity components for most of the measurements made in Japan in February 1999. Also listed in the table are the ratios of pairs of structure parameters. C_U^2/ C_T^2 is equal to the ratio $\alpha_1 \varepsilon/\beta_1 \chi$, the product of the dissipation ratio with the Kolmogorov spectral constant ratio. It shows great variability in a very reduced C_T^2 value. The estimates for turbulent dissipation (ε) are obtained from the relation: $C_U^2 = 2\,\varepsilon^{2/3}$. The column labeled "dyn heat" is the ratio of measured C_T^2 to true C_T^2 if corrections for dynamic heating are not made to the temperature time series. The ratio of the transverse velocity structure parameters to the longitudinal velocity structure parameter should be 4/3 if the inertial sub-range is locally isotropic. On average C_V^2 is and C_W^2 is not. This same result was obtained for the measurements in Australia except for 6 August 1999 which are also shown in Table 1. The measurement duration at level 9650 m was 3000 seconds in contrast to the other levels that day which all were for 1200 seconds. The time series for measurement flight level was dived into two sections. Section A is the eastern half and B is the western half. Level 9560B had the largest structure parameters EGRETT has measured to date. Correspondingly the vertical accelerometer data for section B was intermittently $\pm$ 1.5 g. On the following two days, 7and 8 August, it rained and EGRETT could not make measurements because water in the pressure ports would freeze at altitude. It is of interest to look at the NOAA CDC web site (see above) for these two days. The presence of a low- pressure trough (with closed temperature contours) contiguous to and pole-ward of the jet is the structure we identified as most favorable to extreme turbulence and we sought to investigate whenever possible.

In figure 1 are vertical profiles for C_T^2 , one from Japan and one from Australia that have the peak values for each campaign. With the 660 meter separation between measurement levels in Japan it is possible that the peak value was not sampled. To capture the structure of these narrow layers of extreme turbulence future measurements should probably be between 250 and 300 meter separation in the vertical when extreme turbulence is encountered. Figure 2 contains the vertical profiles of the three components of velocity variance, temperature variance, and the vertical heat flux magnitude (note log plot of amplitude). Figure 3 contains the three Reynolds stress components in a linear plot that sets off the turbulent layer rather well. The curvature of the <uw> profile in the turbulent layer acts as a negative feedback and diminishes a positive mean vertical gradient of the mean wind that produces negative <uw>.

At low spatial wave-numbers, velocity and temperature spectra follow a k_1^{-3} power law and preliminary analysis with the scaling suggested by Lumley (1964) and Weinstock (1978) indicates a non-constant spectral constant in agreement with the aircraft turbulence measurements of Lilly and Lester

(1974). This is an interesting preliminary result but needs more confirmation.

In Table two are show various turbulent parameter ratios and scale calculations. The column $<u\theta>/<w\theta>$ is the horizontal to vertical heat flux ratio. The column $<\theta^2>/w^2>$ is the ratio of temperature variance to vertical velocity variance. The Ri $<w\theta>$ column is the vertical heat flux Richardson number equivalent to ℓ_T^2/ℓ_b^2. The column labeled $<\theta^2>/C_T^2$ is the integral scale estimate obtained from

$(<\theta^2>/C_T^2)^{3/2}$. The next column is the integral scale obtained from $((u^2+v^2+w^2)/2)^{3/2}/\varepsilon = q^3/\varepsilon$. The last column labeled Integral Scale Ratio is the ratio of these two integral scales.

4. Scales and Budgets

TEMPERATURE VARIANCE BUDGET

$\partial\langle\theta^2\rangle/\partial t$ = - advection $-\langle w\theta\rangle\,\partial\Theta/\partial z$ (1 + Horizontal Prod/Vertical stratification Prod) + $-\partial\langle w\theta^2\rangle/\partial z$ (1 + Horizontal TT/Vertical TT) $-\chi$

where χ ($\chi = \kappa\langle(\partial\theta/\partial x_i)^2\rangle$) is dissipation rate of temperature variance and TT stands for turbulent transport by third moments. The temperature structure parameter is obtained from the inertial sub-range temperature spectrum in the form

$\Phi_T(k_1) = 1/4\ C_T^2\ k_1^{-5/3}$

Under Kolmogorov scaling $C_T^2 = 4\beta_1\chi/\varepsilon^{1/3}$ and β_1 is the one dimensional Kolmogorov spectral constant. Under stationarity, horizontal homogeneity, and universal equilibrium, production and dissipation are equal so that:

$-\langle w\theta\rangle\,\partial\Theta/\partial z = \chi = \kappa\langle(\partial\theta/\partial x_i)^2\rangle$;

To derive C_T^2 divide by $\varepsilon^{1/3}/4\beta_1$. The resulting identity evolves as follows:

$4\beta_1/\varepsilon^{1/3}\ \langle w\theta\rangle\,\partial\Theta/\partial z = 4\beta_1 K_H/\varepsilon^{1/3}\,(\partial\Theta/\partial z)^2 = C_T^2 = 4\beta_1\kappa/\varepsilon^{1/3}\ \langle(\partial\theta/\partial x_i)^2\rangle = 4\beta_1 L^{4/3}(\partial\Theta/\partial z)^2$

In the above identity we have replaced mean-square fine scale gradients by the square of the mean gradient times a ratio equivalent to a Reynolds number: $KH/\kappa\ (\partial\Theta/\partial z)2 = \langle(\partial\theta/\partial xi)2\rangle$. The basic problem in modeling CT2 in stable stratification is to determine the composition of L4/3 or KH /ε1/3 which has the dimension of (length)4/3. There are two possibilities suggested by the EGRETT temperature spectra. L is equal to the temperature integral scale, ℓ. The second possibility for $L^{4/3}$ is a combination of length scales: $L^{4/3} = \ell_T^2/\ell^{2/3}$ where ℓ_T is the Ellison scale defined by $\langle\theta^2\rangle = \ell_T^2\,(\partial\Theta/\partial z)^2$. This scale arises naturally in the vertical heat flux conservation equation.

An alternative form for modeling C_T^2 is obtained by replacing the vertical gradient of potential temperature by $N^2\,\Theta_o/g$ not replacing the vertical heat flux by an eddy diffusion coefficient as follows:

$-4\beta_1/\varepsilon^{1/3}\ \langle w\theta\rangle\,\partial\Theta/\partial z = -4\beta_1\, g/\Theta_o\,\langle w\theta\rangle/\varepsilon\ N^2\,(\Theta_o/g)^2\,\varepsilon^{2/3} = = -2\beta_1\, g/\Theta_o\,\langle w\theta\rangle/\varepsilon\ N^2\,(\Theta_o/g)^2$
$C_U^2 = C_T^2$

VERTICAL HEAT FLUX BUDGET

$\partial\langle w\theta\rangle/\partial t$ = - advection $-\langle w^2\rangle\,\partial\Theta/\partial z$ (1 + $\frac{Horizontal - Production}{Vertical - Production}$) + $g/\Theta\,\langle\theta^2\rangle$ - $1/\rho_o\langle\theta\partial p/\partial z\rangle + 2\Omega\cos\varphi\,\langle u\theta\rangle - \partial\langle w^2\theta\rangle/\partial z$ (1 + $\frac{HorTransport}{VertTransport}$) + $\langle w\theta\rangle(\partial U/\partial x + \partial V/\partial y)$

In the stable boundary layer, Wyngaard et. al. (1971) showed the vertical heat flux budget is a balance between a gain from stratification production ($-\langle w^2\rangle\,\partial\Theta/\partial z$) and loss from buoyancy ($+ g/\Theta\,\langle\theta^2\rangle$) and the fluctuating pressure term ($- 1/\rho_o\langle\theta\partial p/\partial z\rangle$. The ratio of buoyancy to stratification production is equivalent to ℓ_T^2/ℓ_b^2 where $\langle w^2\rangle/N^2 = \ell_b^2$. For measurements at the Boulder Tower under conditions of stable stratification, Hunt et. al. (1985) found this ratio was 0.64 for all cases. In the 6 Aug clear air turbulence event this ratio was between 1.4 and 2.4 for the strong turbulence levels. It is not clear at this time what maintains the negative vertical heat flux.

Conclusions

Demonstrated by EGRETT measurements that clear air and refractive turbulence should be sought in the strong shear layers found above and below the jet core of the winter half-season sub-tropical jet stream in both hemispheres when the local anisotropy represented by C_w^2 / C_u^2 ,the ratio of vertical to longitudinal turbulence is weak to moderate: less than 1.33 but greater than 0.6. Future analyses of the correlation of fluctuating velocity and temperature with fluctuating static pressure gradients should confirm its role in controlling anisotropy.

6. References

Derbyshire, S. H. 1993: Local scaling in a simulated stable boundary layer. In *Waves and Turbulence Stably Stratified Flows* (Ed.) S. D. Mobbs and J. C. King. Clarendon Press. Oxford, 465 pp.

Crawford, T. L. and R. J. Dobosy, 1992: A sensitive fast-response probe to measure turbulence and heat flux from any airplane. *Boundary Layer Meteorol.* **59,** 257-278.

Dobosy, R. J., T. L. Crawford, J. L. MacPherson, R. L. Desjardins, R. D. Kelly, S. P. Oncley, and D. H. Lenschow. 1997: Intercomparison among four flux aircraft at BOREAS in 1994. *J. Geophys. Res.,* **102,** 29,101-29,111.

Hunt, J. C. R., J. C. Kaimal and J. E. Gaynor. 1985: Some observations of turbulence structure in stable layers. *Quart. J. R. Met., Soc.,* **111,** 793-815.

Lilly, D. K. and P.F. Lester. 1974: Waves and turbulence in the stratosphere. *J. Atmos. Sci.,* **31**, 800-812

Lumley, J. L. 1964: The spectrum of nearly inertial turbulence in a stably stratified fluid. *J. Atmos. Sci.***21,** 99-102.

_____ and H. A. Panofsky, 1964: The Structure of Atmospheric Turbulence. New York, Interscience-Wiley, 239pp.

Weinstock, J. 1978: Vertical turbulent diffusion in a stably stratified fluid. *J. Atmos. Sci.*, 35, 1022-1027

Wyngaard, J. C. 1973: On surface-layer turbulence in *Workshop on Micrometeorology.* D. A. Haugen (Ed.) American Meteorology Society, Boston, 392pp.

_____, O. R. Cote and Y. Izumi 1971: Local free convection, similarity, and the budgets of shear stress and heat flux., *J. Atmos. Sci.,* **28**, 1171-1182.

Van Atta, C. 1990: Comment on "The scaling of turbulence in the presence of vertical stratification" by A. E. Gargett. *J. Geophys. Res.*, **95**, 11,673-11,674.

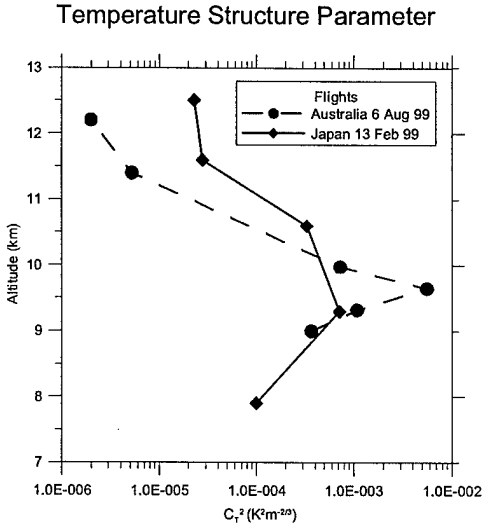

Figure 1. Vertical Profiles of Temperature Structure Parameter.

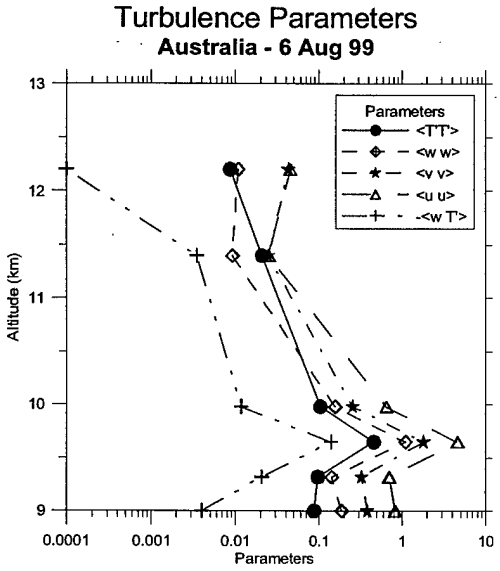

Figure 2. Vertical profiles of temperature variance, turbulent velocity components, and the vertical heat flux (multiplied by −1).

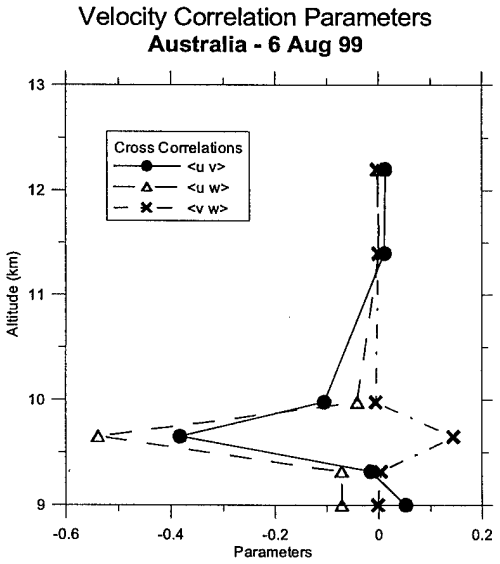

Figure 3. Vertical Profiles of Three Components of Reynolds Stress.

Table 1. Structure function parameters and ratio

Date	Altitude	C_t^2	C_u^2	C_w^2	C_v^2	Cu2/Ct2	dyn heat factor- u2	Cw2/Cu2	Cv2/Cu2	ε (m^2/s^3)
Japan	(meters)									
12-Feb-99	11,849	1.40E-04	1.20E-03	5.90E-04	1.50E-03	8.6	1.3	0.49	1.25	1.47E-05
	9,231	1.60E-05	1.60E-03	1.30E-04	2.60E-03	**100.0**	4.6	0.08	1.63	2.26E-05
	8,932	**1.25E-06**	7.00E-05	1.70E-05	5.80E-05	**56.0**	3	0.24	0.83	2.07E-07
	7,694	1.50E-05	3.00E-04	1.60E-04	1.30E-03	20.0	1.5	0.53	4.33	1.84E-06
13-Feb-99	12,537	2.30E-05	9.00E-05	2.30E-05	1.40E-04	3.9	1.1	0.26	1.56	3.02E-07
	11,580	2.80E-05	5.60E-03	9.30E-04	4.50E-03	**200.0**	8.2	0.17	0.80	1.48E-04
	10,595	3.30E-04	4.20E-03	2.40E-03	4.60E-03	12.7	1.5	0.57	1.10	9.62E-05
	9,325	**7.20E-04**	3.60E-03	1.76E-03	5.30E-03	5.0	1.2	0.49	1.47	7.64E-05
	7,898	1.00E-04	**1.00E-02**	1.10E-03	1.30E-02	**100.0**	4.6	0.11	1.30	**3.54E-04**
22-Feb-99	12,343	1.40E-05	3.90E-03	4.10E-04	4.80E-03	**278.6**	11.1	0.11	1.23	8.61E-05
	12,362	1.70E-05	5.00E-04	2.70E-04	5.00E-04	**29.4**	2.1	0.54	1.00	3.95E-06
	11,751	2.50E-04	4.00E-03	2.70E-03	5.10E-03	16.0	1.6	0.67	1.27	8.94E-05
	9,850	1.60E-05	?	7.40E-05	?	?		?	?	?
	9,242	7.50E-06	1.20E-04	2.75E-05	7.50E-05	16.0	1.6	0.23	0.63	4.65E-07
23-Feb-99	12,282	2.70E-05	1.70E-04	6.60E-05	2.20E-04	6.3	1.2	0.39	1.29	7.84E-07
	11,662	9.00E-06	2.10E-03	1.00E-03	3.80E-03	**233.3**	9.4	0.48	1.81	3.40E-05
	10,243	7.00E-05	**1.20E-02**	5.50E-03	1.15E-02	**171.4**	7.2	0.46	0.96	**4.65E-04**
	9,969	3.30E-05	2.60E-04	7.20E-05	3.30E-04	7.9	1.3	0.28	1.27	1.48E-06
	9,536	5.70E-05	1.40E-03	5.70E-04	1.80E-03	24.6	1.9	0.41	1.29	1.85E-05
Australia										
6-Aug-99	12,200	2.00E-06	5.30E-05	2.05E-05	5.33E-05	26	10	0.38	1	1.36E-07
	11,400	5.26E-06	1.68E-04	3.94E-05	5.20E-04	319	7.5	0.23	1.26	7.70E-07
	9,980	7.27E-04	1.79E-02	1.03E-02	2.30E-02	24.6	14	0.58	1.3	8.45E-04
	A 9,650	3.66E-04	1.34E-02	5.75E-03	1.48E-02	36.6	16	0.43	1.1	5.48E-04
	B 9,650	**5.57E-03**	**1.20E-01**	**1.00E-01**	**1.31E-01**	21.5	18	0.83	1.1	1.47E-02
	9,320	1.08E-03	3.42E-02	1.80E-02	3.43E-02	31.5	17	0.52	1	2.24E-03
	9,000	3.67E-04	1.90E-02	1.16E-02	2.66E-02	51.8	32	0.61	1.4	9.26E-04

Table 2 Summary of turbulence measurements for 6 August 1999.

Altitude	u w	w^2	g	Z RI (w θ)	< >/C_T^2	q3/ε	C_T^2/ C_T^2 max	Integral Scale Ratio
9000	-40	0.465	3.48	1.6	2.6 km	629 m	15	3.3
9320	-9	0.682	3.48	2.4	0.94 km	201 m	5	1.4
B 9650	-6.7	0.418	3.48	1.4	0.75 km	500 m	1	1.3
9980	-16	0.668	3.48	2.3	1.7 km	460 m	7.7	2.4
11400	0.8	2.26	3.48	7.8	25 km	6.6 km	1060	11.3
12200	13	0.8	3.48	2.8	288 km	82 km	2800	2.3

APPENDIX B: Flight and Altitude Plots

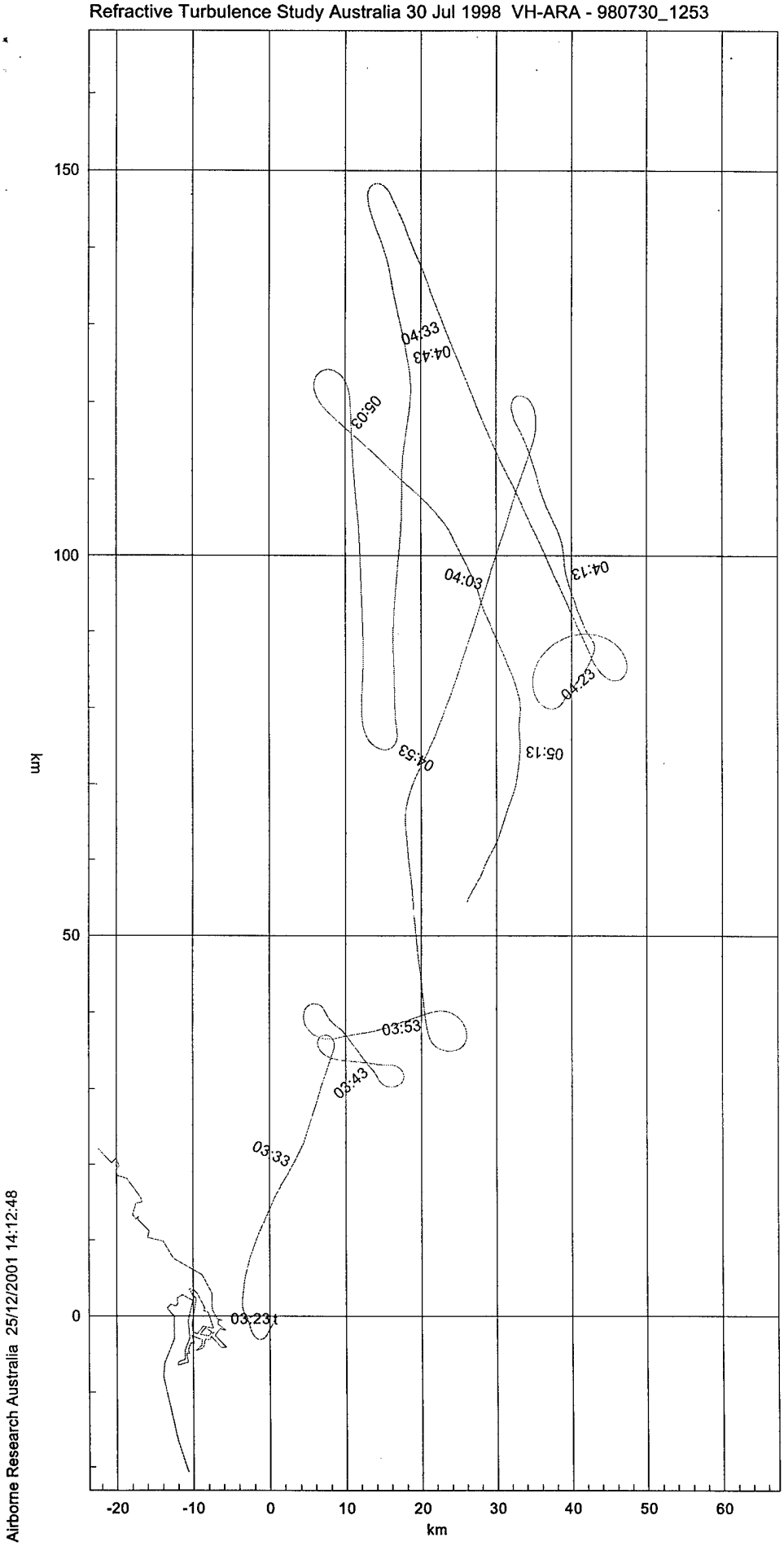
Refractive Turbulence Study Australia 30 Jul 1998 VH-ARA - 980730_1253
150
100
50
0
km
04:33
04:43
05:03
04:03
04:13
04:23
04:53
05:13
03:53
03:43
03:33
03:23
-20
-10
0
10
20
30
40
50
60
km
Airborne Research Australia 25/12/2001 14:12:48

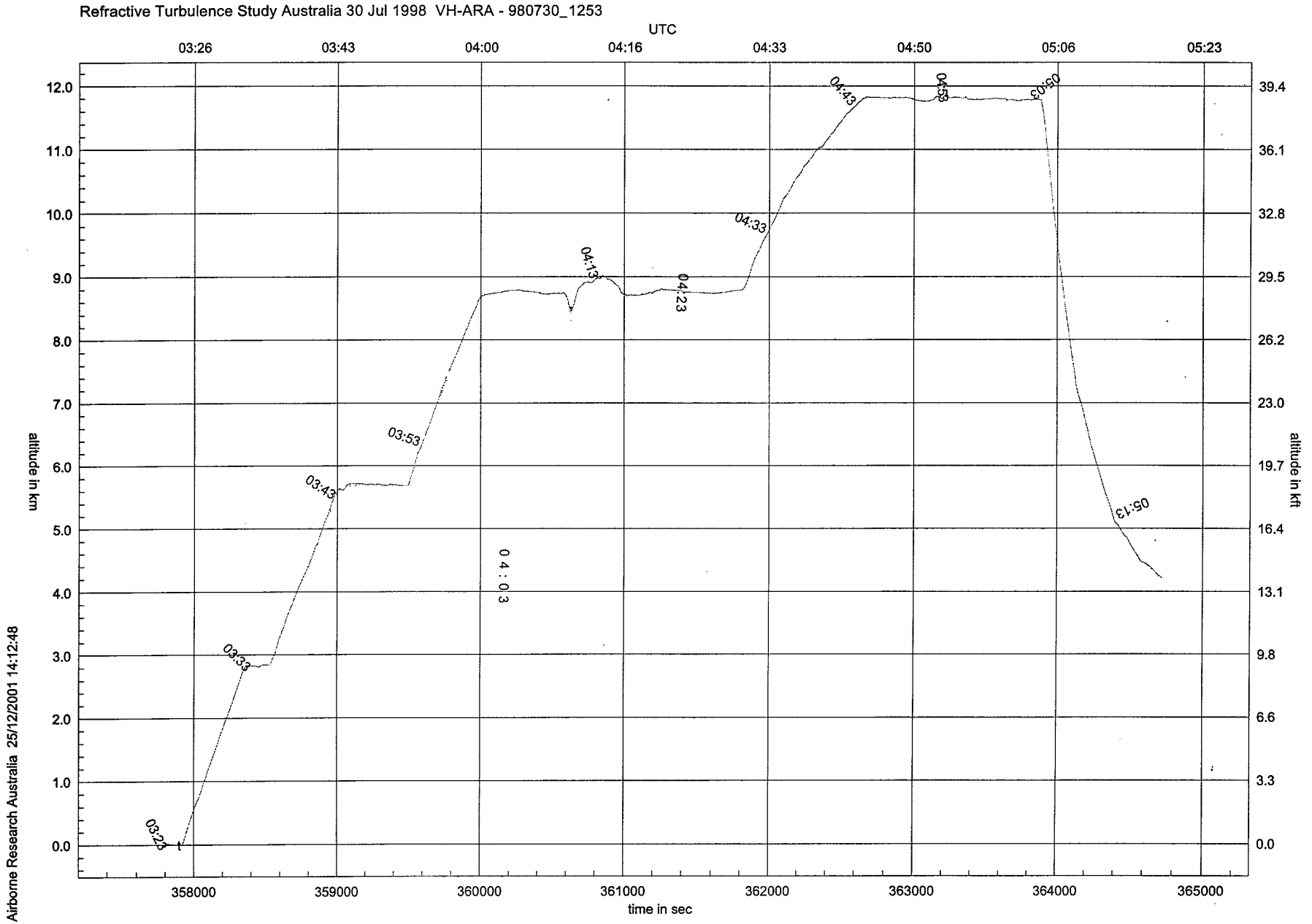
Refractive Turbulence Study Australia 30 Jul 1998 VH-ARA - 980730_1253
UTC
03:26
03:43
04:00
04:16
04:33
04:50
05:06
05:23
12.0
11.0
10.0
9.0
8.0
7.0
6.0
5.0
4.0
3.0
2.0
1.0
0.0
39.4
36.1
32.8
29.5
26.2
23.0
19.7
16.4
13.1
9.8
6.6
3.3
0.0
altitude in km
altitude in kft
03:23
03:33
03:43
03:53
04:13
04:23
04:33
04:43
04:53
05:03
05:13
04:03
358000
359000
360000
361000
362000
363000
364000
365000
time in sec
Airborne Research Australia 25/12/2001 14:12:48

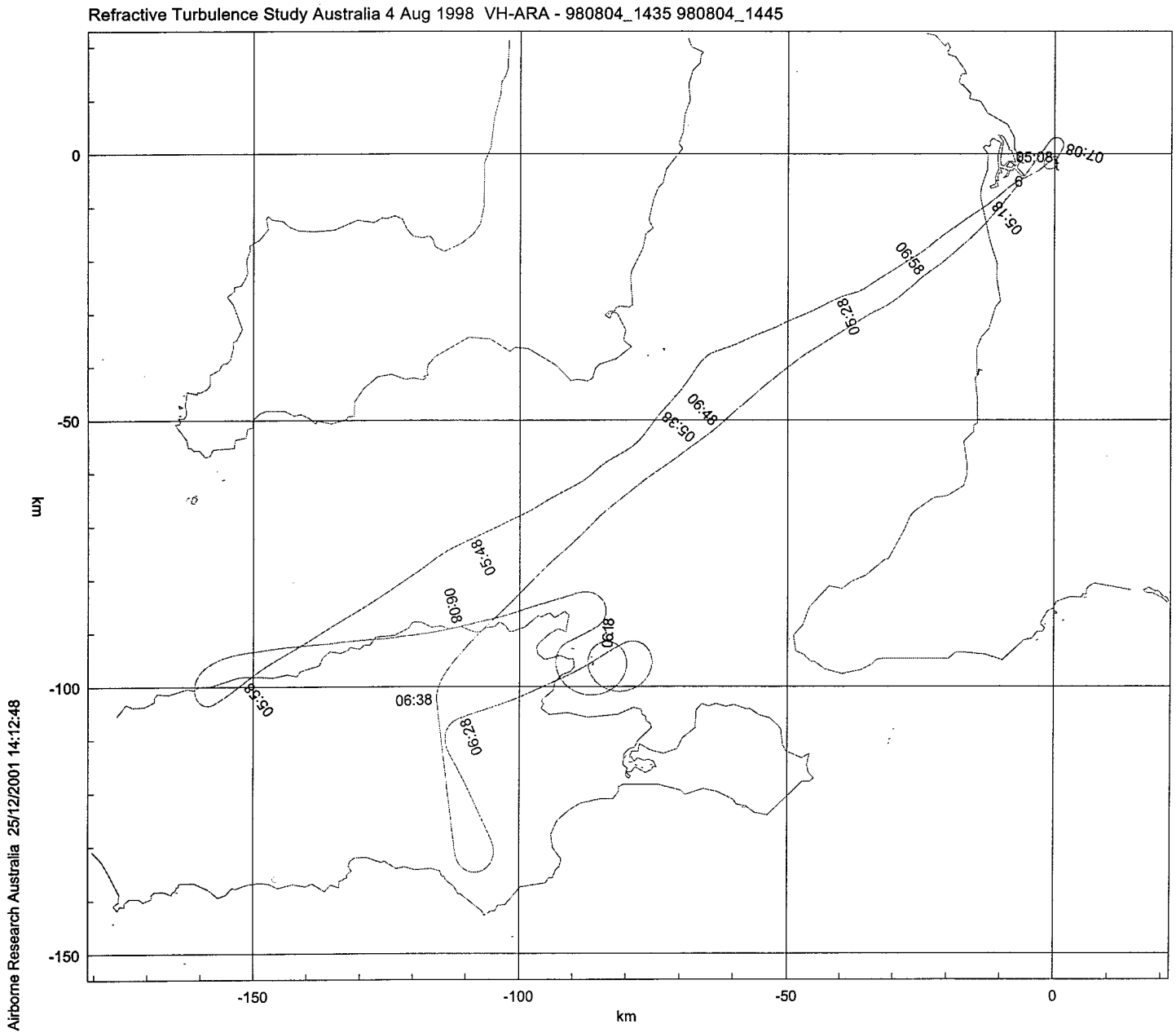
Refractive Turbulence Study Australia 4 Aug 1998 VH-ARA - 980804_1435 980804_1445
0
-50
-100
-150
km
-150
-100
-50
0
km
Airborne Research Australia 25/12/2001 14:12:48
07:08
05:08
05:18
05:28
05:38
05:48
06:38
06:28
06:18
06:08

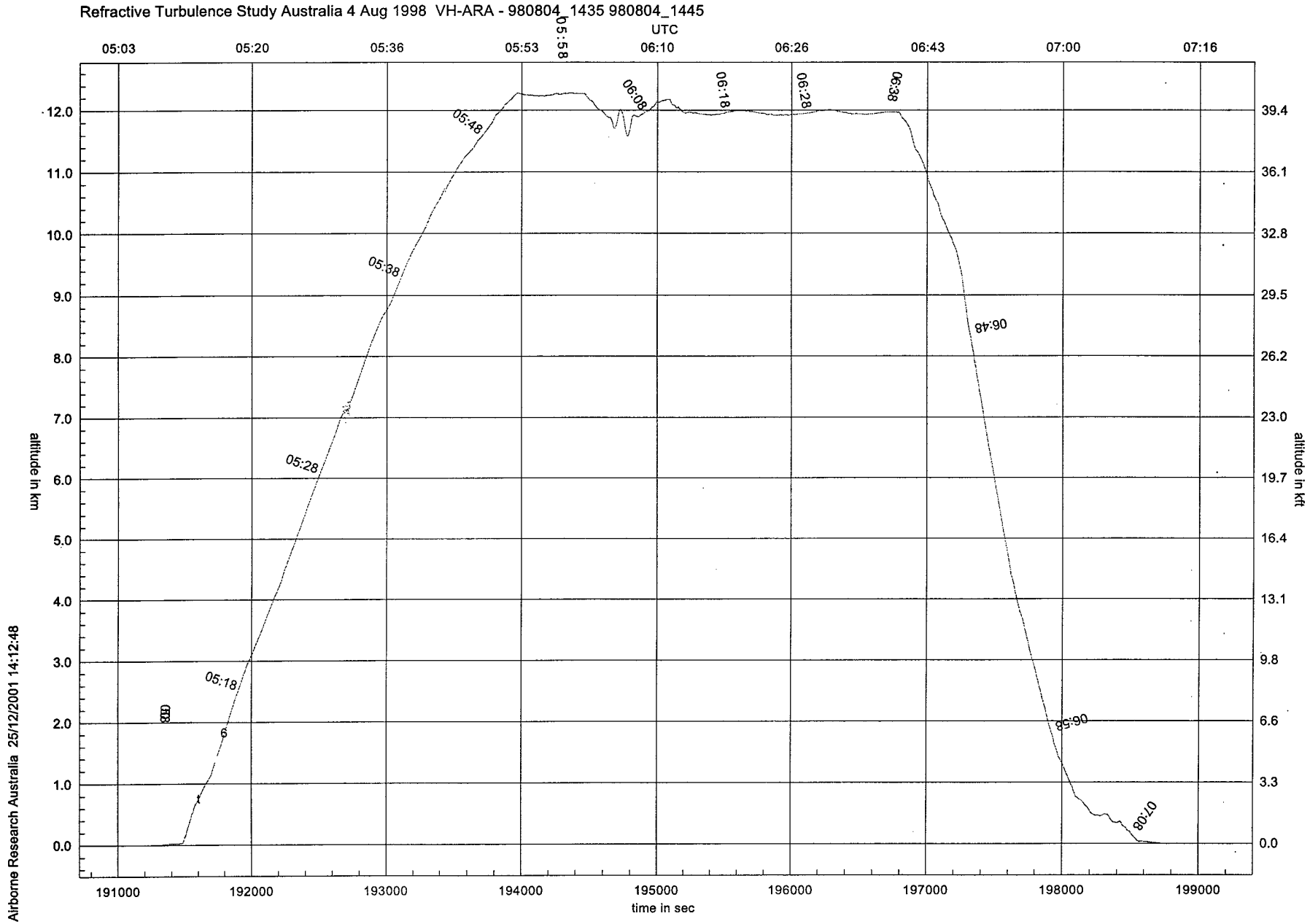
Refractive Turbulence Study Australia 4 Aug 1998 VH-ARA - 980804_1435 980804_1445
UTC
05:03
05:20
05:36
05:53
05:58
06:10
06:26
06:43
07:00
07:16
05:48
06:08
06:18
06:28
06:38
05:38
06:48
05:28
05:18
06:58
07:08
12.0
11.0
10.0
9.0
8.0
7.0
6.0
5.0
4.0
3.0
2.0
1.0
0.0
39.4
36.1
32.8
29.5
26.2
23.0
19.7
16.4
13.1
9.8
6.6
3.3
0.0
altitude in km
altitude in kft
191000
192000
193000
194000
195000
196000
197000
198000
199000
time in sec
Airborne Research Australia 25/12/2001 14:12:48

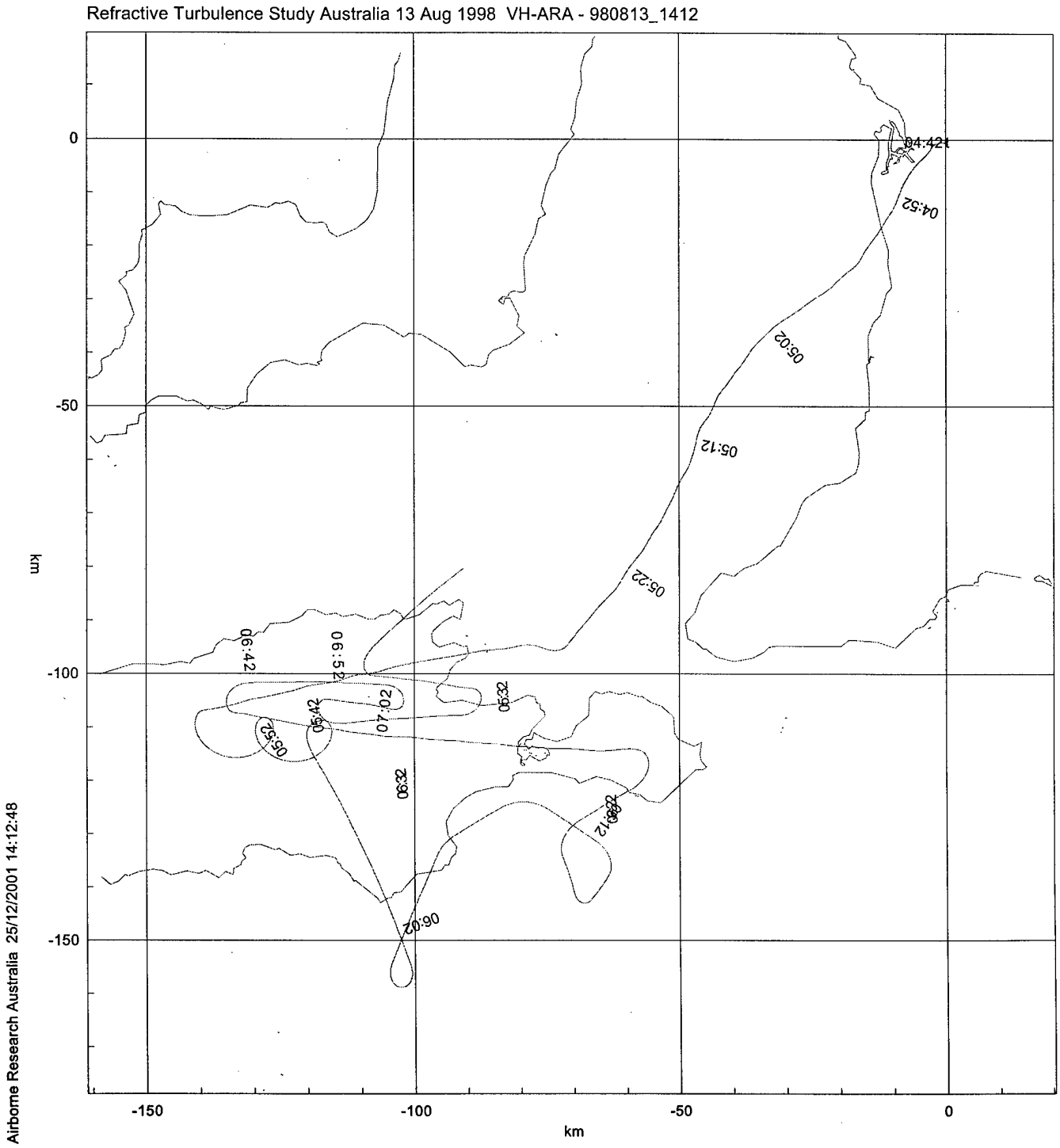
Refractive Turbulence Study Australia 13 Aug 1998 VH-ARA - 980813_1412
0
-50
-100
-150
km
-150
-100
-50
0
km
04:42
04:52
05:02
05:12
05:22
06:42
06:52
07:02
Airborne Research Australia 25/12/2001 14:12:48

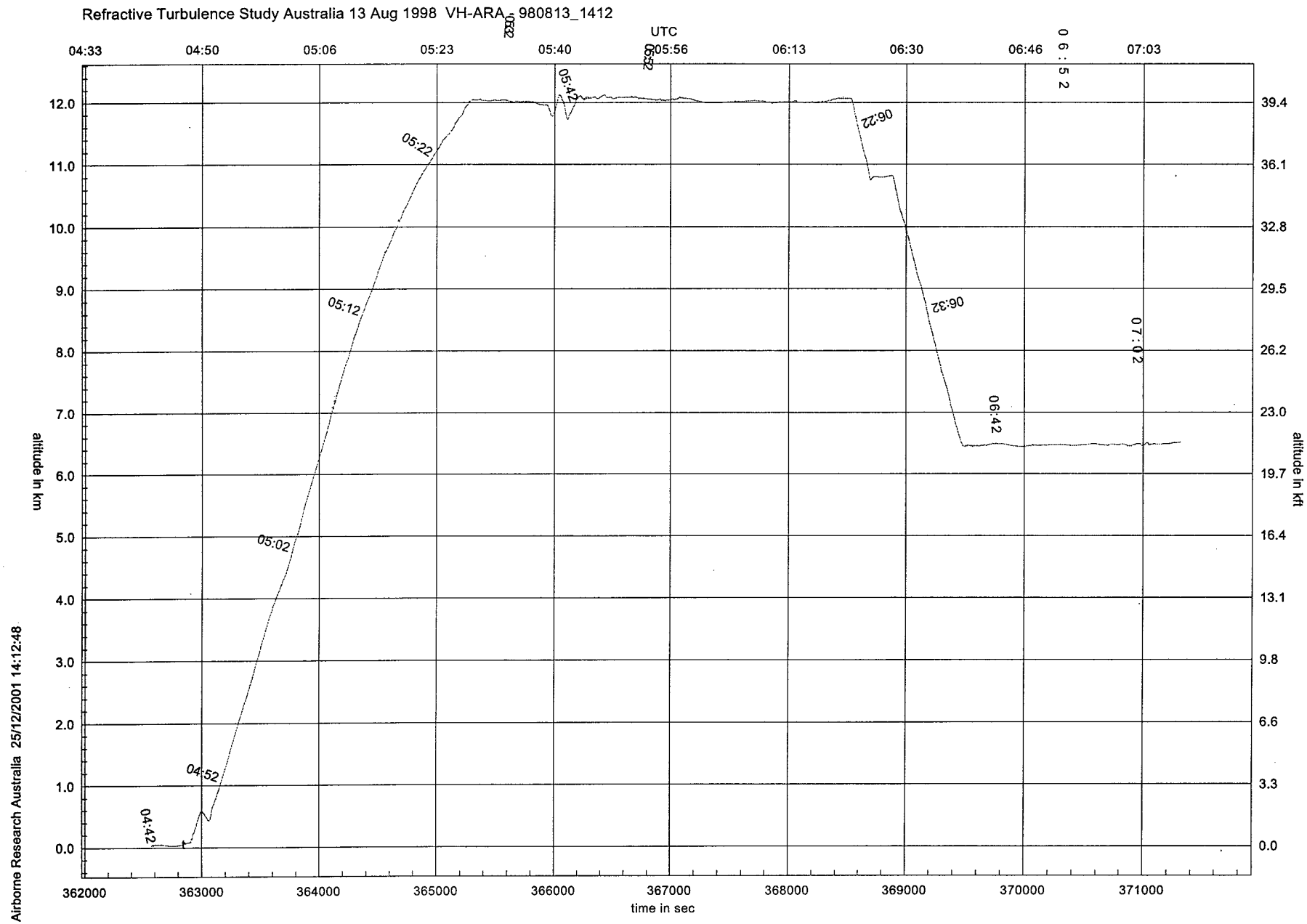
Refractive Turbulence Study Australia 13 Aug 1998 VH-ARA 980813_1412
UTC
04:33
04:50
05:06
05:23
05:40
05:56
06:13
06:30
06:46
07:03
05:32
05:52
06:52
07:02
05:42
06:22
06:32
06:42
05:22
05:12
05:02
04:52
04:42
12.0
11.0
10.0
9.0
8.0
7.0
6.0
5.0
4.0
3.0
2.0
1.0
0.0
39.4
36.1
32.8
29.5
26.2
23.0
19.7
16.4
13.1
9.8
6.6
3.3
0.0
altitude in km
altitude in kft
362000
363000
364000
365000
366000
367000
368000
369000
370000
371000
time in sec
Airborne Research Australia 25/12/2001 14:12:48

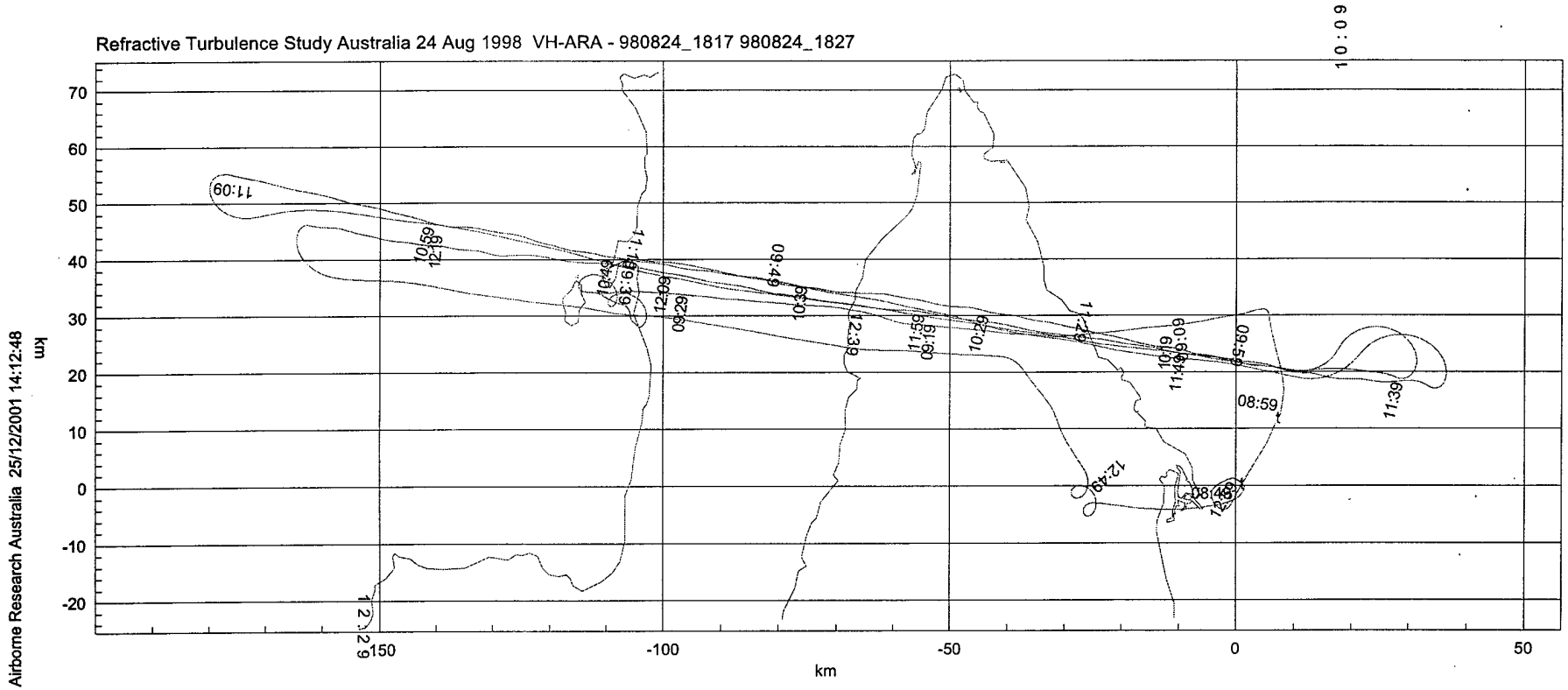
Refractive Turbulence Study Australia 24 Aug 1998 VH-ARA - 980824_1817 980824_1827
Airborne Research Australia 25/12/2001 14:12:48
km
km
70
60
50
40
30
20
10
0
-10
-20
-150
-100
-50
0
50
11:09
10:09
09:09
08:59
08:49
11:39
12:49
12:29

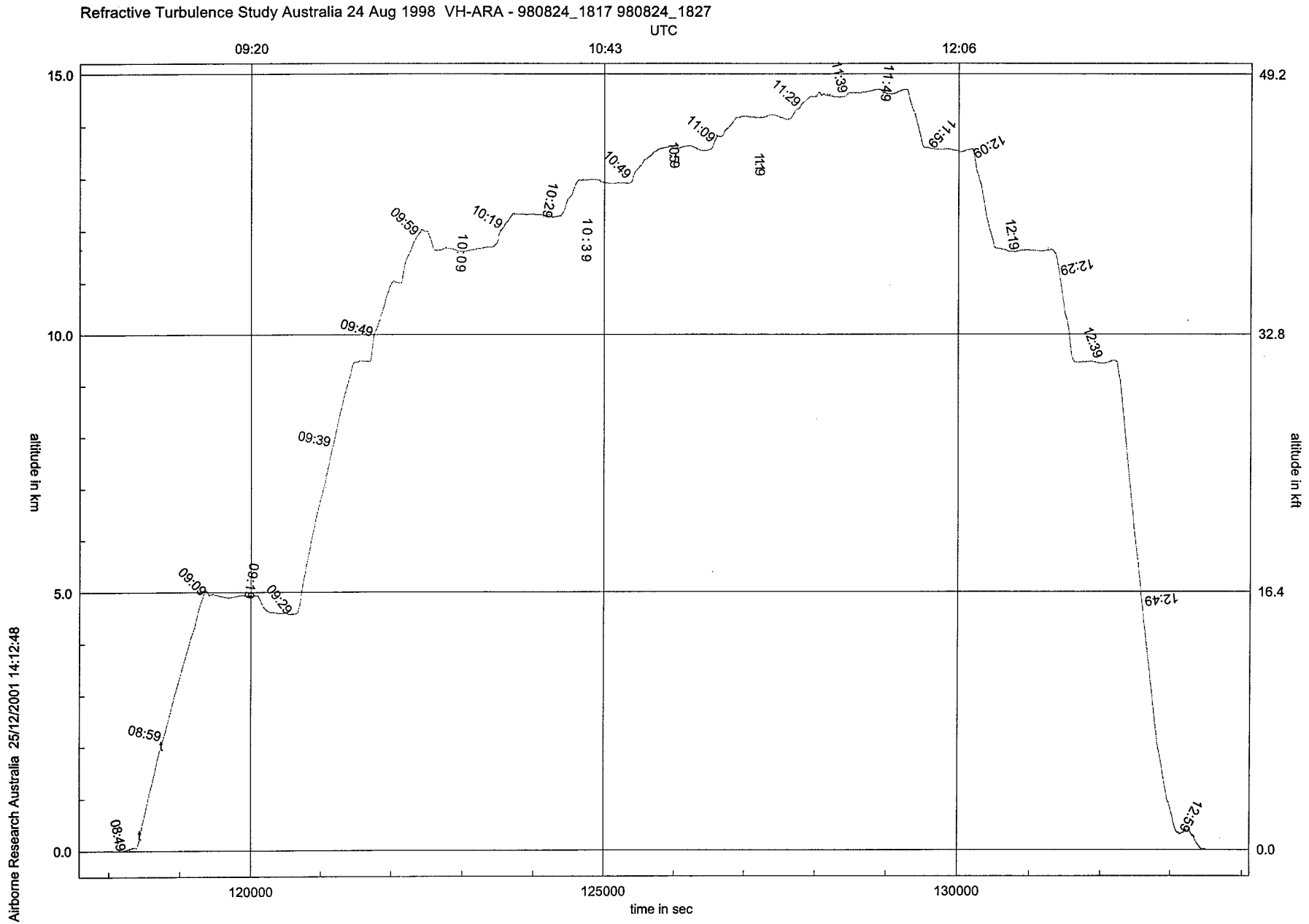
Refractive Turbulence Study Australia 24 Aug 1998 VH-ARA - 980824_1817 980824_1827
UTC
09:20
10:43
12:06
15.0
10.0
5.0
0.0
49.2
32.8
16.4
0.0
altitude in km
altitude in kft
Airborne Research Australia 25/12/2001 14:12:48
120000
125000
130000
time in sec
08:49
08:59
09:09
09:19
09:29
09:39
09:49
09:59
10:09
10:19
10:29
10:39
10:49
10:59
11:09
11:19
11:29
11:39
11:49
11:59
12:09
12:19
12:29
12:39
12:49
12:59

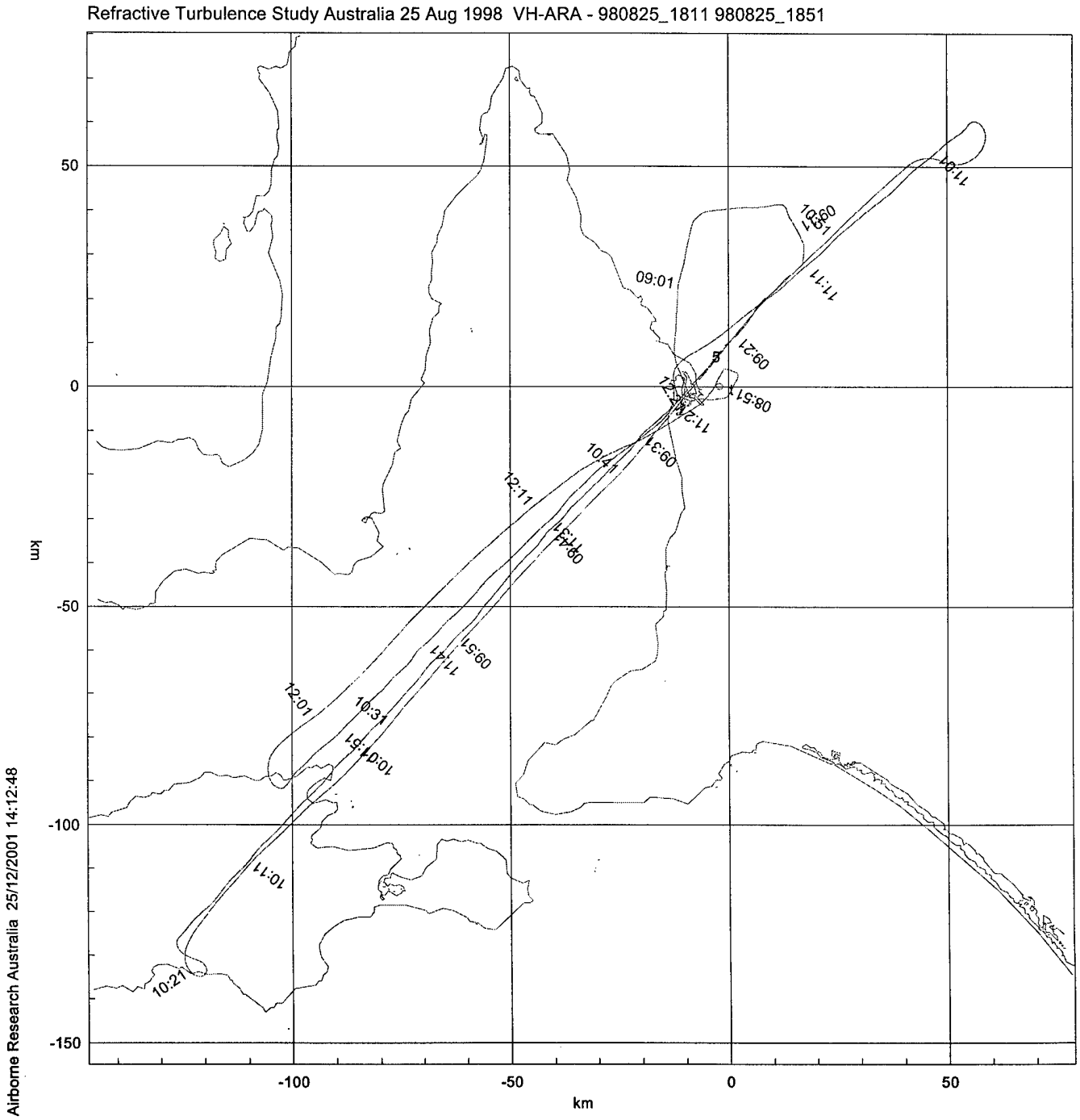
Refractive Turbulence Study Australia 25 Aug 1998 VH-ARA - 980825_1811 980825_1851
50
0
-50
-100
-150
km
-100
-50
0
50
km
09:01
10:31
11:01
11:11
09:21
08:51
11:21
09:31
10:41
12:11
09:41
09:51
11:41
09:51
12:01
10:31
10:01:51
10:11
10:21
Airborne Research Australia 25/12/2001 14:12:48

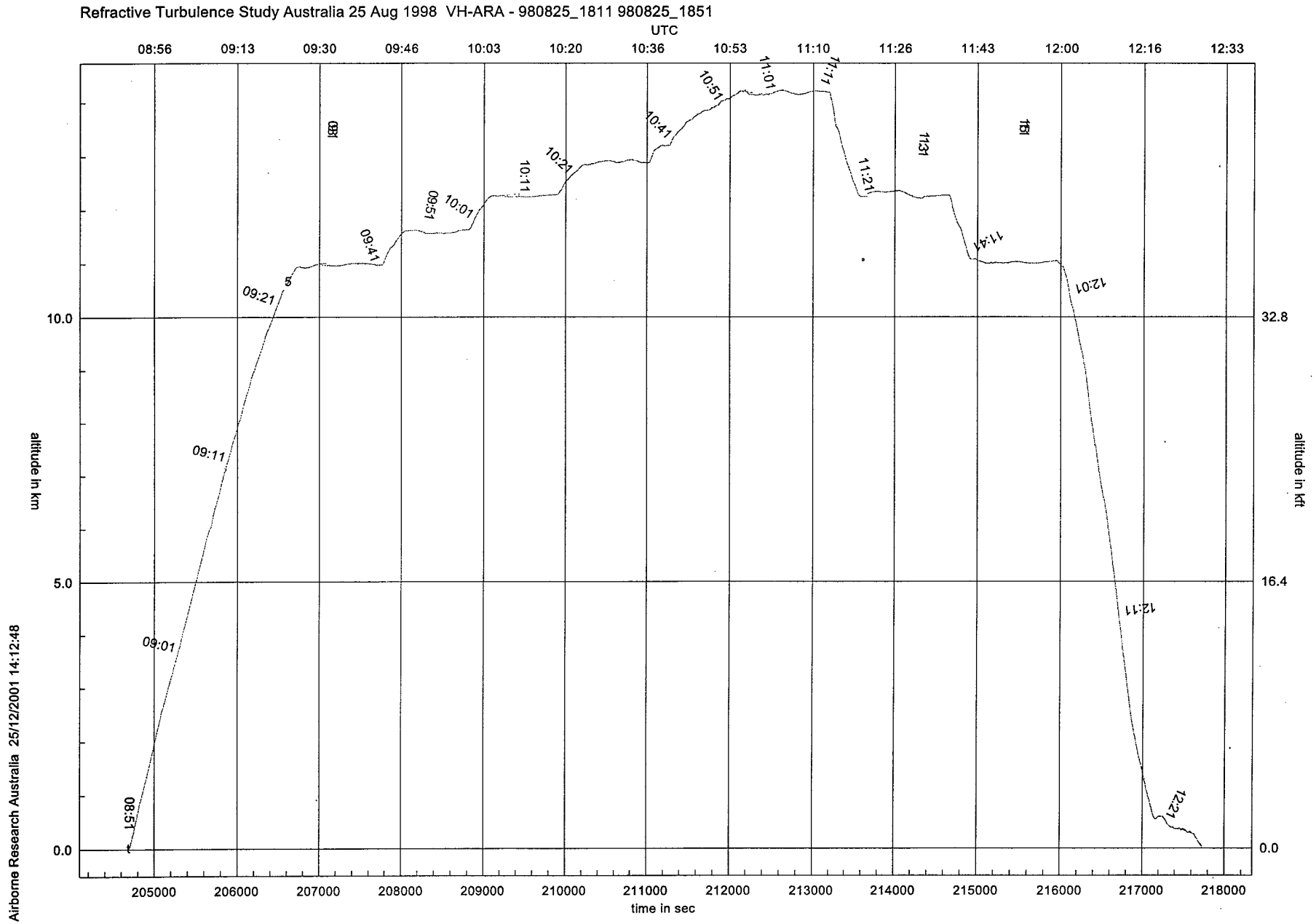
Refractive Turbulence Study Australia 25 Aug 1998 VH-ARA - 980825_1811 980825_1851
UTC
08:56
09:13
09:30
09:46
10:03
10:20
10:36
10:53
11:10
11:26
11:43
12:00
12:16
12:33
09:21
09:41
09:51
10:01
10:11
10:21
10:41
10:51
11:01
11:21
11:41
12:01
09:11
09:01
08:51
12:11
12:27
10.0
5.0
0.0
32.8
16.4
0.0
altitude in km
altitude in kft
205000
206000
207000
208000
209000
210000
211000
212000
213000
214000
215000
216000
217000
218000
time in sec
Airborne Research Australia 25/12/2001 14:12:48

Refractive Turbulence Study Australia 26 Aug 1998 VH-ARA - 980826_1742 980826_1806 980826_1859 980826_2000

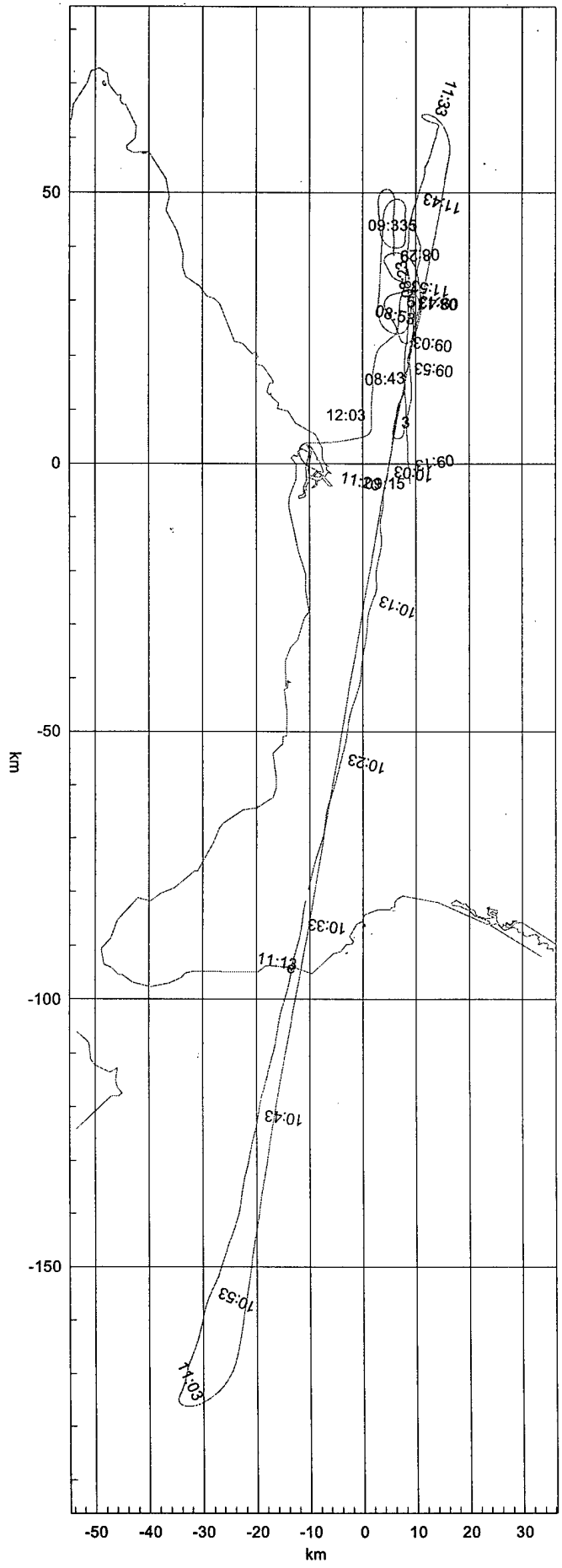

Airborne Research Australia 25/12/2001 14:12:48

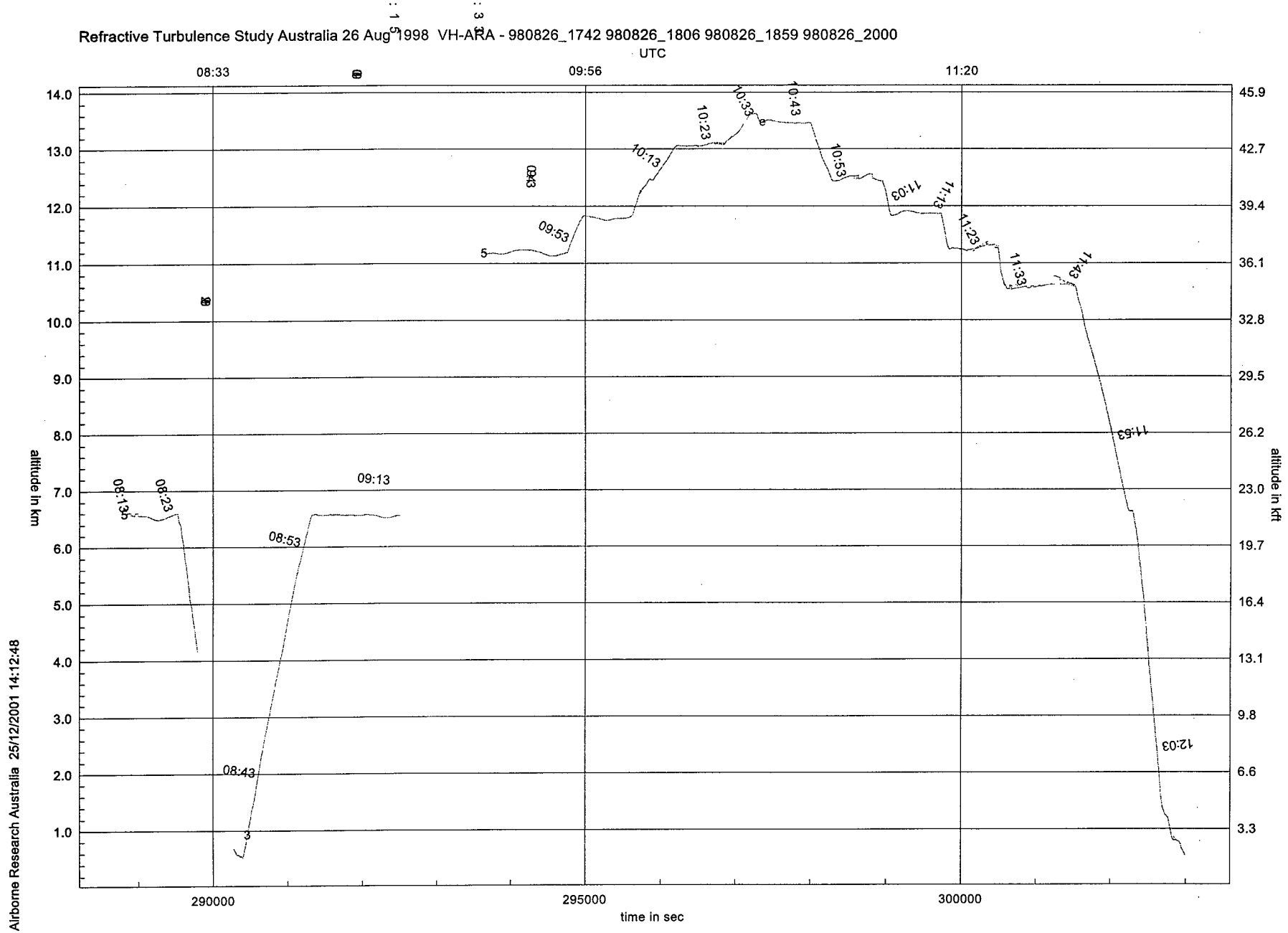
Refractive Turbulence Study Australia 26 Aug 1998 VH-ARA - 980826_1742 980826_1806 980826_1859 980826_2000
UTC
08:33
09:56
11:20
altitude in km
altitude in kft
time in sec
290000
295000
300000
Airborne Research Australia 25/12/2001 14:12:48

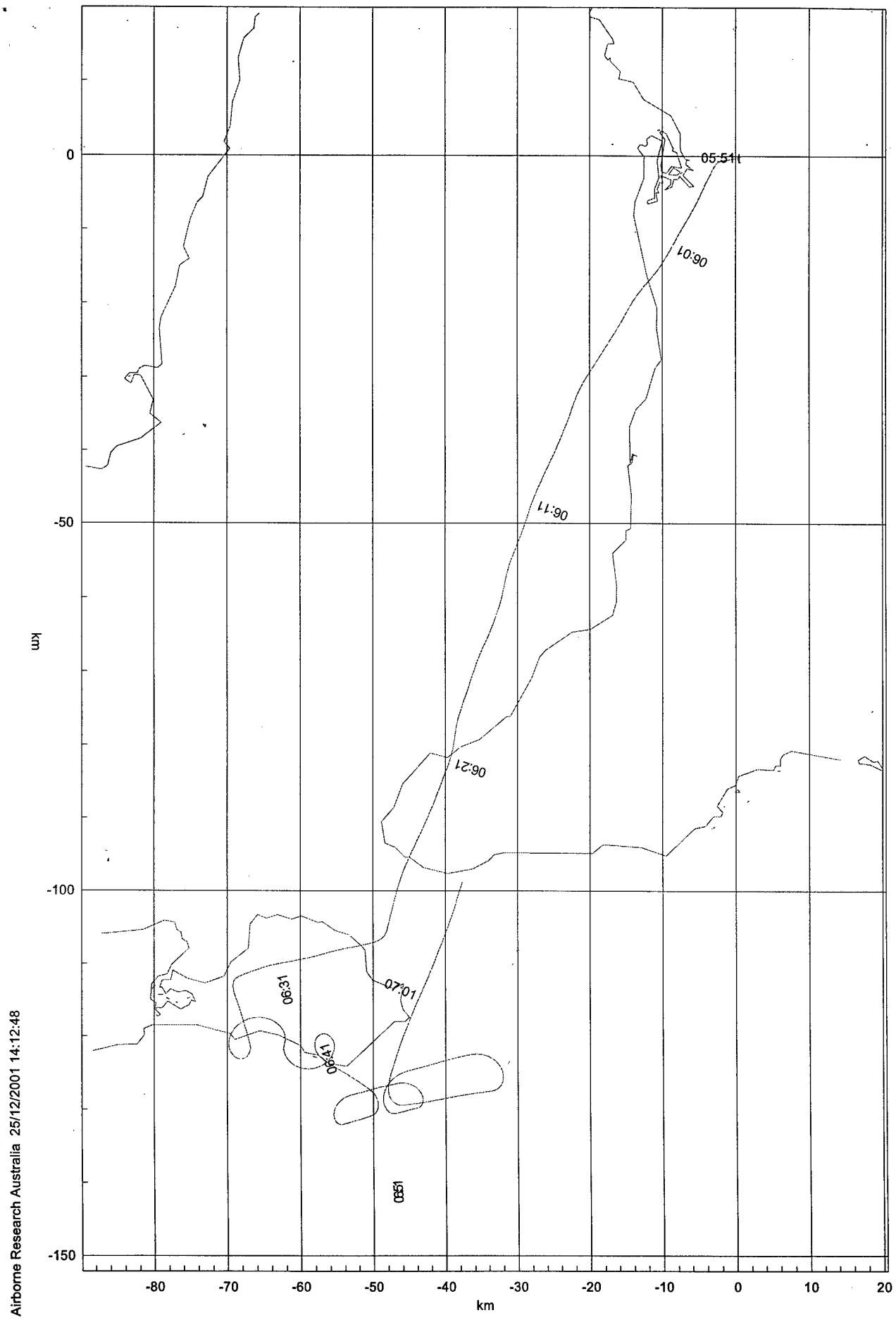
Refractive Turbulence Study Australia 31 Aug 1998 VH-ARA - 980831_1519
0
-50
-100
-150
km
-80
-70
-60
-50
-40
-30
-20
-10
0
10
20
km
05:51
06:07
06:11
06:21
06:31
06:41
07:01
Airborne Research Australia 25/12/2001 14:12:48

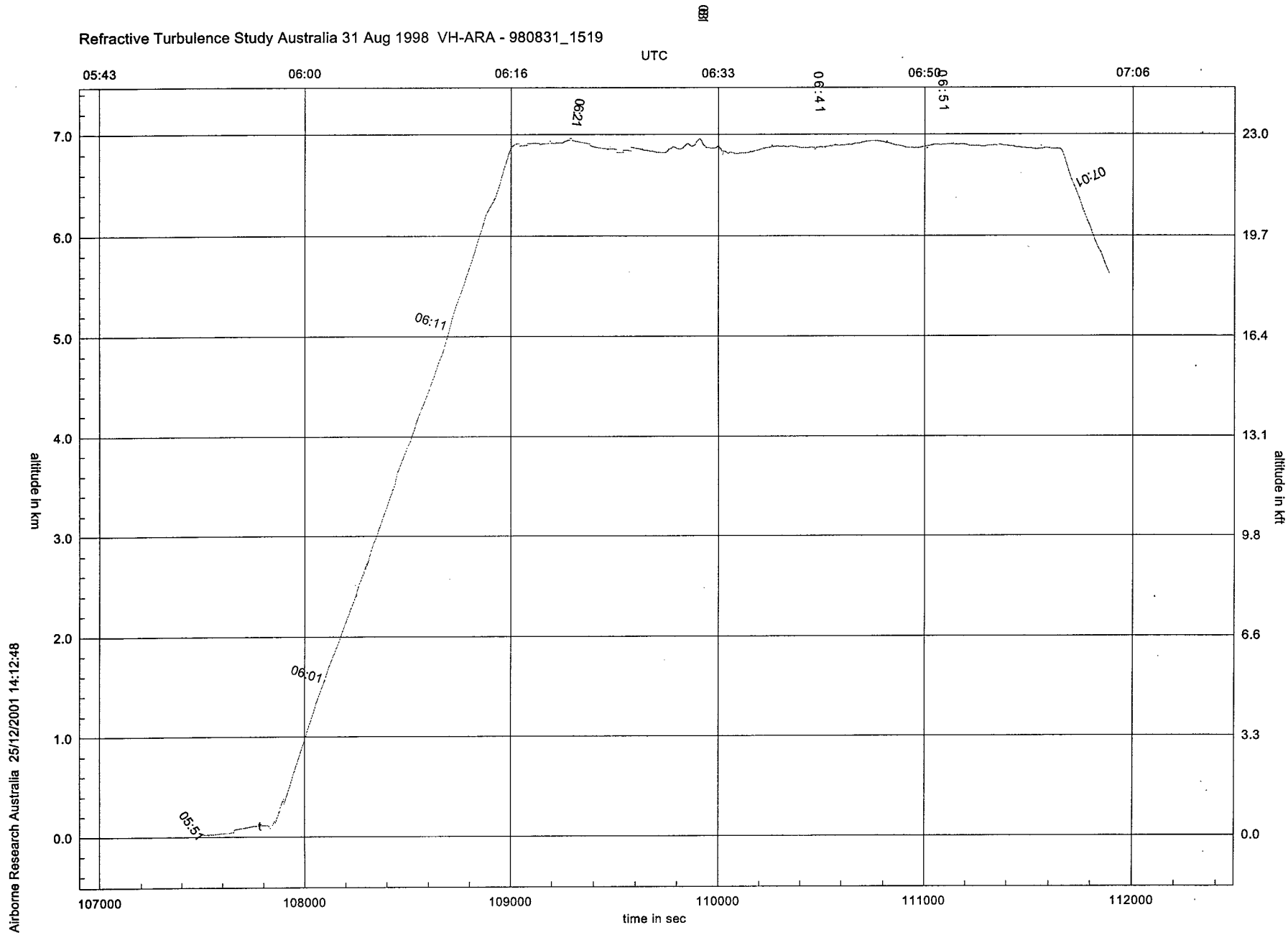
Refractive Turbulence Study Australia 31 Aug 1998 VH-ARA - 980831_1519
UTC
05:43
06:00
06:16
06:33
06:50
07:06
06:21
06:41
06:51
07:01
06:11
06:01
05:51
7.0
6.0
5.0
4.0
3.0
2.0
1.0
0.0
23.0
19.7
16.4
13.1
9.8
6.6
3.3
0.0
altitude in km
altitude in kft
107000
108000
109000
110000
111000
112000
time in sec
Airborne Research Australia 25/12/2001 14:12:48

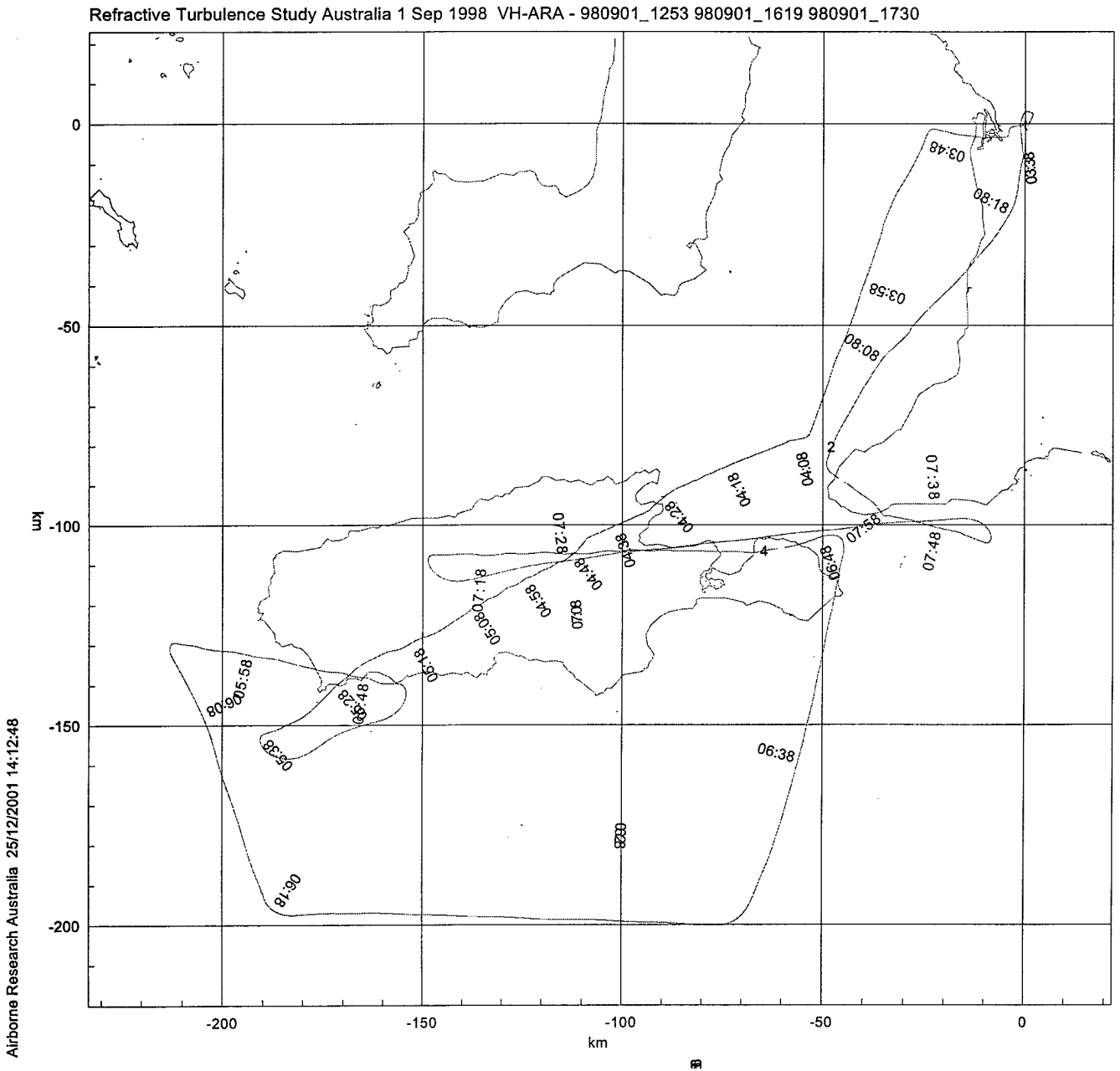
Refractive Turbulence Study Australia 1 Sep 1998 VH-ARA - 980901_1253 980901_1619 980901_1730
0
-50
-100
-150
-200
km
-200
-150
-100
-50
0
km
Airborne Research Australia 25/12/2001 14:12:48
03:48
03:58
04:08
04:18
04:28
04:38
04:48
04:58
05:08
05:18
05:28
05:38
05:48
05:58
06:08
06:18
06:28
06:38
06:48
07:28
07:38
08:08
08:18
08:38

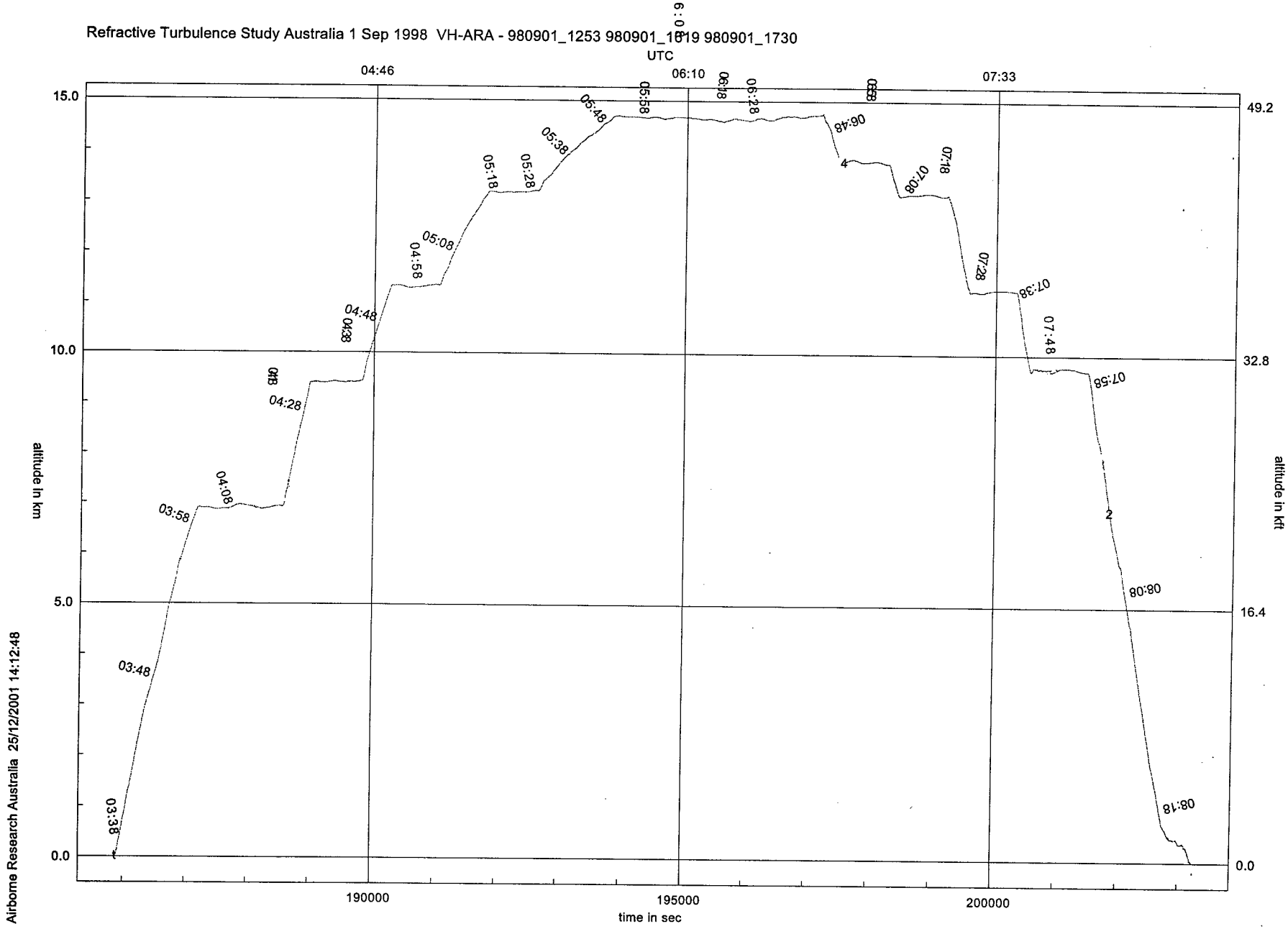
Refractive Turbulence Study Australia 1 Sep 1998 VH-ARA - 980901_1253 980901_1819 980901_1730
UTC
04:46
06:10
07:33
15.0
10.0
5.0
0.0
49.2
32.8
16.4
0.0
altitude in km
altitude in kft
Airborne Research Australia 25/12/2001 14:12:48
190000
195000
200000
time in sec

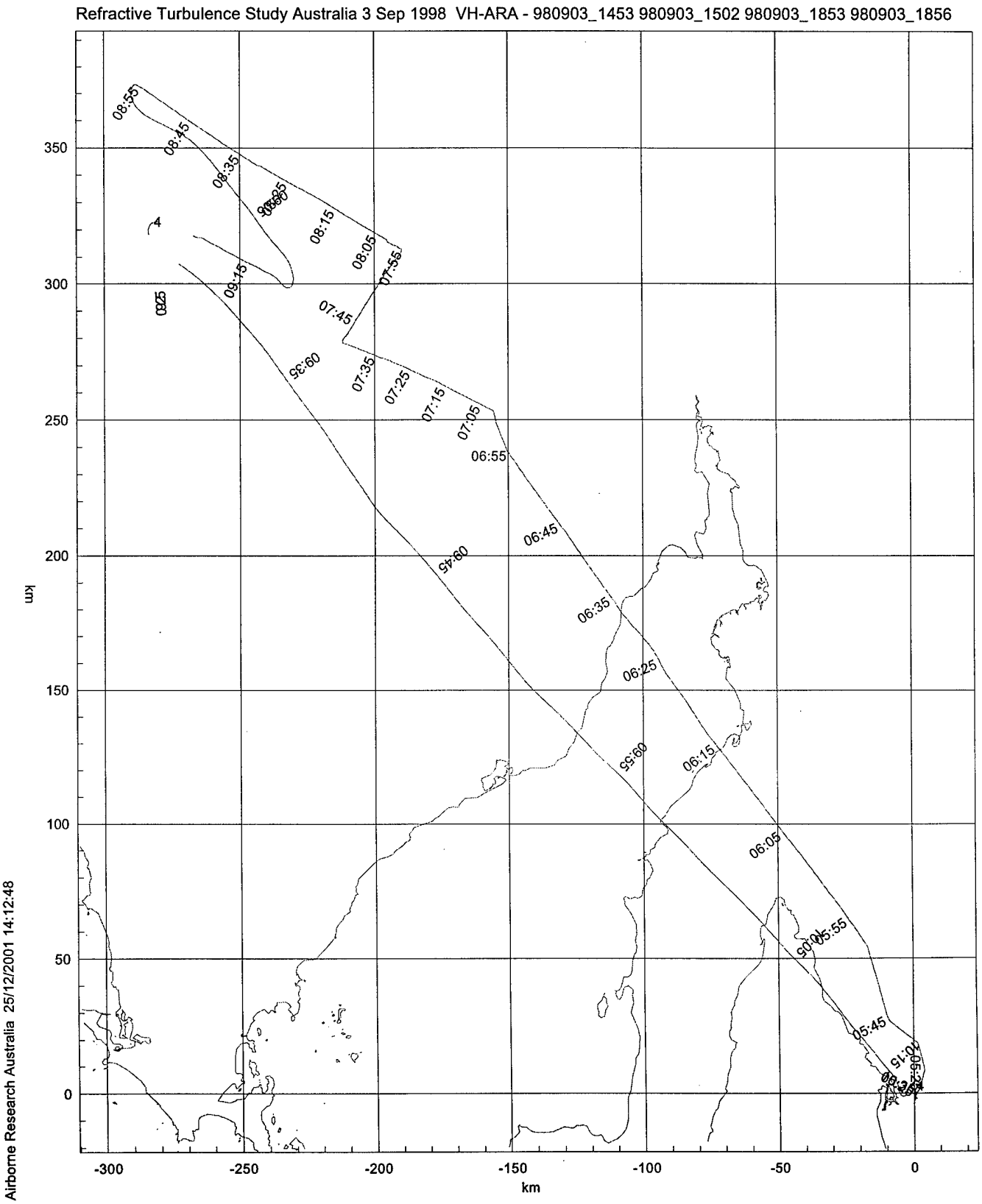
Refractive Turbulence Study Australia 3 Sep 1998 VH-ARA - 980903_1453 980903_1502 980903_1853 980903_1856
km
350
300
250
200
150
100
50
0
-300
-250
-200
-150
-100
-50
0
km
08:55
08:45
08:35
08:15
08:05
07:55
07:45
07:35
07:25
07:15
07:05
06:55
06:45
06:35
06:25
06:15
06:05
05:55
05:45
09:35
09:45
09:55
Airborne Research Australia 25/12/2001 14:12:48

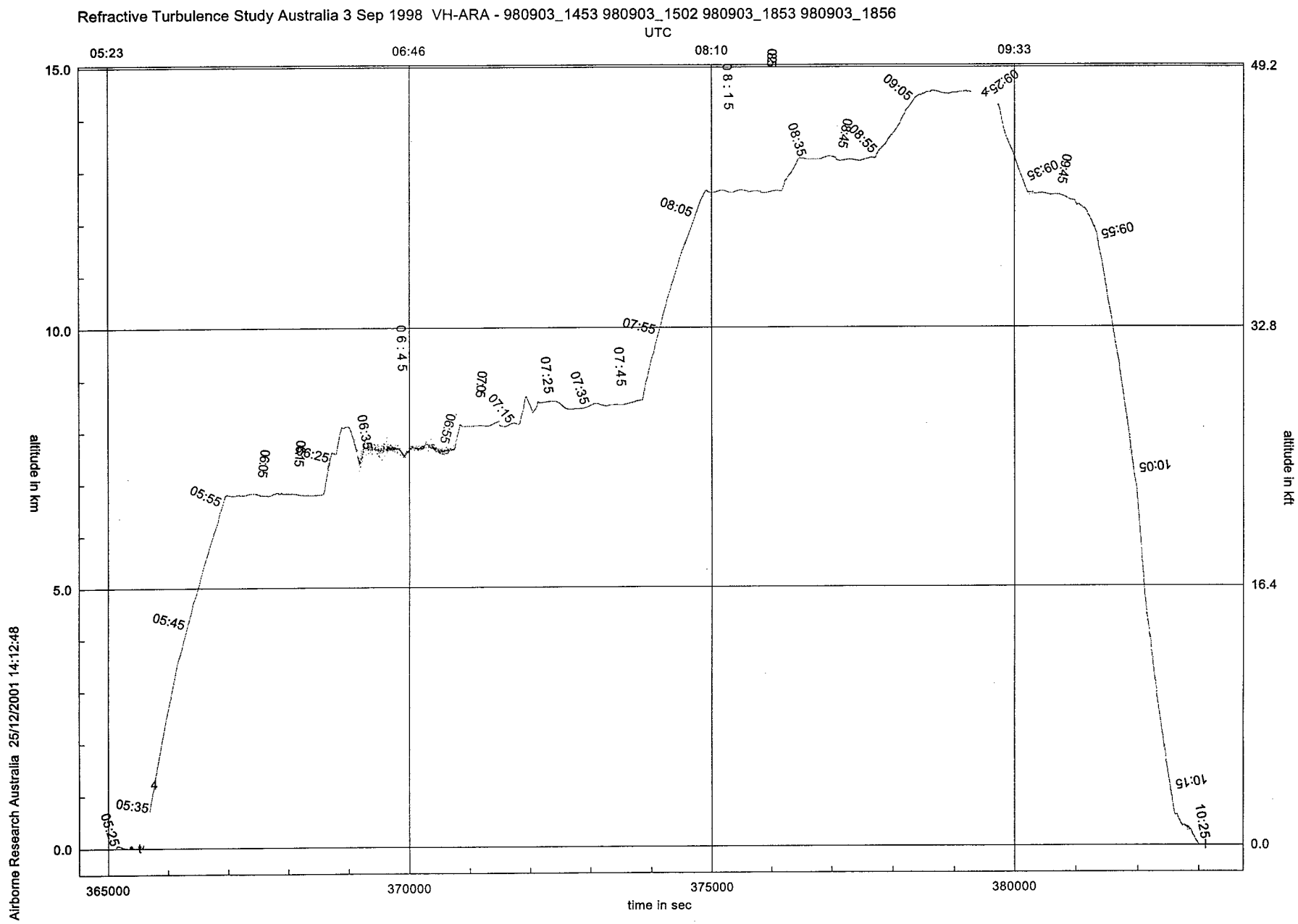
Refractive Turbulence Study Australia 3 Sep 1998 VH-ARA - 980903_1453 980903_1502 980903_1853 980903_1856
UTC
05:23
06:46
08:10
09:33
15.0
10.0
5.0
0.0
49.2
32.8
16.4
0.0
altitude in km
altitude in kft
time in sec
365000
370000
375000
380000
Airborne Research Australia 25/12/2001 14:12:48

Refractive Turbulence Study Australia 9 Sep 1998 VH-ARA - 980909_1353 980909_1407

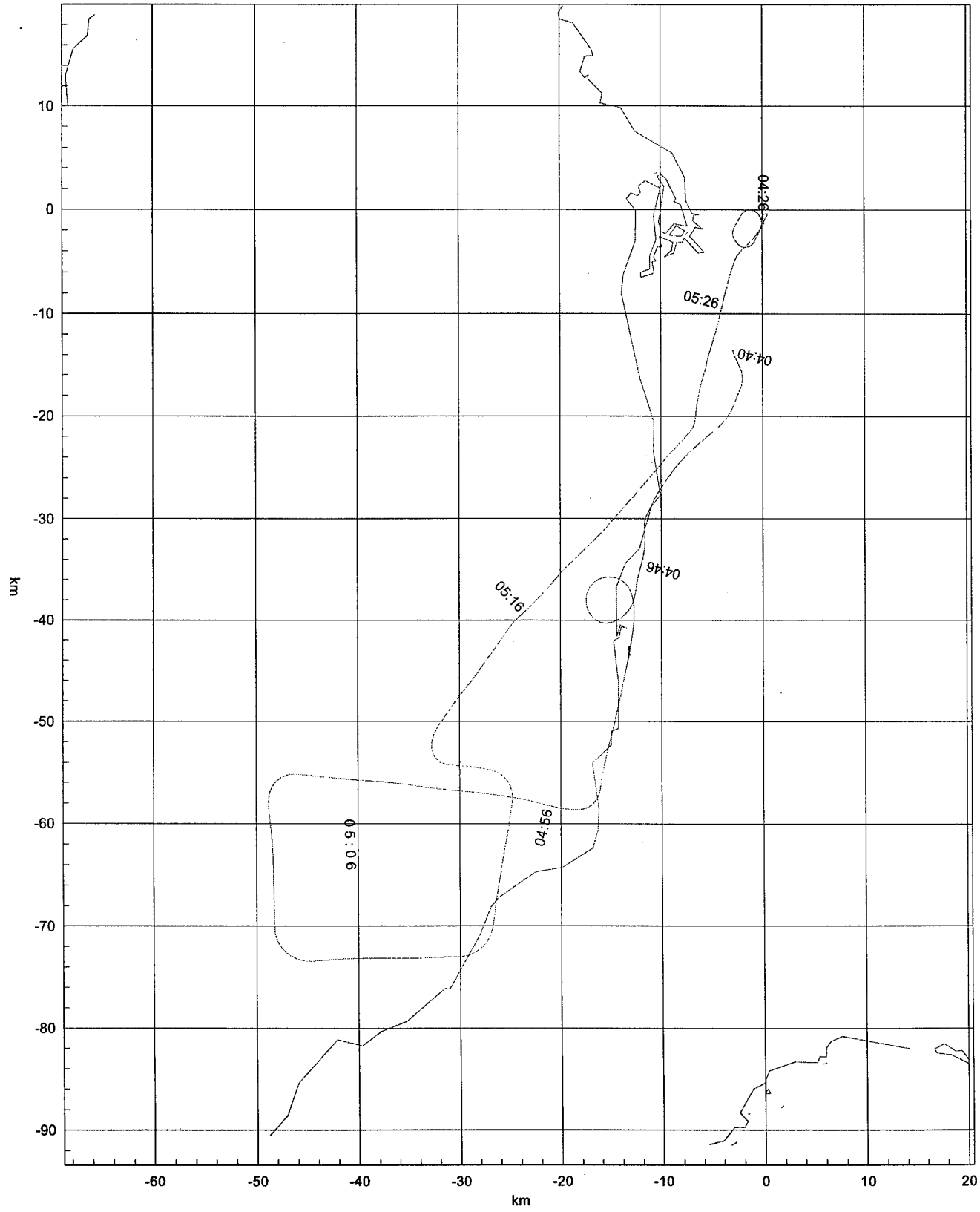

Airborne Research Australia 25/12/2001 14:12:48

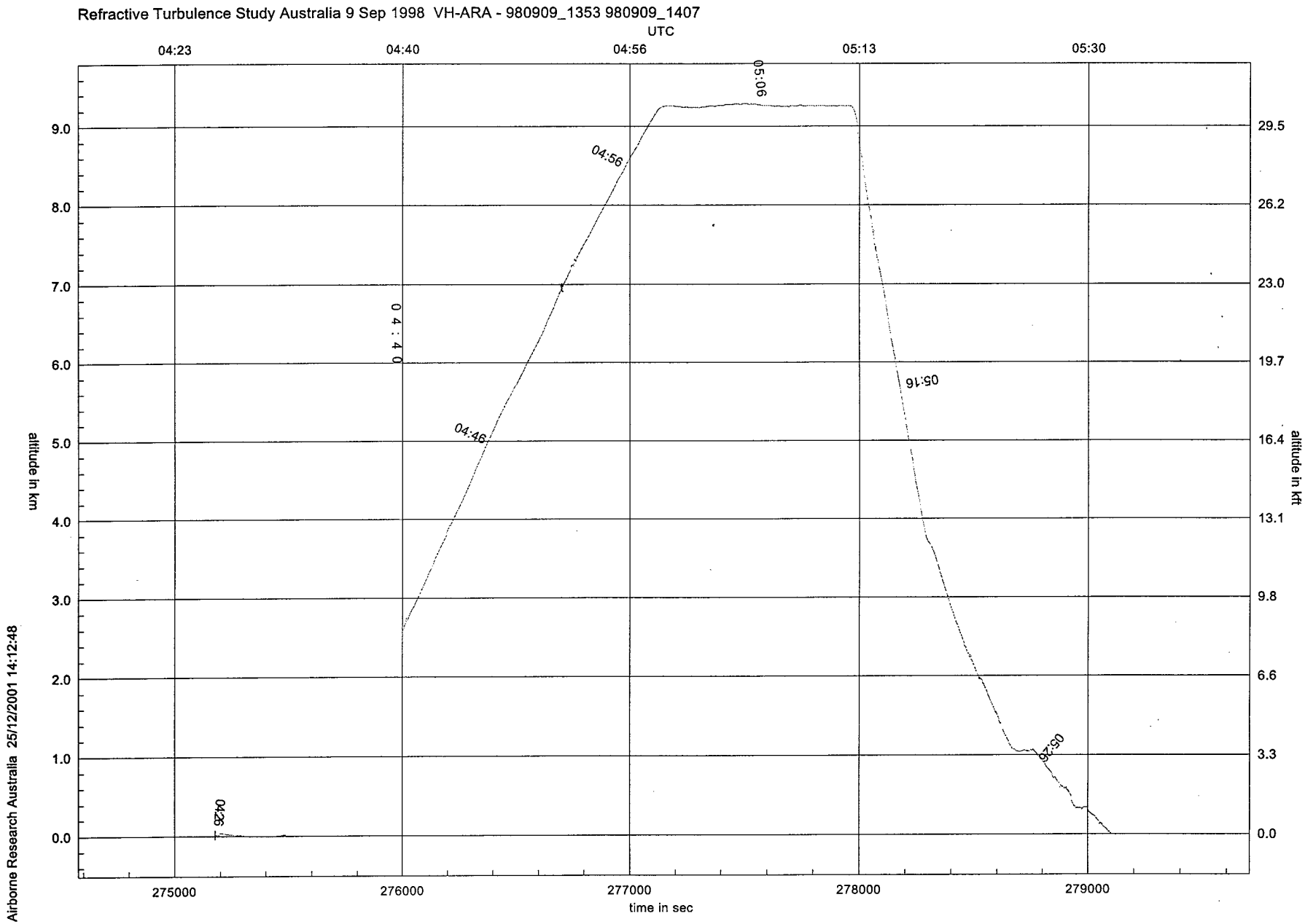
Refractive Turbulence Study Australia 9 Sep 1998 VH-ARA - 980909_1353 980909_1407
UTC
04:23
04:40
04:56
05:13
05:30
05:06
04:56
04:40
04:46
05:16
05:26
04:36
9.0
8.0
7.0
6.0
5.0
4.0
3.0
2.0
1.0
0.0
29.5
26.2
23.0
19.7
16.4
13.1
9.8
6.6
3.3
0.0
altitude in km
altitude in kft
275000
276000
277000
278000
279000
time in sec
Airborne Research Australia 25/12/2001 14:12:48

Refractive Turbulence Study Australia 6 Nov 1998 VH-ARA - 981106_1509

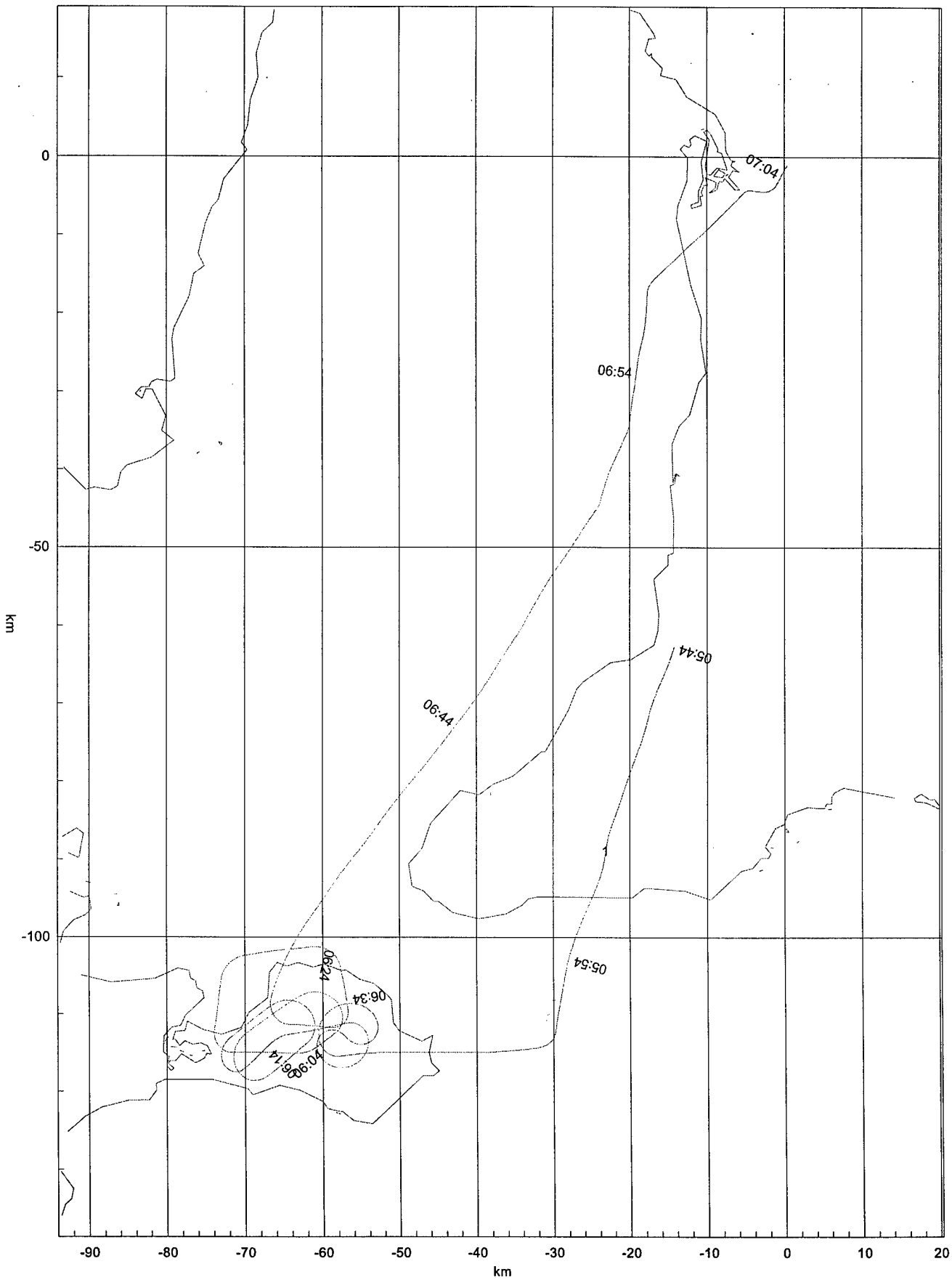

Airborne Research Australia 25/12/2001 14:12:48

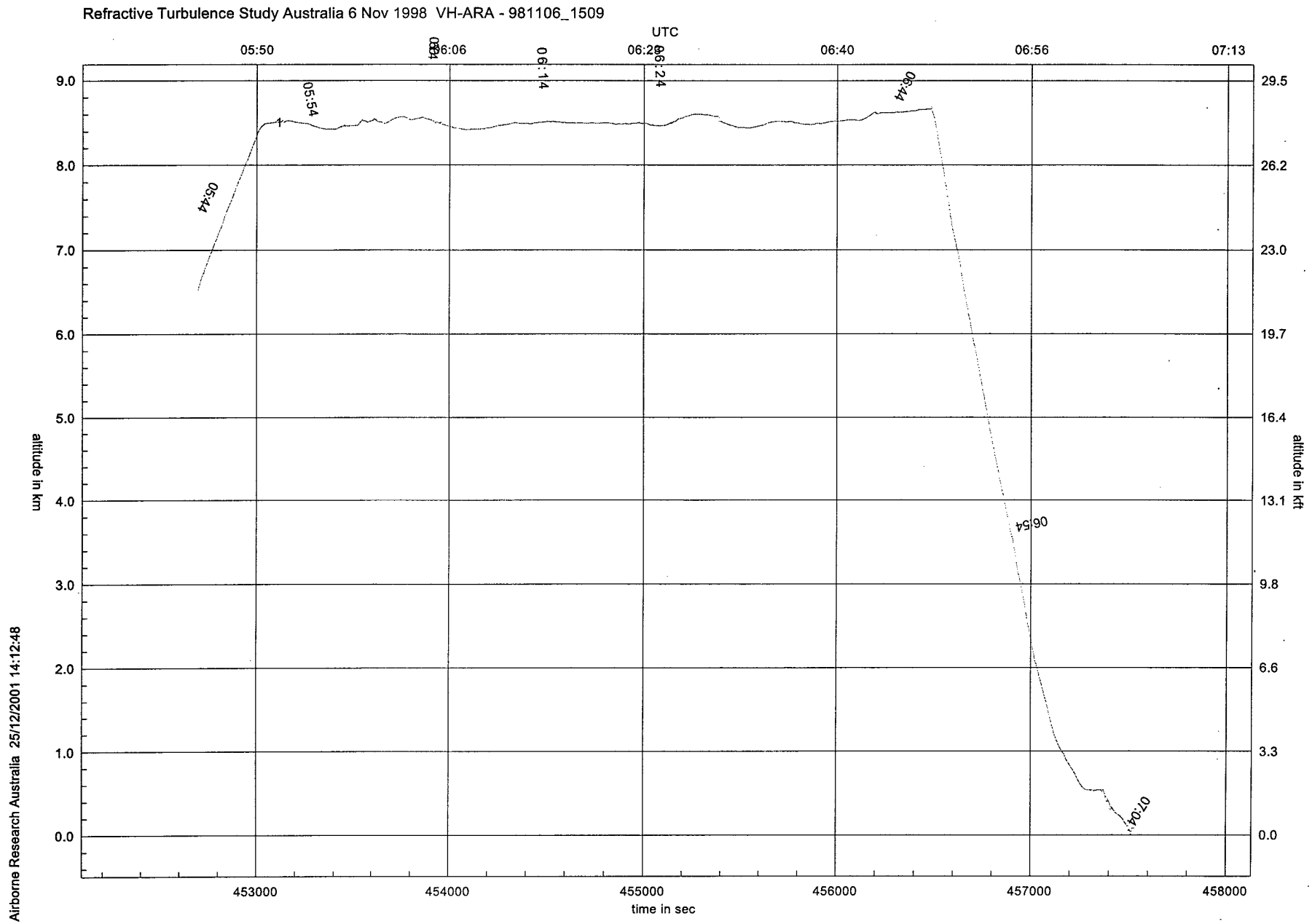
Refractive Turbulence Study Australia 6 Nov 1998 VH-ARA - 981106_1509
UTC
05:50
06:06
06:14
06:24
06:40
06:56
07:13
05:44
05:54
06:44
06:54
07:04
9.0
8.0
7.0
6.0
5.0
4.0
3.0
2.0
1.0
0.0
29.5
26.2
23.0
19.7
16.4
13.1
9.8
6.6
3.3
0.0
altitude in km
altitude in kft
453000
454000
455000
456000
457000
458000
time in sec
Airborne Research Australia 25/12/2001 14:12:48

Refractive Turbulence Study Japan 8 Feb 1999 VH-ARA - 990208_1113 990208_1455 990208_1502 990208_1600

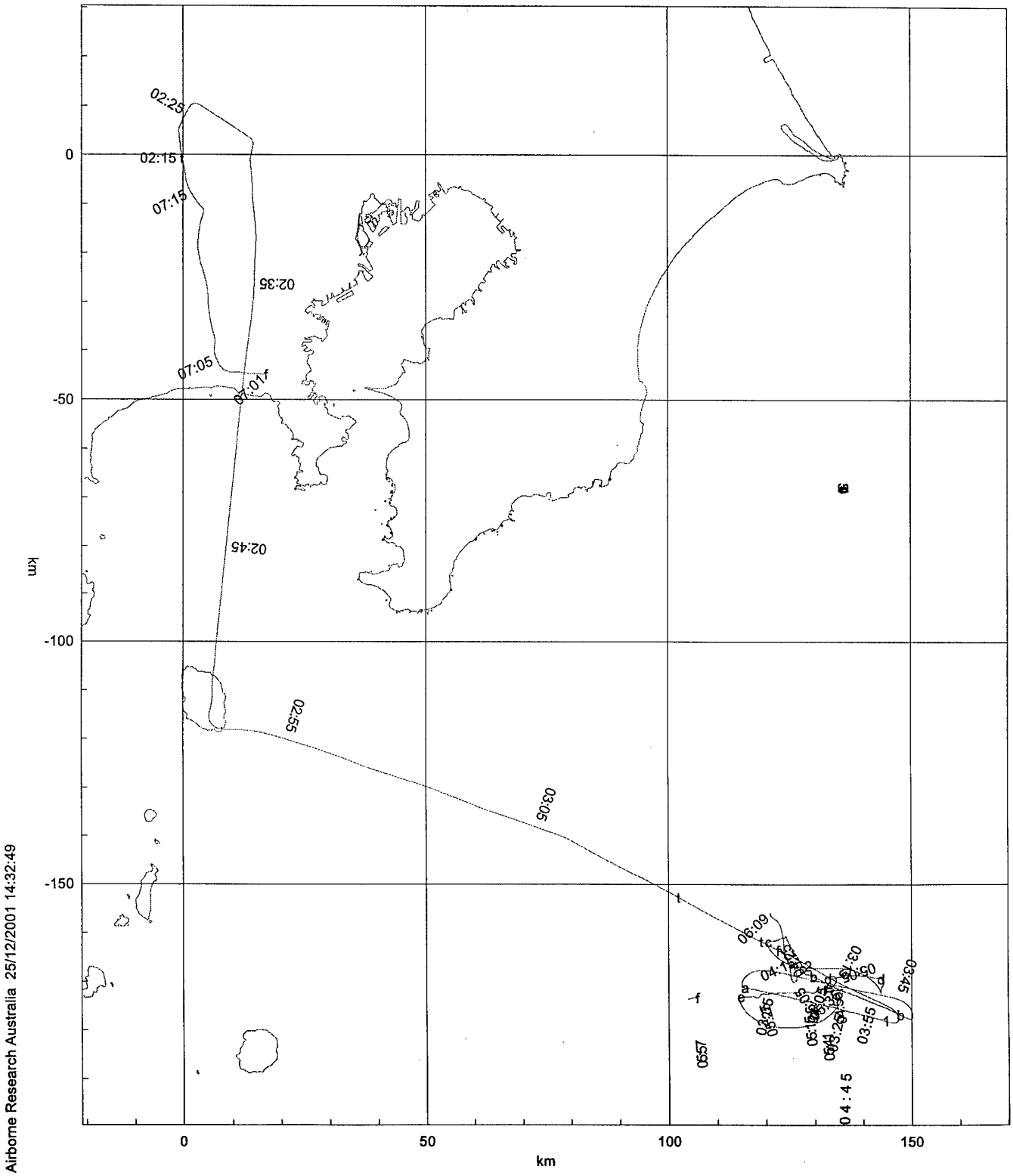

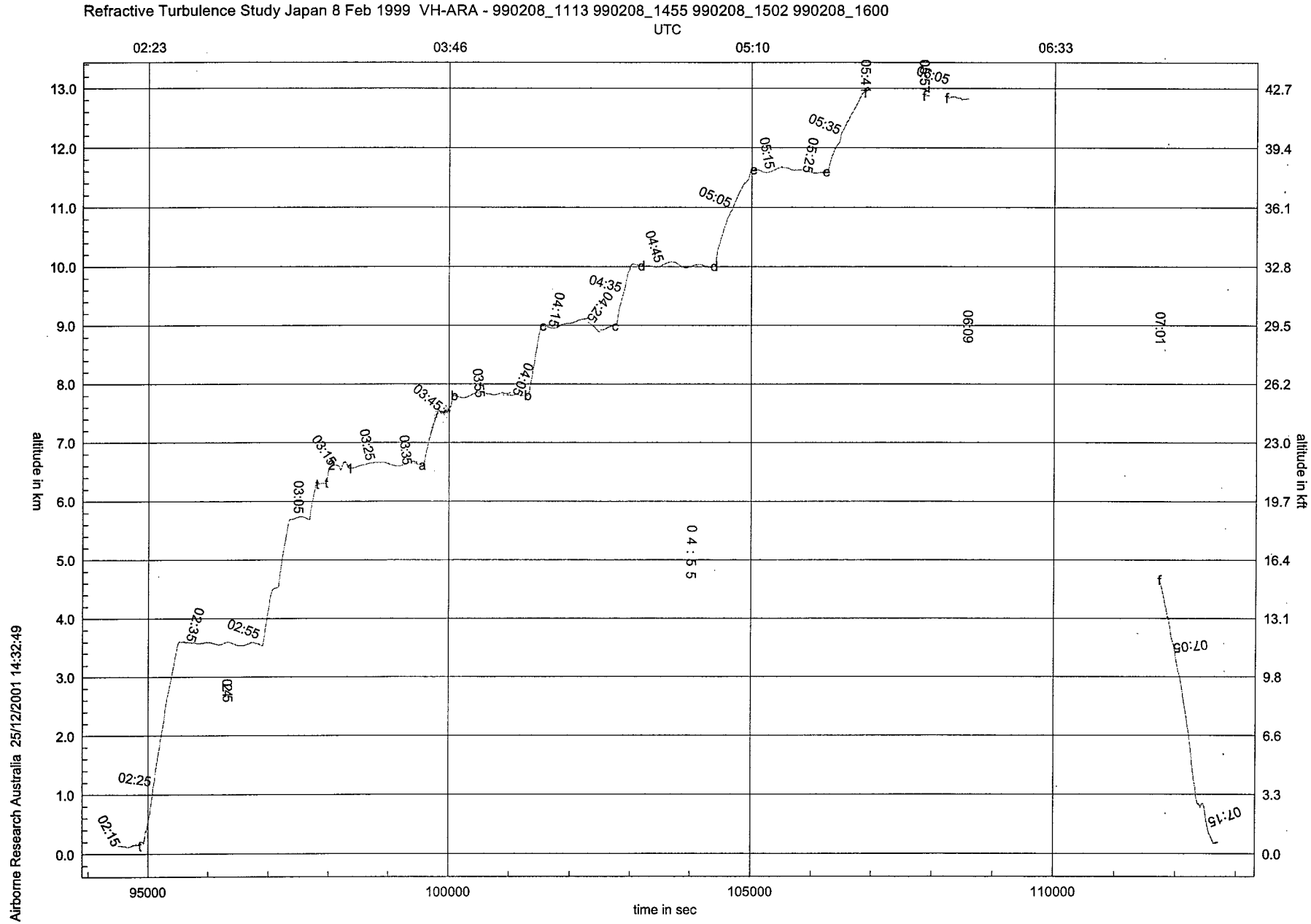
Refractive Turbulence Study Japan 8 Feb 1999 VH-ARA - 990208_1113 990208_1455 990208_1502 990208_1600
UTC
02:23
03:46
05:10
06:33
altitude in km
altitude in kft
time in sec
95000
100000
105000
110000
Airborne Research Australia 25/12/2001 14:32:49

Refractive Turbulence Study Japan 9 Feb 1999 VH-ARA - 990209_1210 990209_1226 990209_1407 990209_1435 990209_

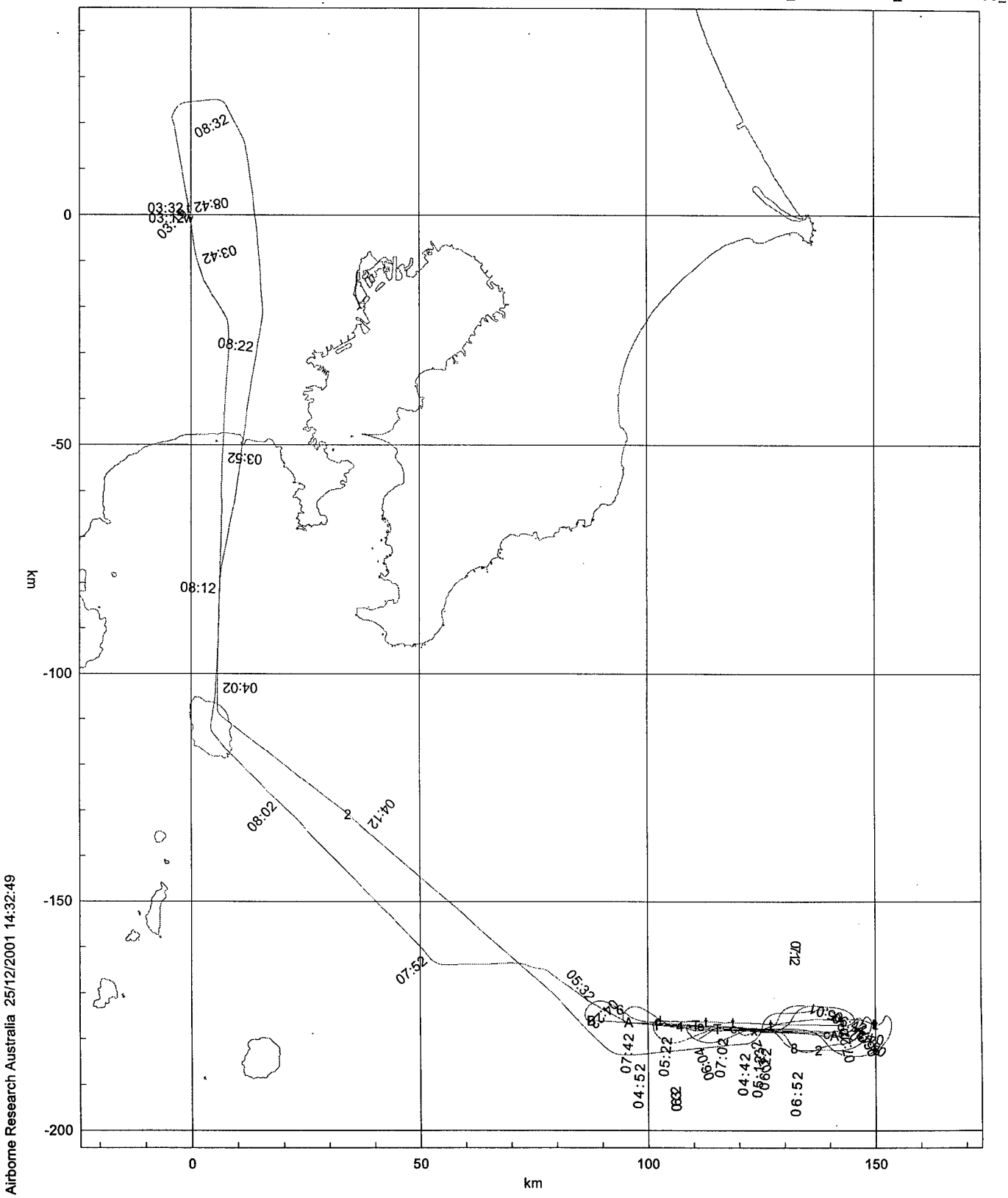

Airborne Research Australia 25/12/2001 14:32:49

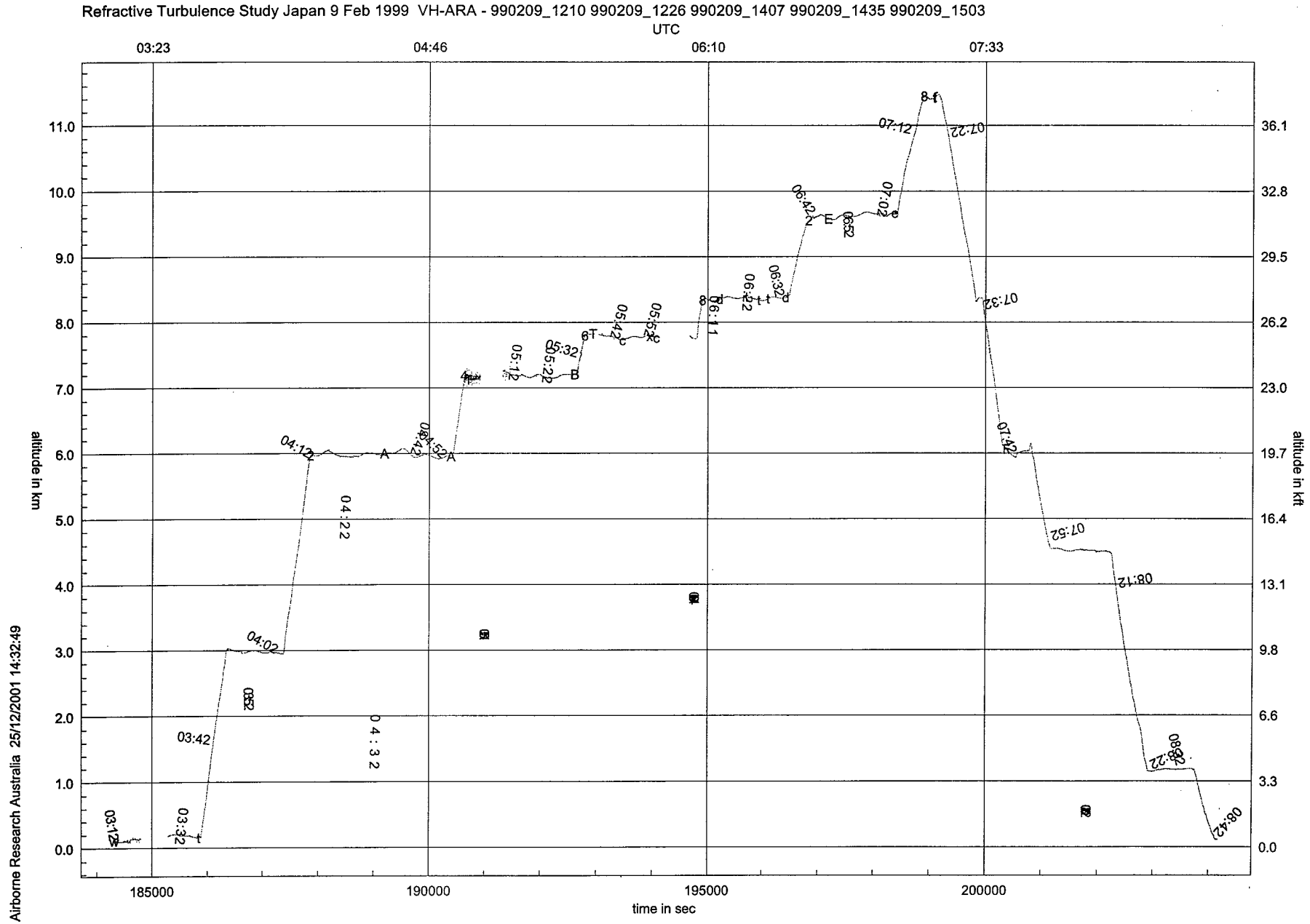
Refractive Turbulence Study Japan 9 Feb 1999 VH-ARA - 990209_1210 990209_1226 990209_1407 990209_1435 990209_1503
UTC
03:23
04:46
06:10
07:33
altitude in km
altitude in kft
time in sec
185000
190000
195000
200000
11.0
10.0
9.0
8.0
7.0
6.0
5.0
4.0
3.0
2.0
1.0
0.0
36.1
32.8
29.5
26.2
23.0
19.7
16.4
13.1
9.8
6.6
3.3
0.0
Airborne Research Australia 25/12/2001 14:32:49

Refractive Turbulence Study Japan 12 Feb 1999 VH-ARA - 990212_1158 990212_1515 990212_1720

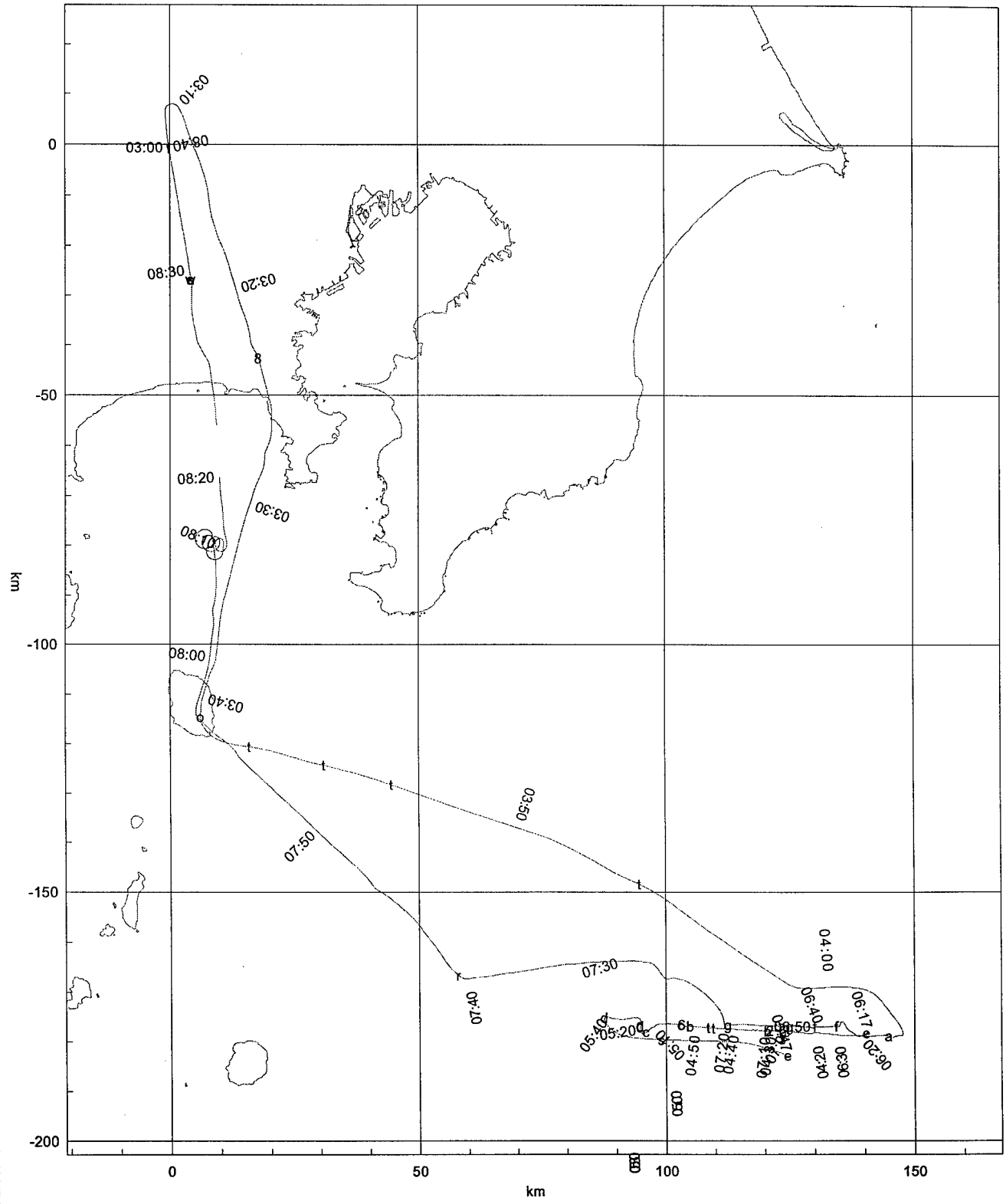

Airborne Research Australia 25/12/2001 14:32:49

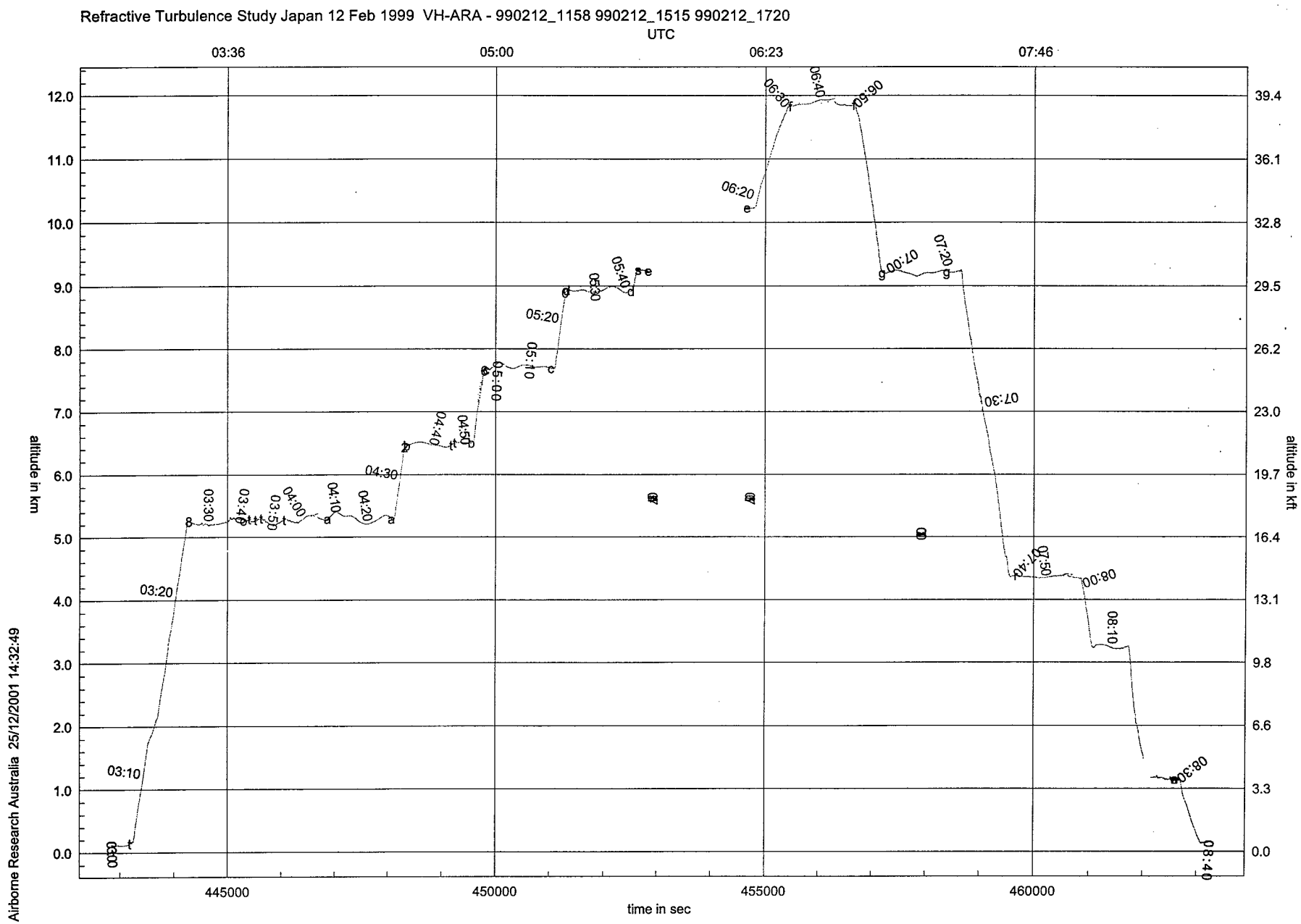
Refractive Turbulence Study Japan 12 Feb 1999 VH-ARA - 990212_1158 990212_1515 990212_1720
UTC
03:36
05:00
06:23
07:46
altitude in km
altitude in kft
time in sec
445000
450000
455000
460000
Airborne Research Australia 25/12/2001 14:32:49

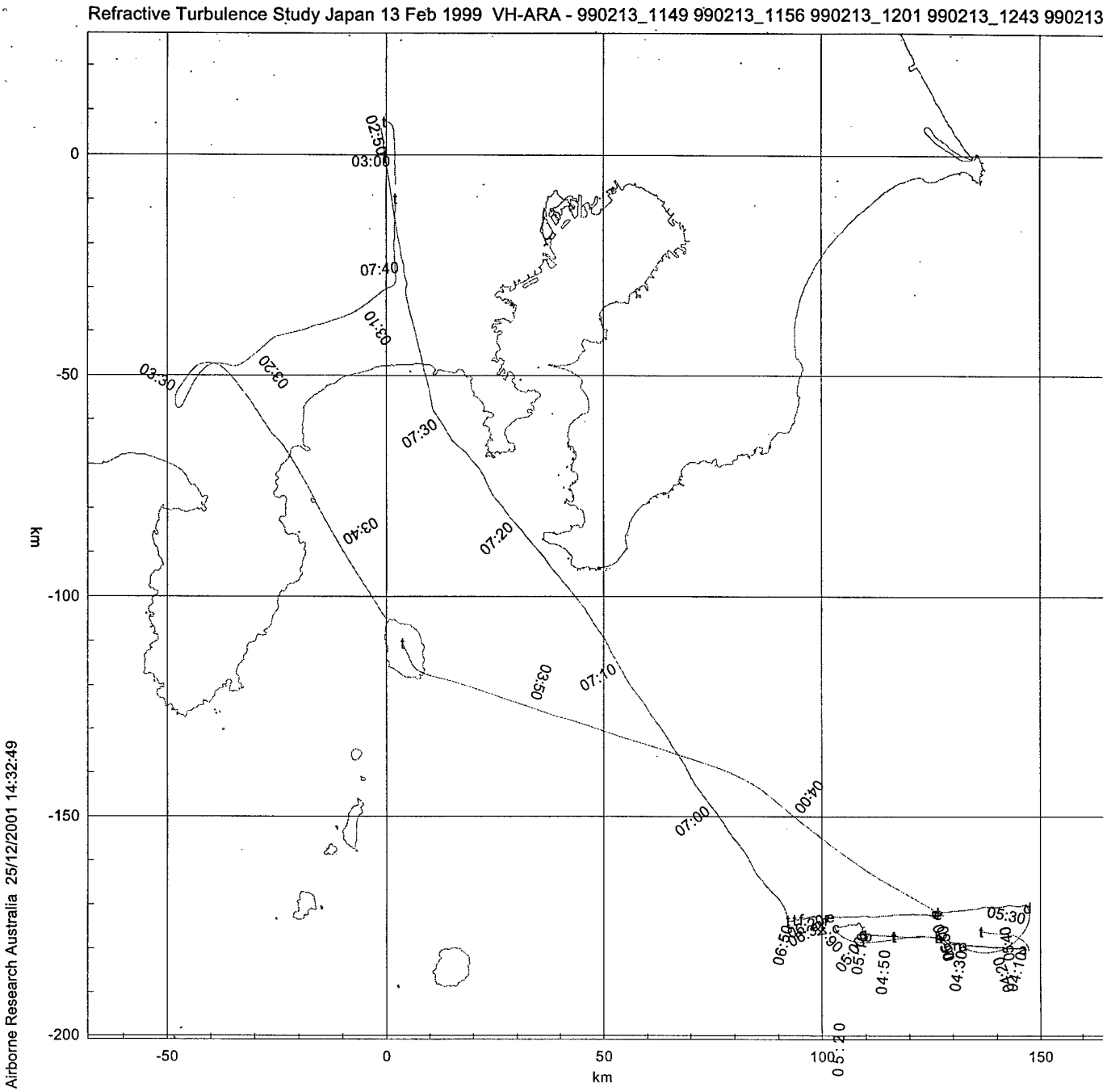
Refractive Turbulence Study Japan 13 Feb 1999 VH-ARA - 990213_1149 990213_1156 990213_1201 990213_1243 990213
Airborne Research Australia 25/12/2001 14:32:49
km
km
0
-50
-100
-150
-200
-50
0
50
100
150
02:50
03:00
03:10
03:20
03:30
03:40
03:50
04:00
04:10
04:20
04:30
04:40
04:50
05:00
05:10
05:20
05:30
06:10
06:30
06:50
07:00
07:10
07:20
07:30
07:40

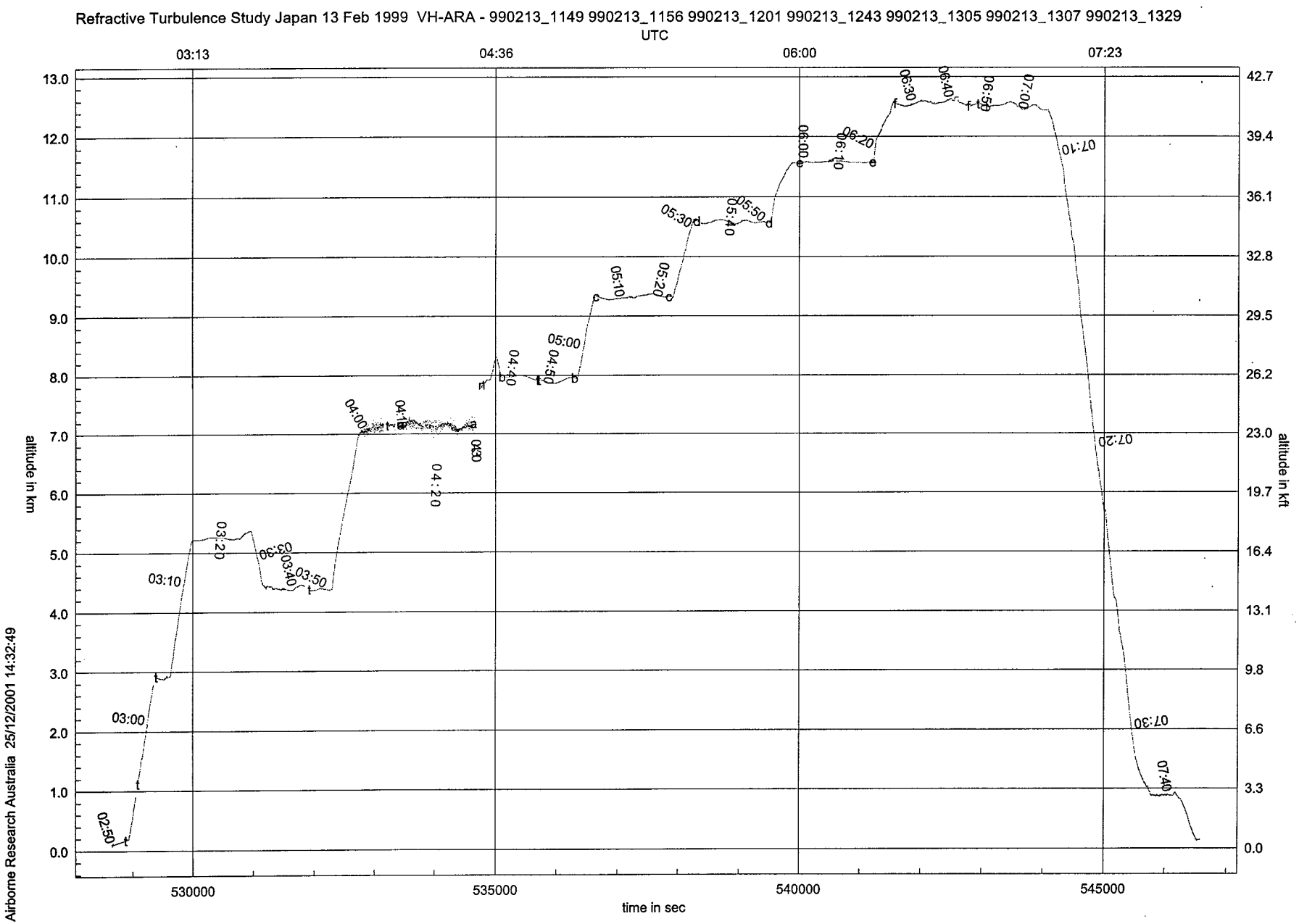
Refractive Turbulence Study Japan 13 Feb 1999 VH-ARA - 990213_1149 990213_1156 990213_1201 990213_1243 990213_1305 990213_1307 990213_1329
UTC
03:13
04:36
06:00
07:23
altitude in km
altitude in kft
time in sec
530000
535000
540000
545000
Airborne Research Australia 25/12/2001 14:32:49

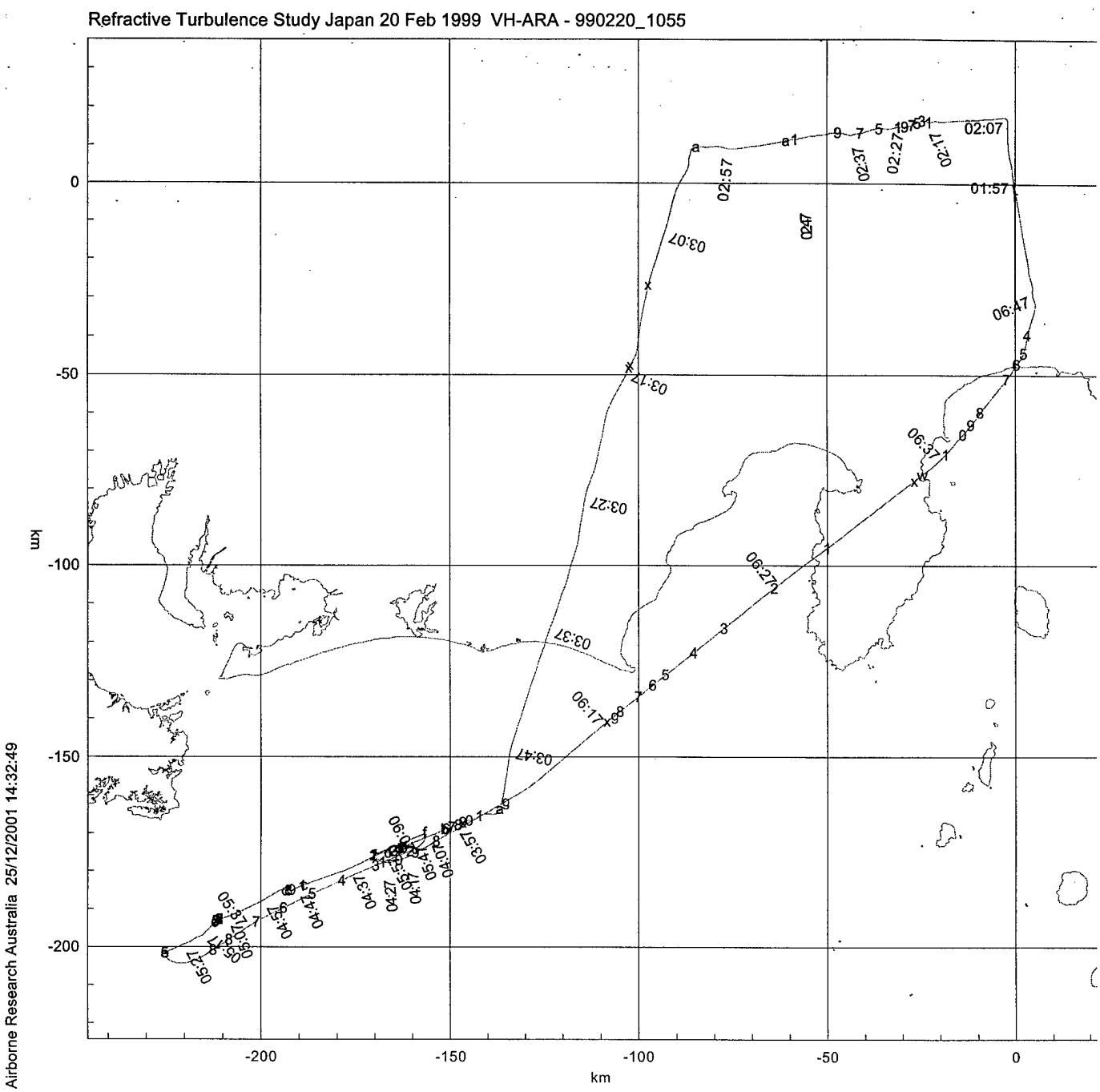
Refractive Turbulence Study Japan 20 Feb 1999 VH-ARA - 990220_1055
Airborne Research Australia 25/12/2001 14:32:49
km
0
-50
-100
-150
-200
-200
-150
-100
-50
0
02:07
01:57
02:57
03:07
03:17
03:27
03:37
03:47
06:47
06:37
06:27
06:17
06:07
05:57
05:47
05:37
05:27
05:17
05:07
04:57
04:47
04:37
04:27
04:17
04:07
03:57

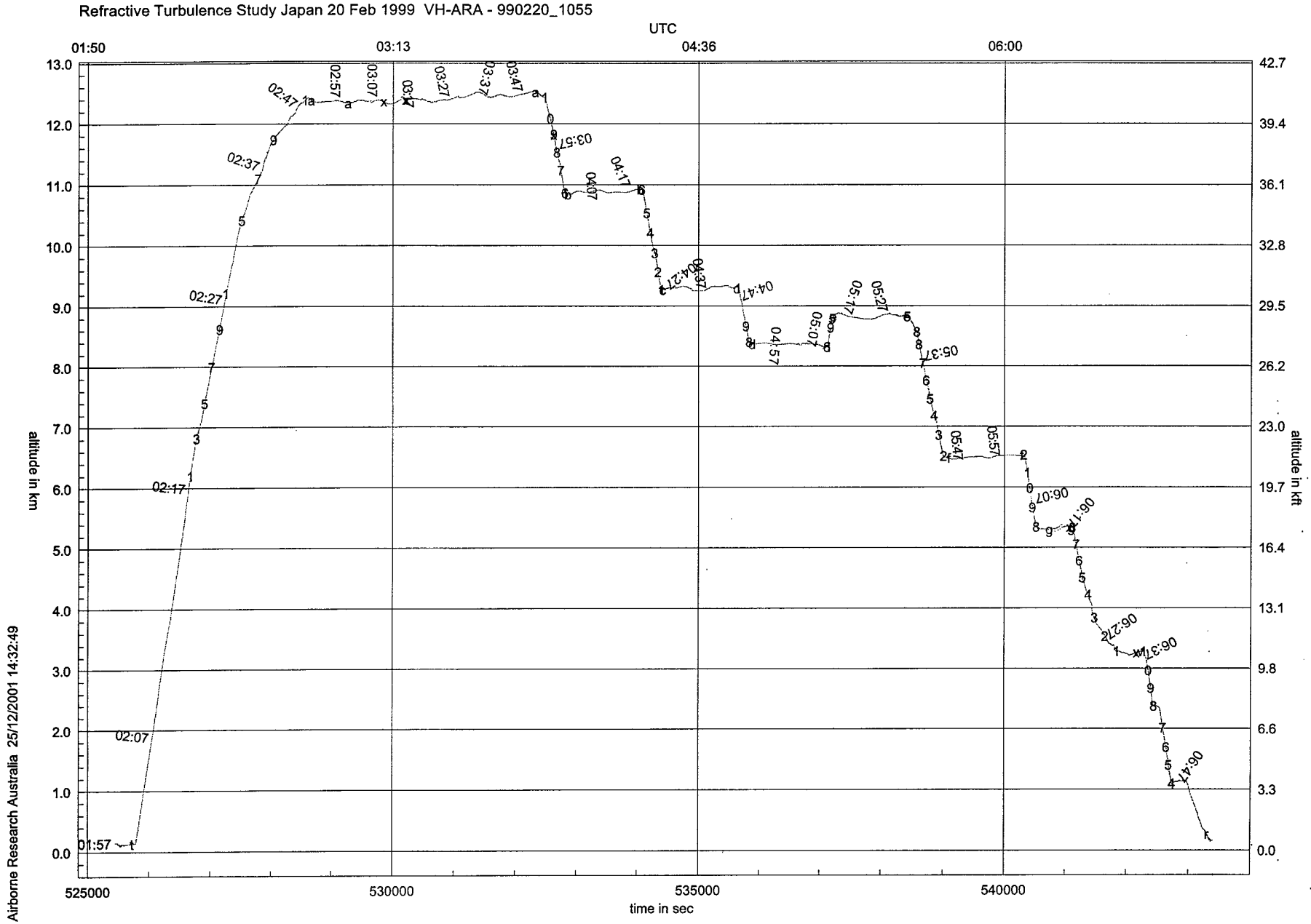
Refractive Turbulence Study Japan 20 Feb 1999 VH-ARA - 990220_1055
UTC
01:50
03:13
04:36
06:00
altitude in km
altitude in kft
time in sec
525000
530000
535000
540000
Airborne Research Australia 25/12/2001 14:32:49

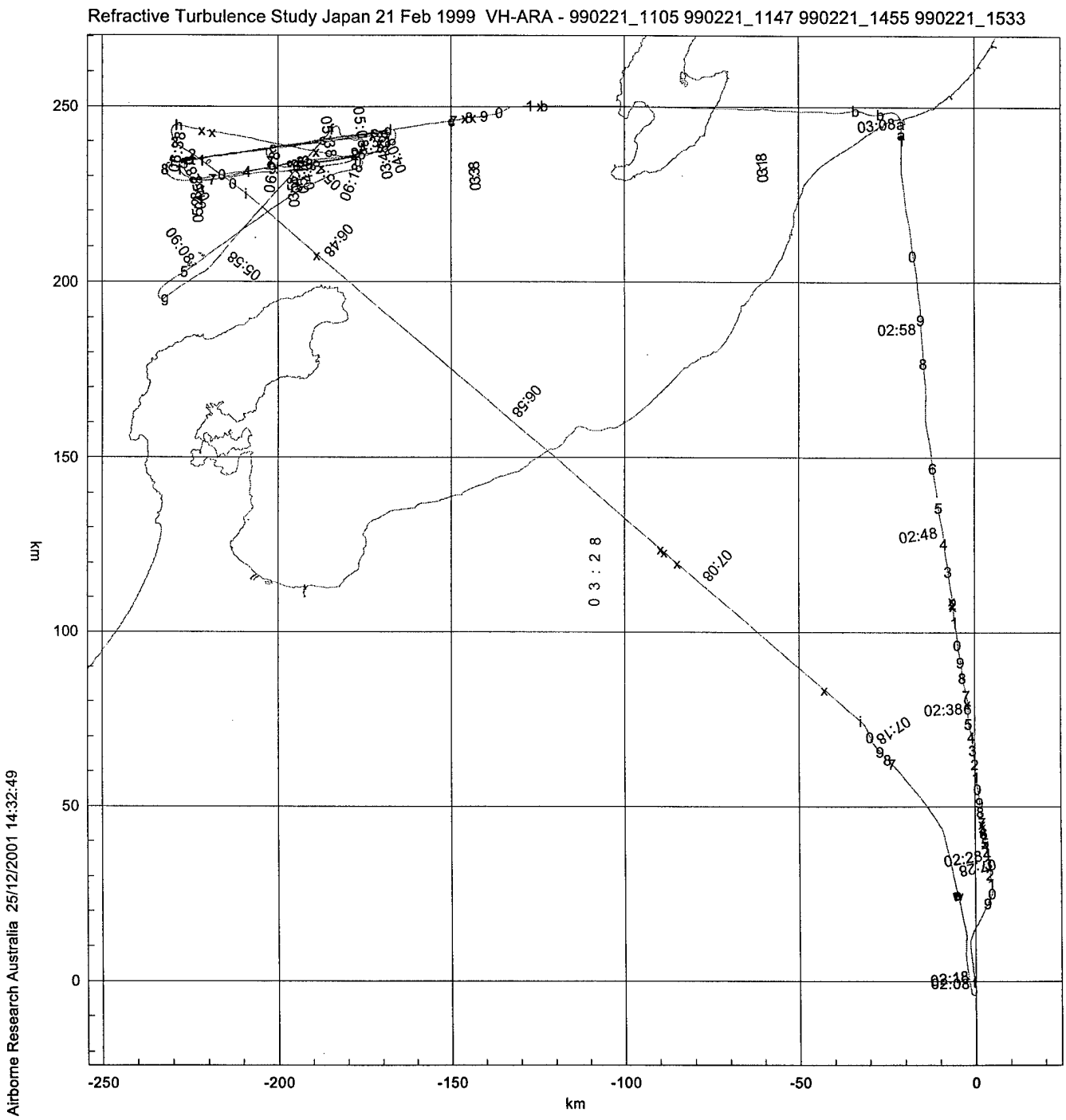
Refractive Turbulence Study Japan 21 Feb 1999 VH-ARA - 990221_1105 990221_1147 990221_1455 990221_1533
250
200
150
100
50
0
km
-250
-200
-150
-100
-50
0
km
Airborne Research Australia 25/12/2001 14:32:49

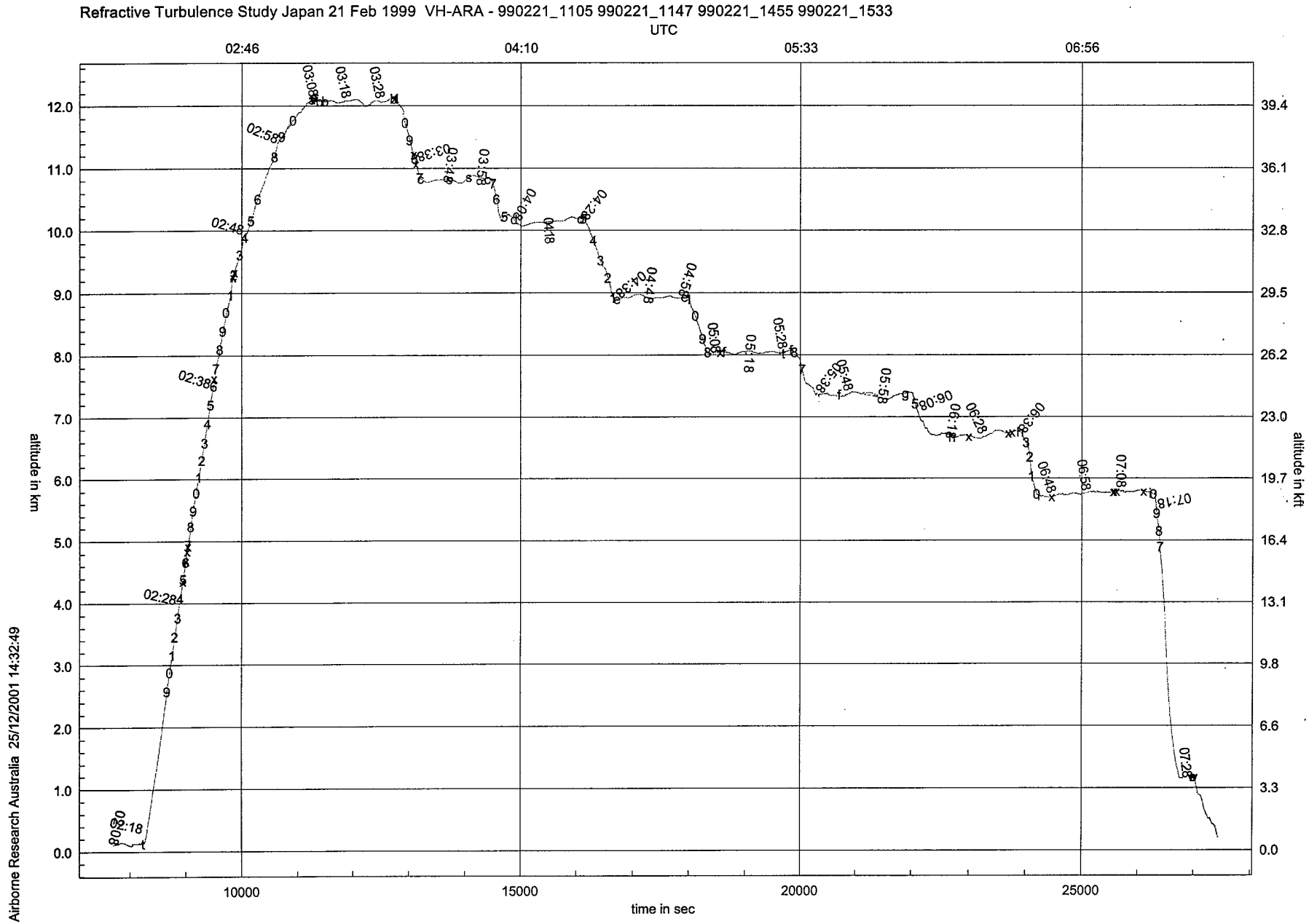
Refractive Turbulence Study Japan 21 Feb 1999 VH-ARA - 990221_1105 990221_1147 990221_1455 990221_1533
UTC
02:46
04:10
05:33
06:56
altitude in km
altitude in kft
time in sec
Airborne Research Australia 25/12/2001 14:32:49

Refractive Turbulence Study Japan 22 Feb 1999 VH-ARA - 990222_1104

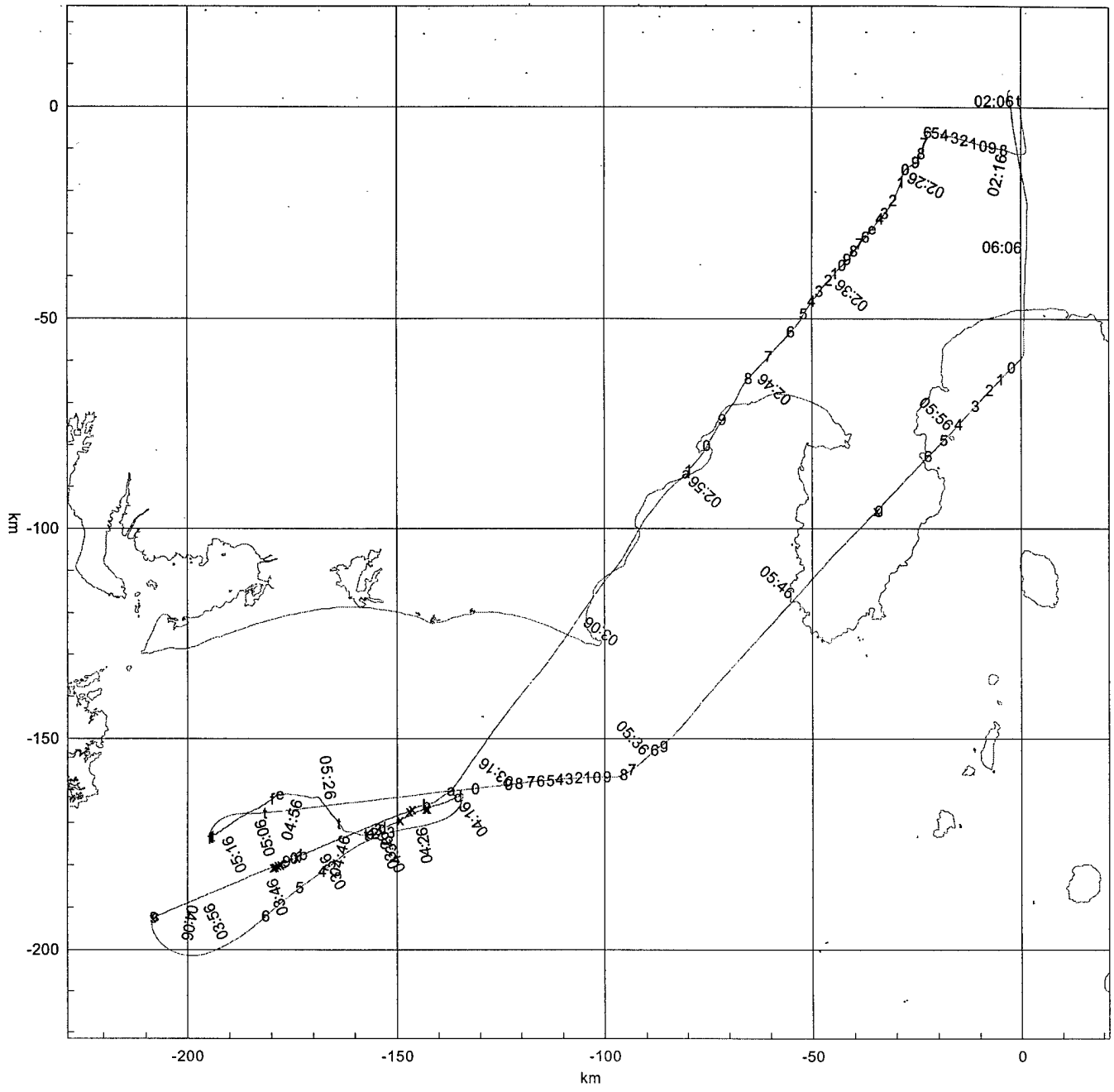

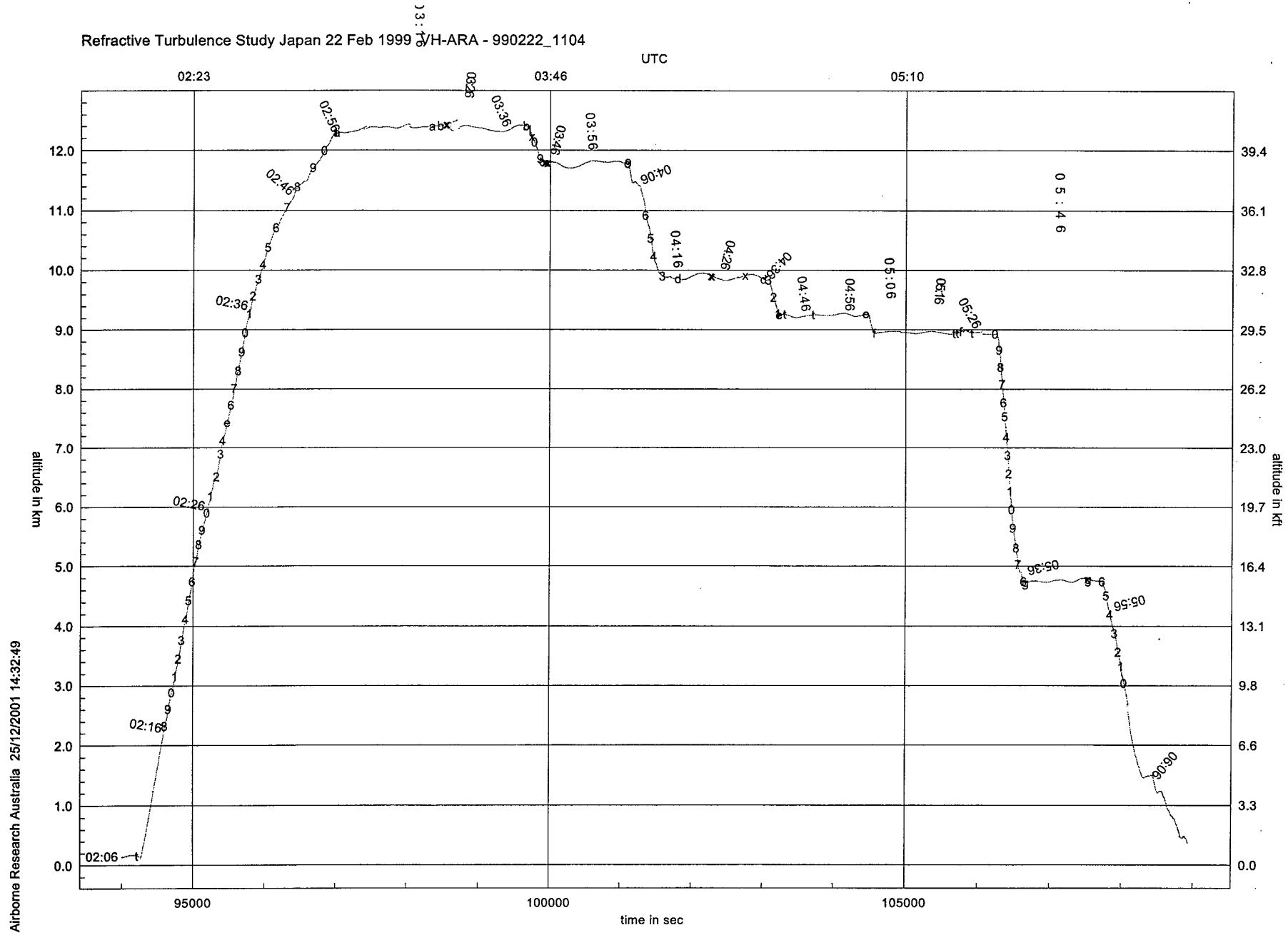
Refractive Turbulence Study Japan 22 Feb 1999 VH-ARA - 990222_1104
UTC
02:23
03:46
05:10
altitude in km
altitude in kft
time in sec
95000
100000
105000
Airborne Research Australia 25/12/2001 14:32:49

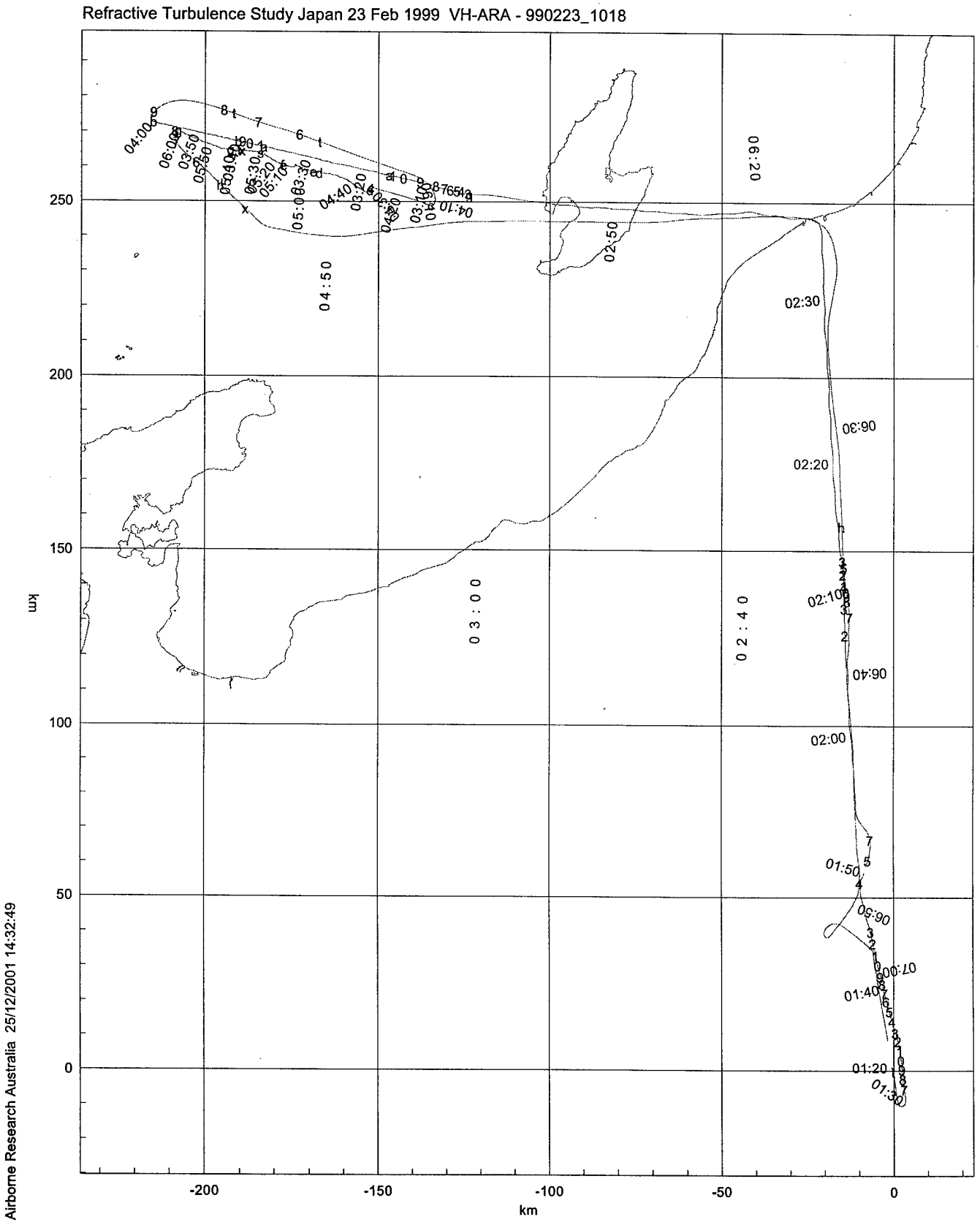
Refractive Turbulence Study Japan 23 Feb 1999 VH-ARA - 990223_1018
km
250
200
150
100
50
0
-200
-150
-100
-50
0
km
04:50
03:00
02:40
02:30
02:20
02:10
02:00
01:50
01:40
01:20
02:50
06:20
06:30
06:40
06:50
07:00
Airborne Research Australia 25/12/2001 14:32:49

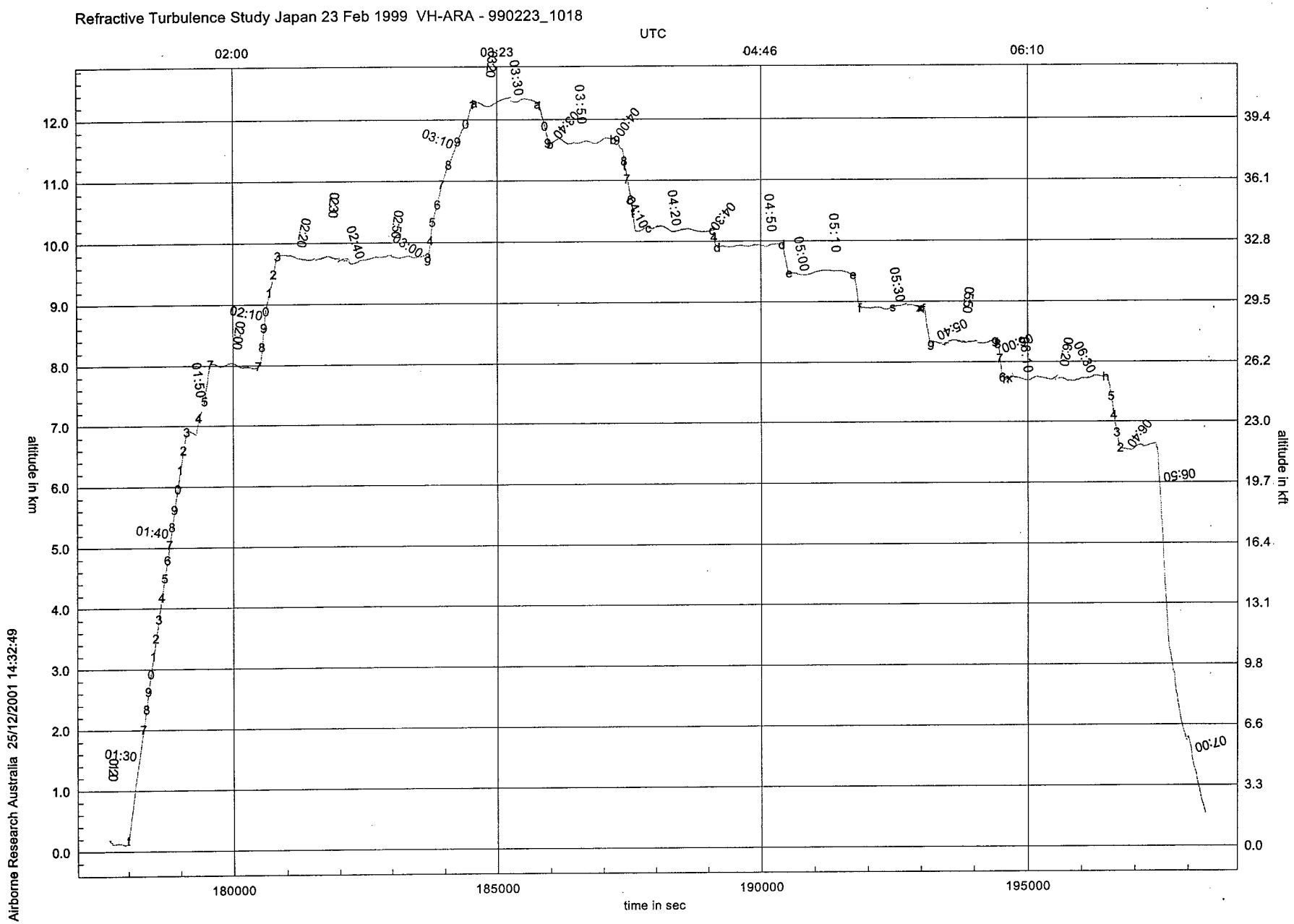
Refractive Turbulence Study Japan 23 Feb 1999 VH-ARA - 990223_1018
UTC
02:00
03:23
04:46
06:10
altitude in km
altitude in kft
time in sec
180000
185000
190000
195000
0.0
1.0
2.0
3.0
4.0
5.0
6.0
7.0
8.0
9.0
10.0
11.0
12.0
0.0
3.3
6.6
9.8
13.1
16.4
19.7
23.0
26.2
29.5
32.8
36.1
39.4
Airborne Research Australia 25/12/2001 14:32:49

Refractive Turbulence Study Australia 16 Jul 1999 VH-ARA - 990716_1412

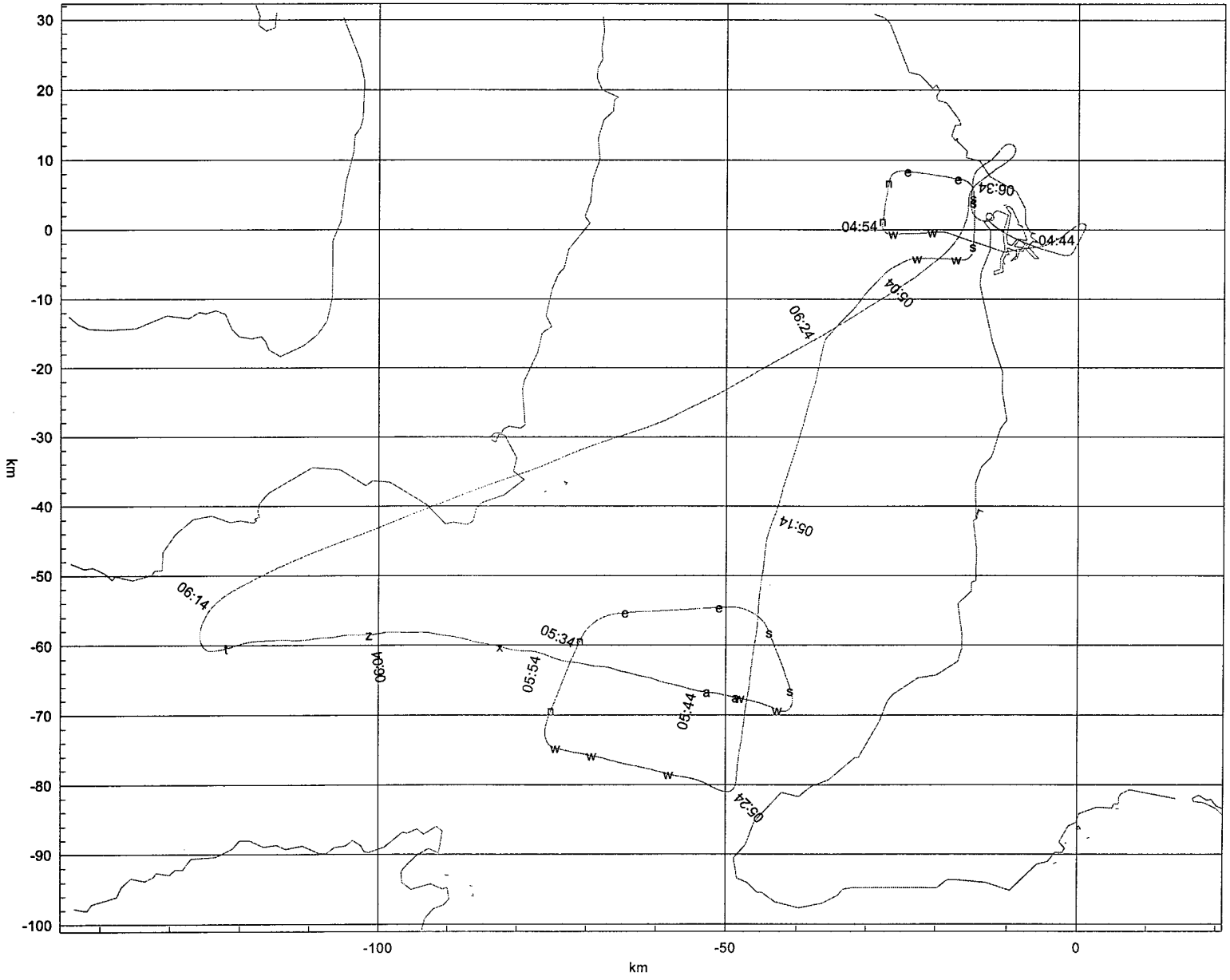

Airborne Research Australia 25/12/2001 15:29:44

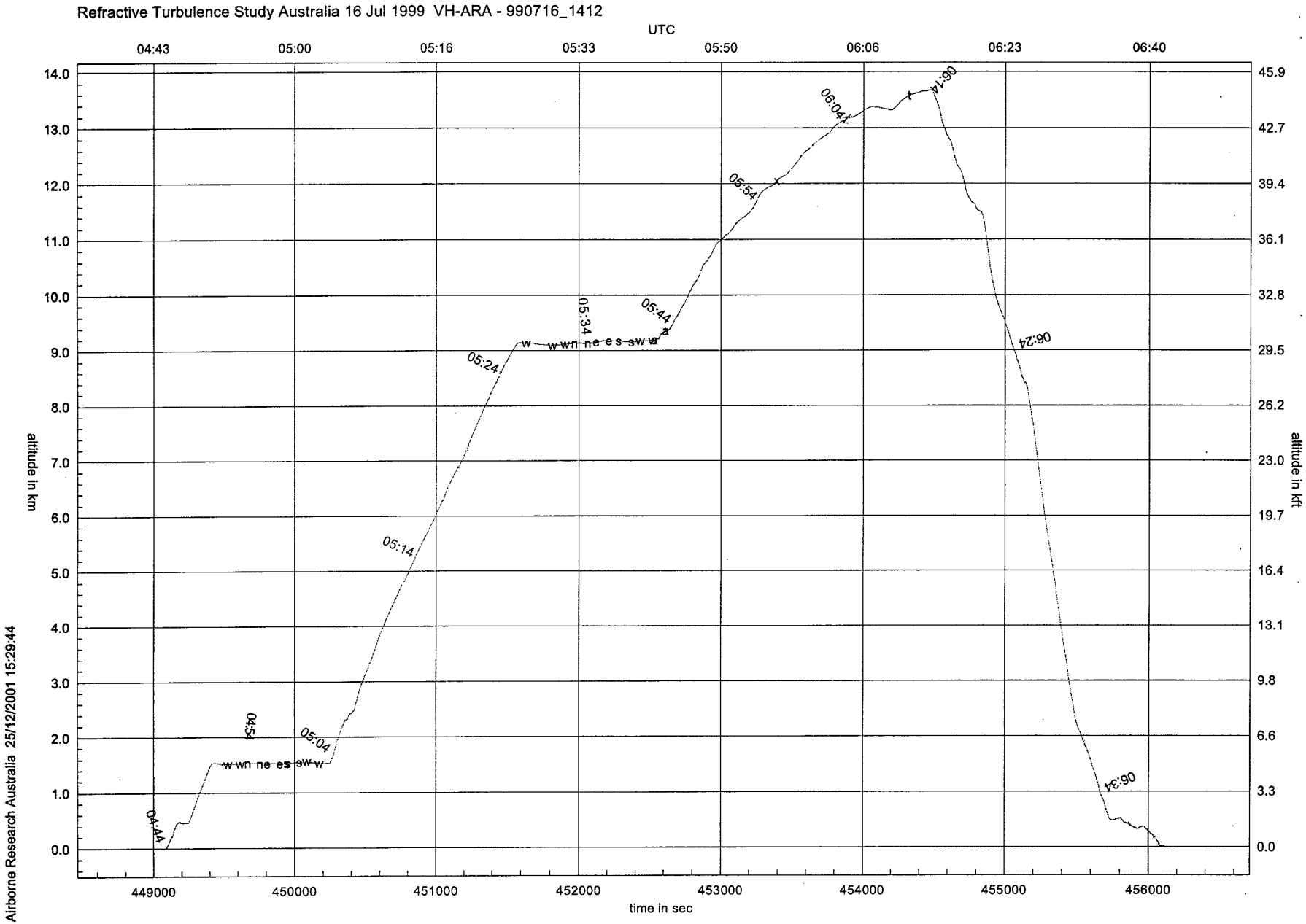
Refractive Turbulence Study Australia 16 Jul 1999 VH-ARA - 990716_1412
UTC
04:43
05:00
05:16
05:33
05:50
06:06
06:23
06:40
14.0
13.0
12.0
11.0
10.0
9.0
8.0
7.0
6.0
5.0
4.0
3.0
2.0
1.0
0.0
45.9
42.7
39.4
36.1
32.8
29.5
26.2
23.0
19.7
16.4
13.1
9.8
6.6
3.3
0.0
altitude in km
altitude in kft
04:44
04:54
05:04
05:14
05:24
05:34
05:44
05:54
06:04
06:14
06:24
06:34
w wn ne es sw w
449000
450000
451000
452000
453000
454000
455000
456000
time in sec
Airborne Research Australia 25/12/2001 15:29:44

Refractive Turbulence Study Australia 28 Jul 1999 VH-ARA - 990728_1254 990728_1309 990728_1343 990728_1506

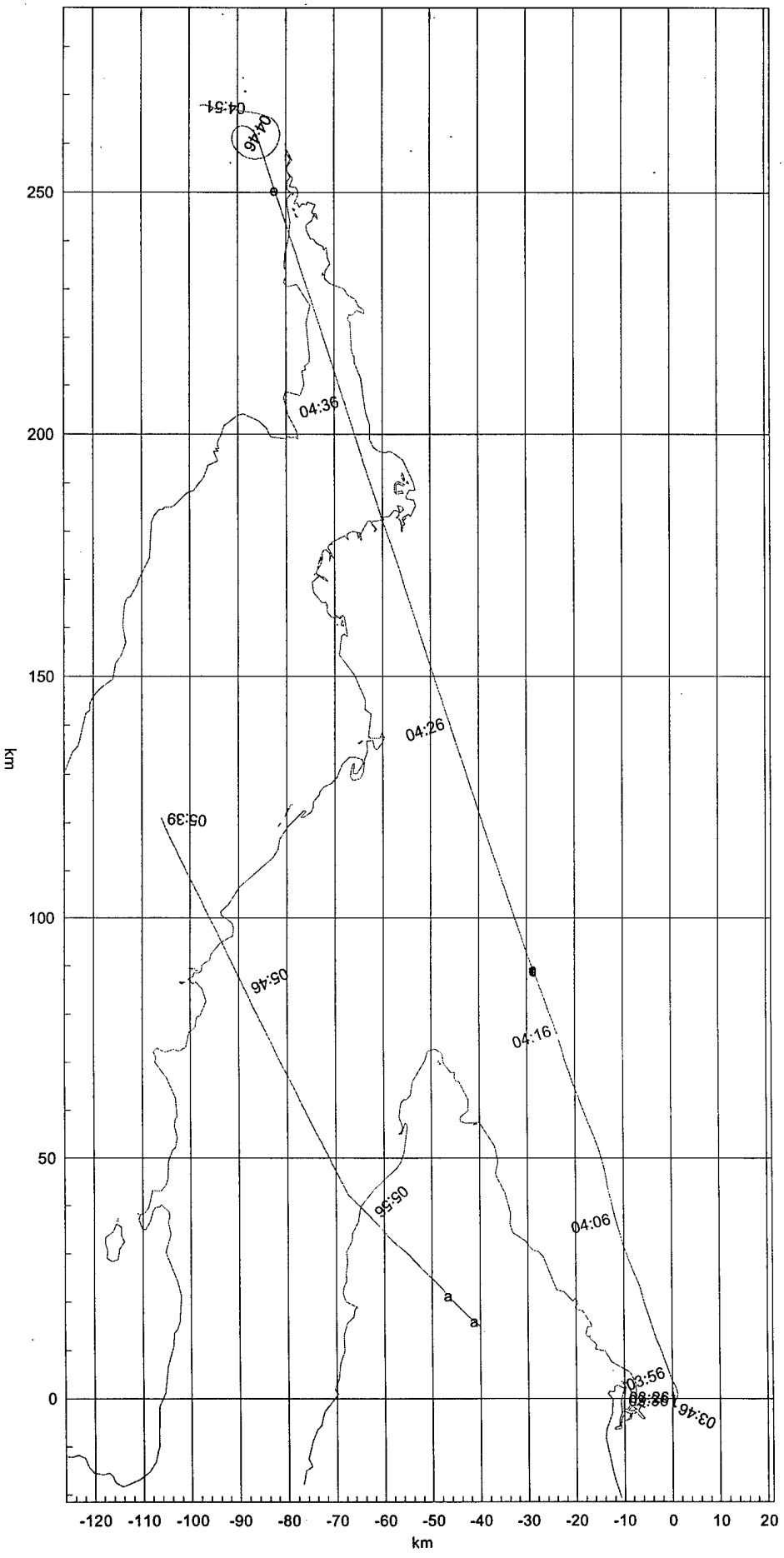

Airborne Research Australia 25/12/2001 15:29:44

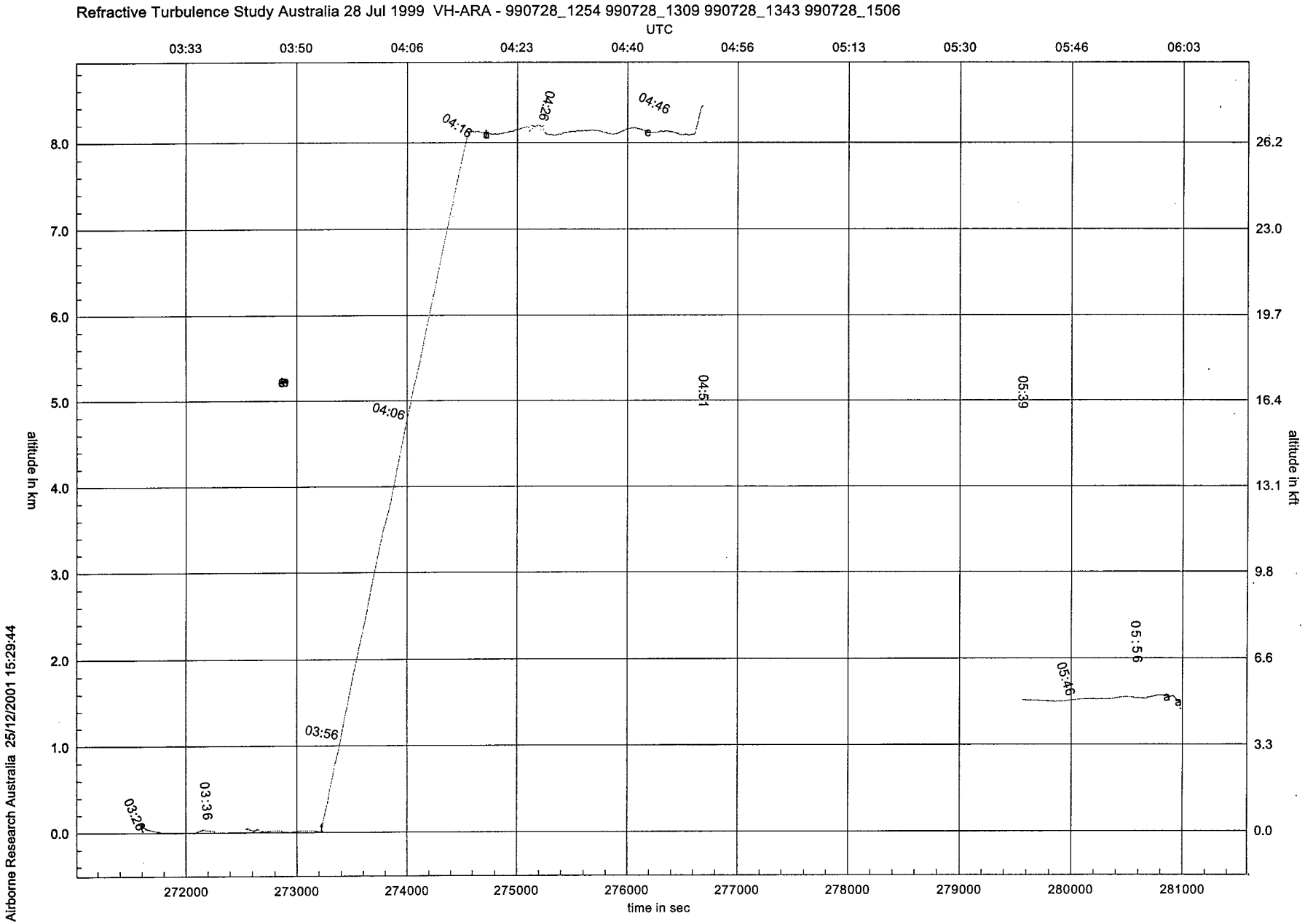
Refractive Turbulence Study Australia 28 Jul 1999 VH-ARA - 990728_1254 990728_1309 990728_1343 990728_1506
UTC
03:33
03:50
04:06
04:23
04:40
04:56
05:13
05:30
05:46
06:03
04:16
04:26
04:46
04:06
04:51
05:39
05:56
05:46
03:56
03:36
03:26
8.0
7.0
6.0
5.0
4.0
3.0
2.0
1.0
0.0
altitude in km
26.2
23.0
19.7
16.4
13.1
9.8
6.6
3.3
0.0
altitude in kft
272000
273000
274000
275000
276000
277000
278000
279000
280000
281000
time in sec
Airborne Research Australia 25/12/2001 15:29:44

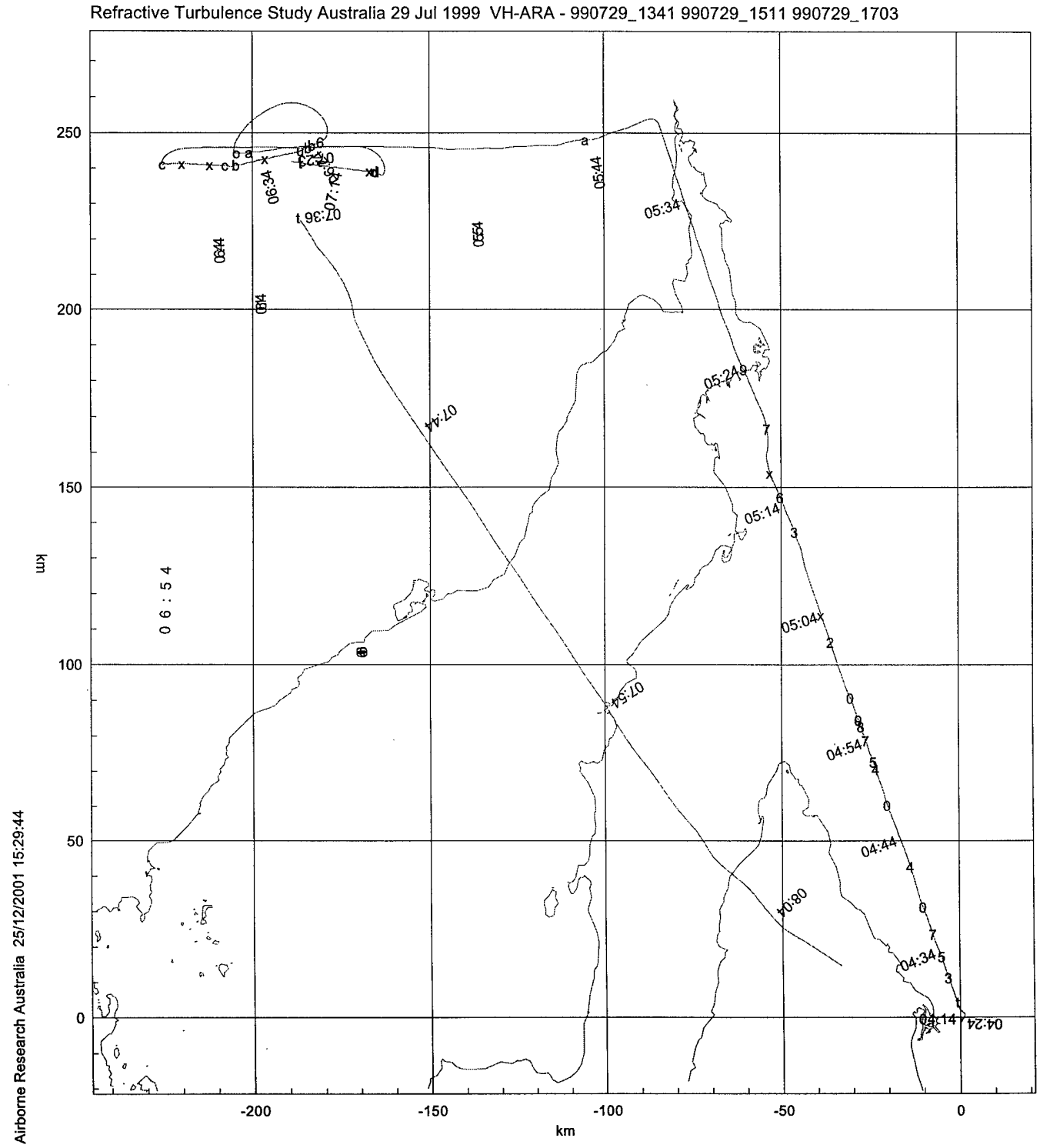
Refractive Turbulence Study Australia 29 Jul 1999 VH-ARA - 990729_1341 990729_1511 990729_1703
250
200
150
100
50
0
km
-200
-150
-100
-50
0
km
Airborne Research Australia 25/12/2001 15:29:44

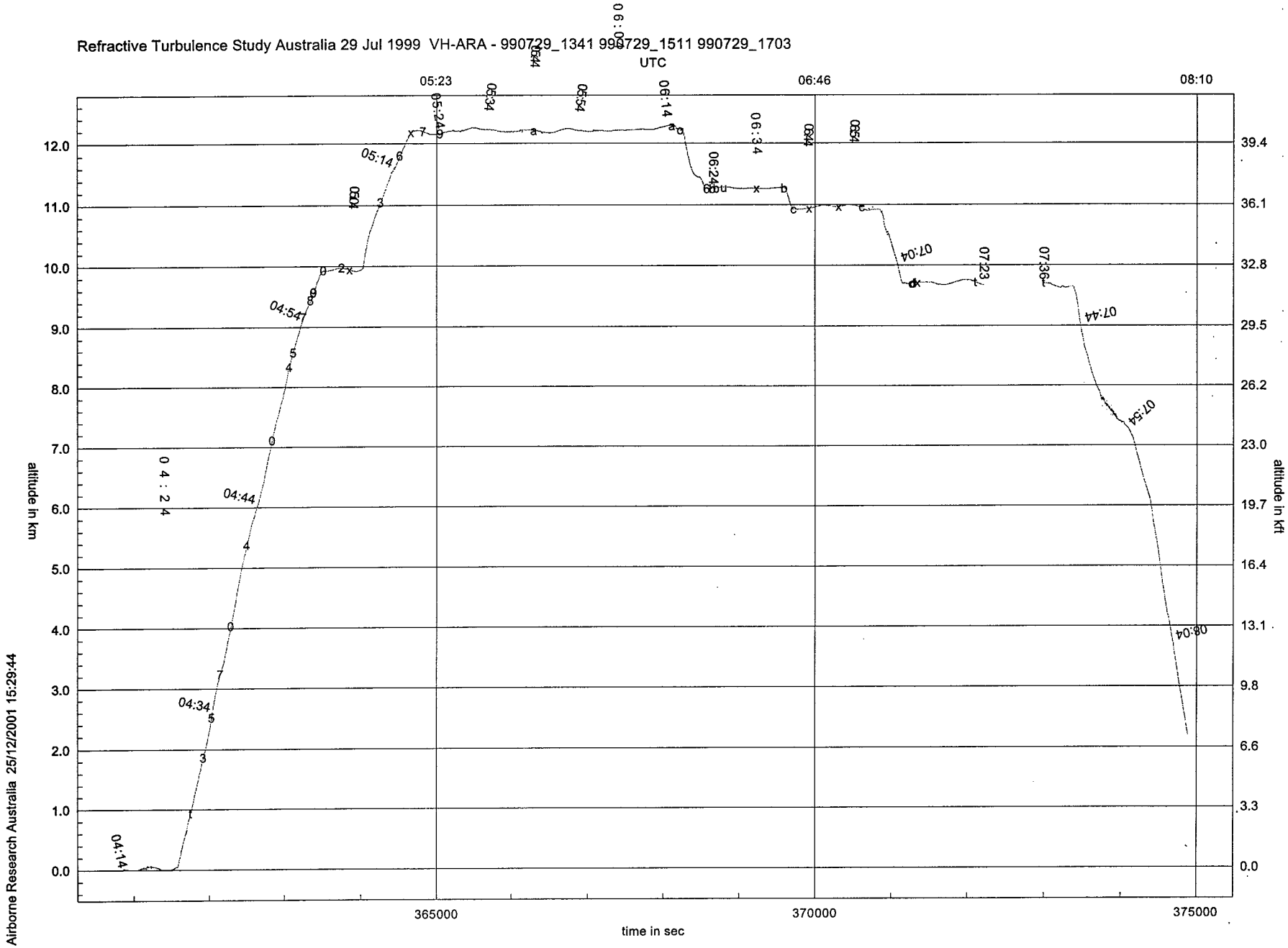
Refractive Turbulence Study Australia 29 Jul 1999 VH-ARA - 990729_1341 990729_1511 990729_1703
UTC
05:23
06:46
08:10
altitude in km
altitude in kft
time in sec
365000
370000
375000
Airborne Research Australia 25/12/2001 15:29:44

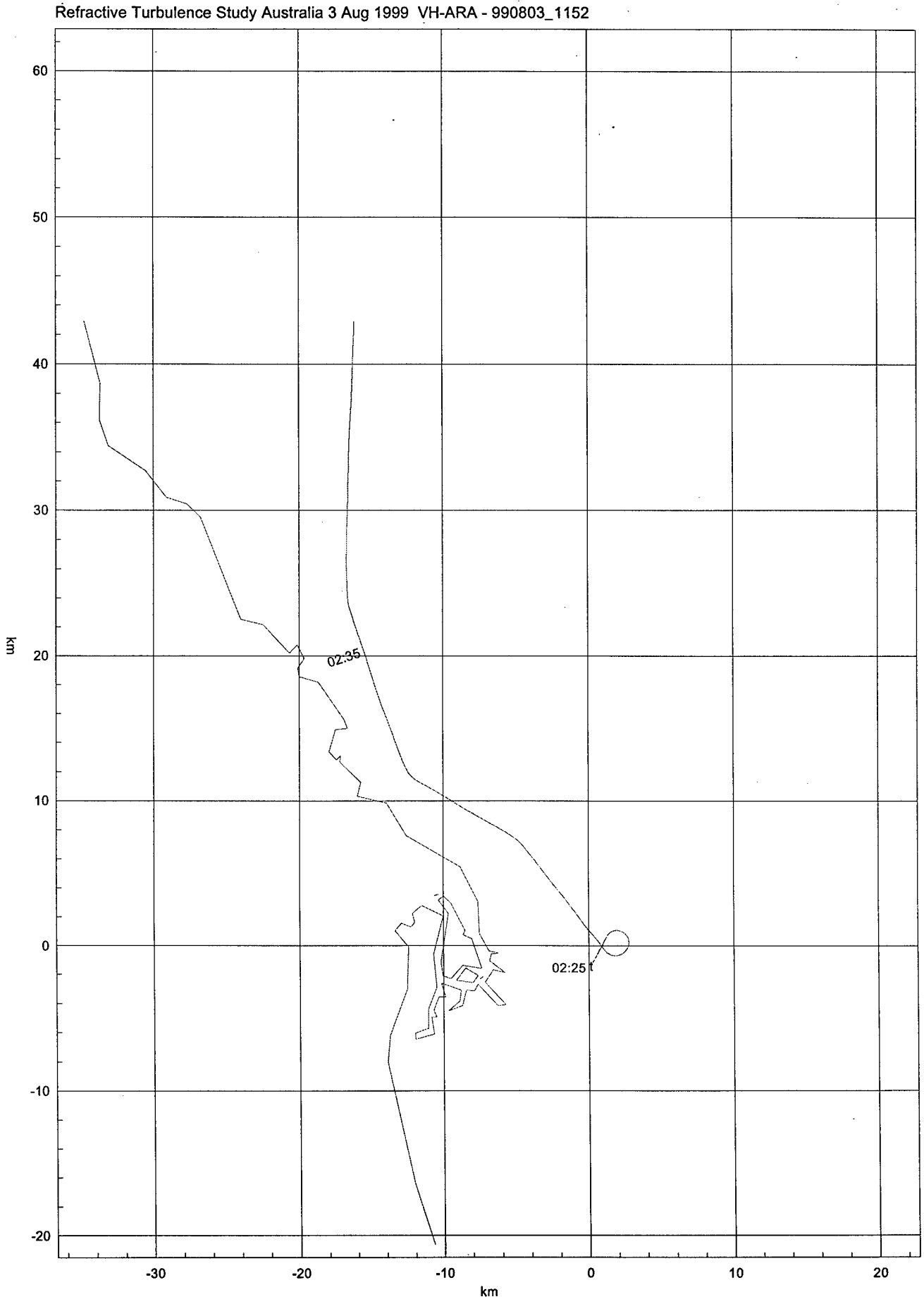
Refractive Turbulence Study Australia 3 Aug 1999 VH-ARA - 990803_1152
60
50
40
30
20
10
0
-10
-20
km
02:35
02:25
-30
-20
-10
0
10
20
km
Airborne Research Australia 25/12/2001 15:29:44

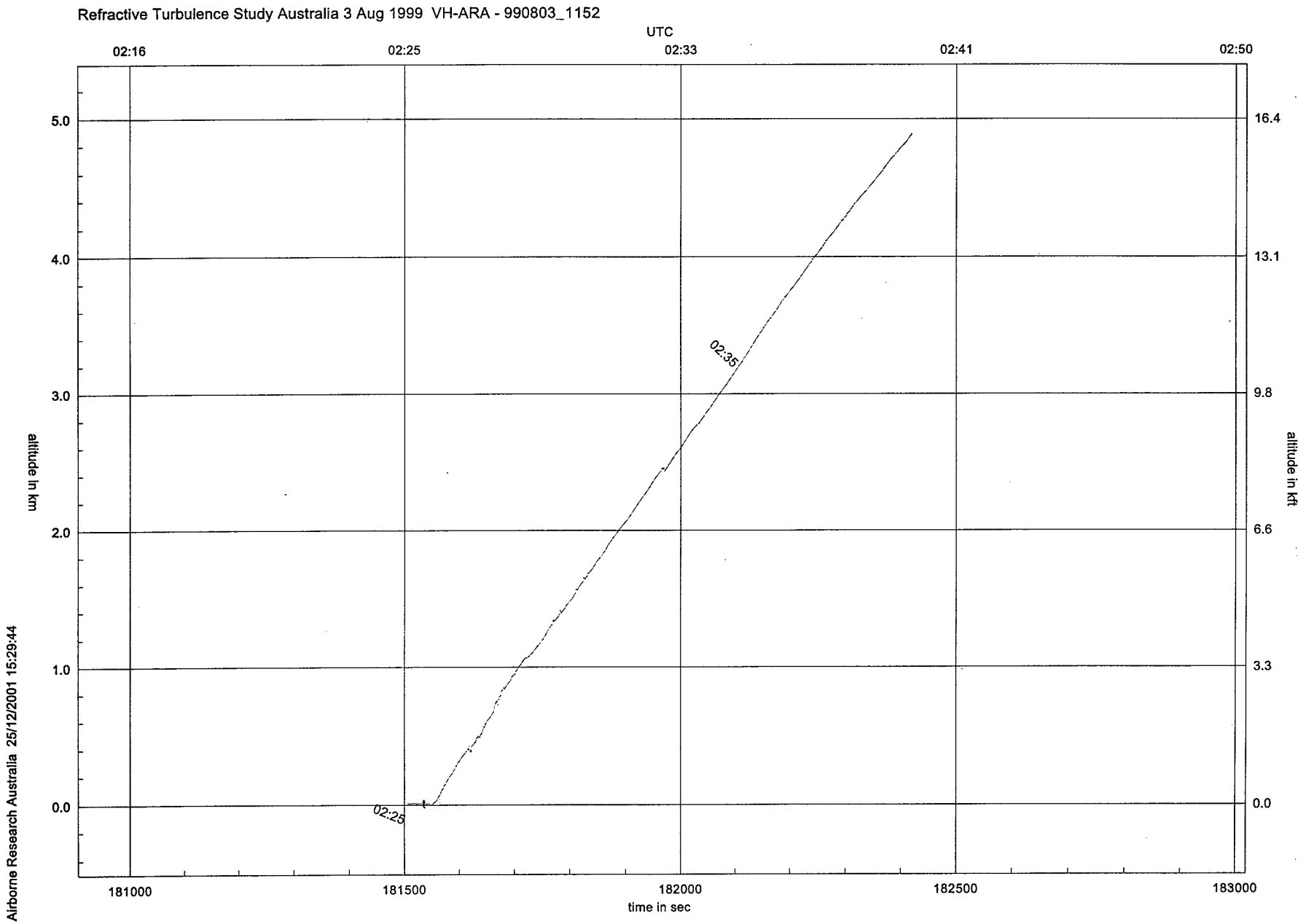
Refractive Turbulence Study Australia 3 Aug 1999 VH-ARA - 990803_1152
UTC
02:16
02:25
02:33
02:41
02:50
5.0
4.0
3.0
2.0
1.0
0.0
16.4
13.1
9.8
6.6
3.3
0.0
02:35
02:25
altitude in km
altitude in kft
181000
181500
182000
182500
183000
time in sec
Airborne Research Australia 25/12/2001 15:29:44

Refractive Turbulence Study Australia 5 Aug 1999 VH-ARA - 990805_1500 990805_1624 990805_1631 990805_1636 990805

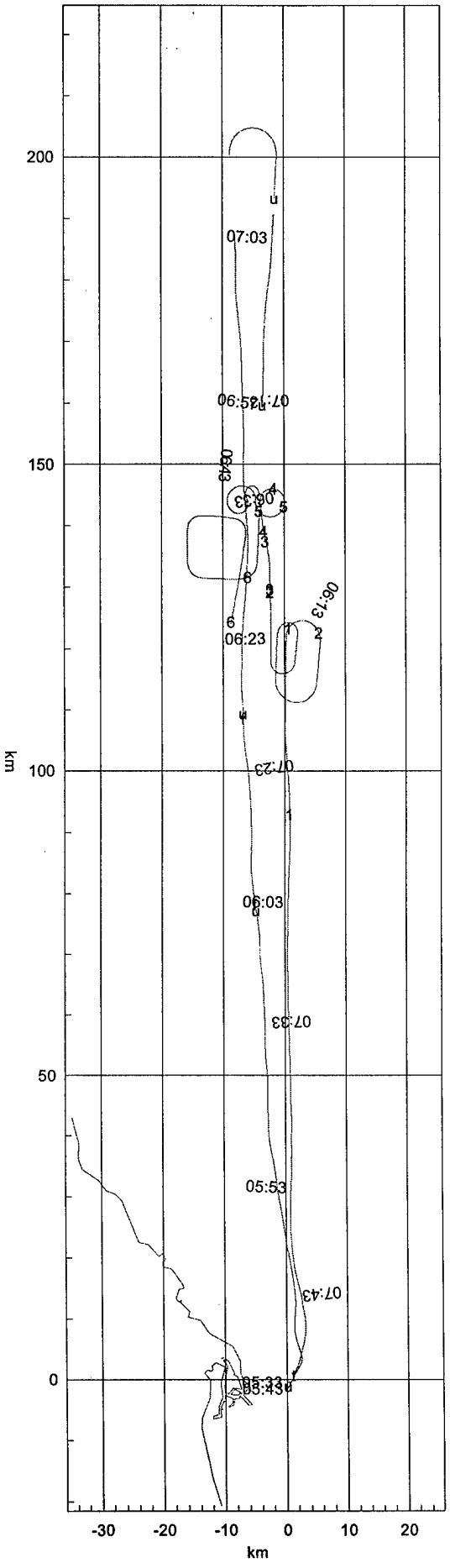

Airborne Research Australia 25/12/2001 15:29:44

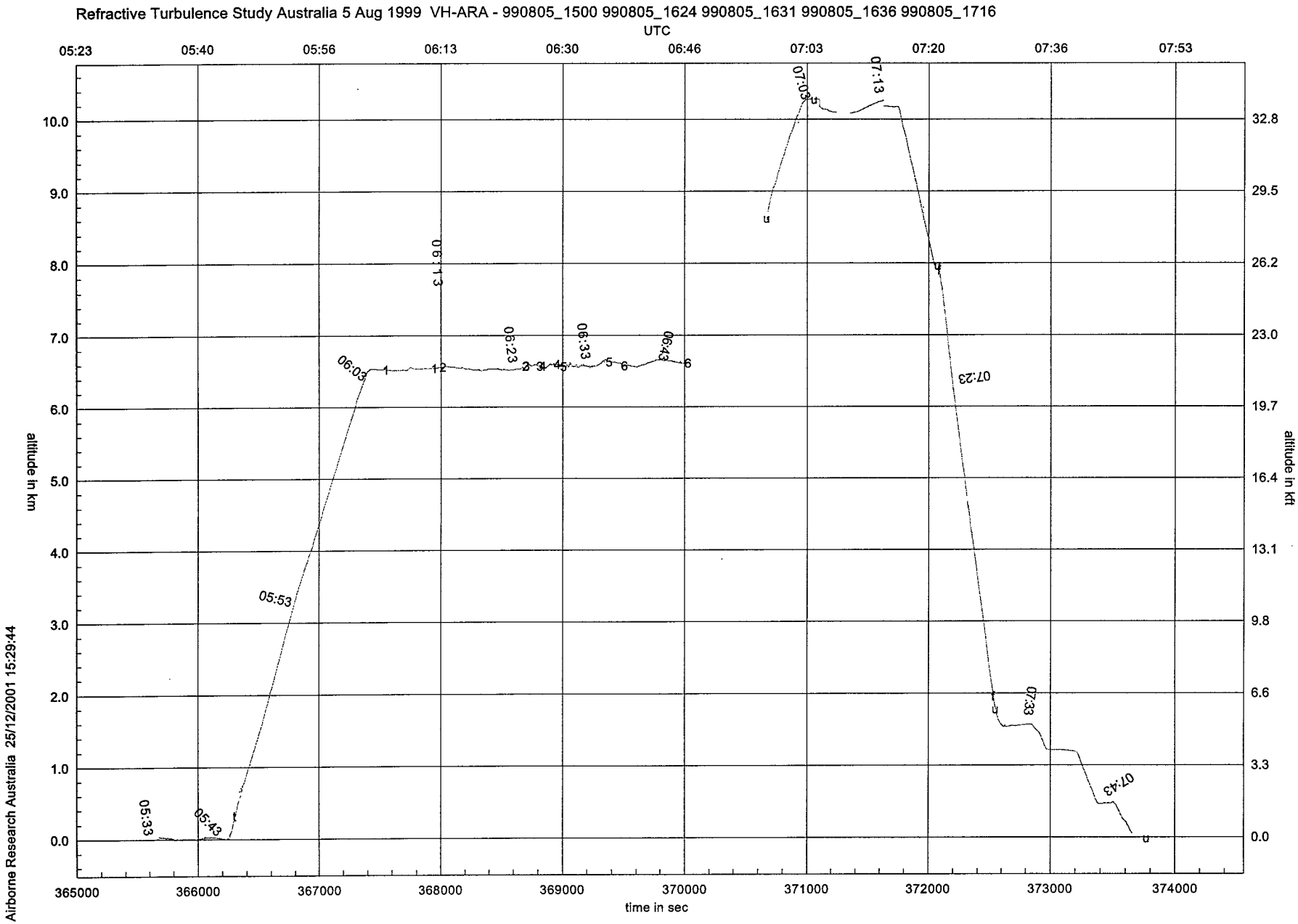
Refractive Turbulence Study Australia 5 Aug 1999 VH-ARA - 990805_1500 990805_1624 990805_1631 990805_1636 990805_1716
UTC
05:23
05:40
05:56
06:13
06:30
06:46
07:03
07:20
07:36
07:53
10.0
9.0
8.0
7.0
6.0
5.0
4.0
3.0
2.0
1.0
0.0
32.8
29.5
26.2
23.0
19.7
16.4
13.1
9.8
6.6
3.3
0.0
altitude in km
altitude in kft
05:33
05:43
05:53
06:03
06:13
06:23
06:33
06:43
07:03
07:13
07:23
07:33
07:43
365000
366000
367000
368000
369000
370000
371000
372000
373000
374000
time in sec
Airborne Research Australia 25/12/2001 15:29:44

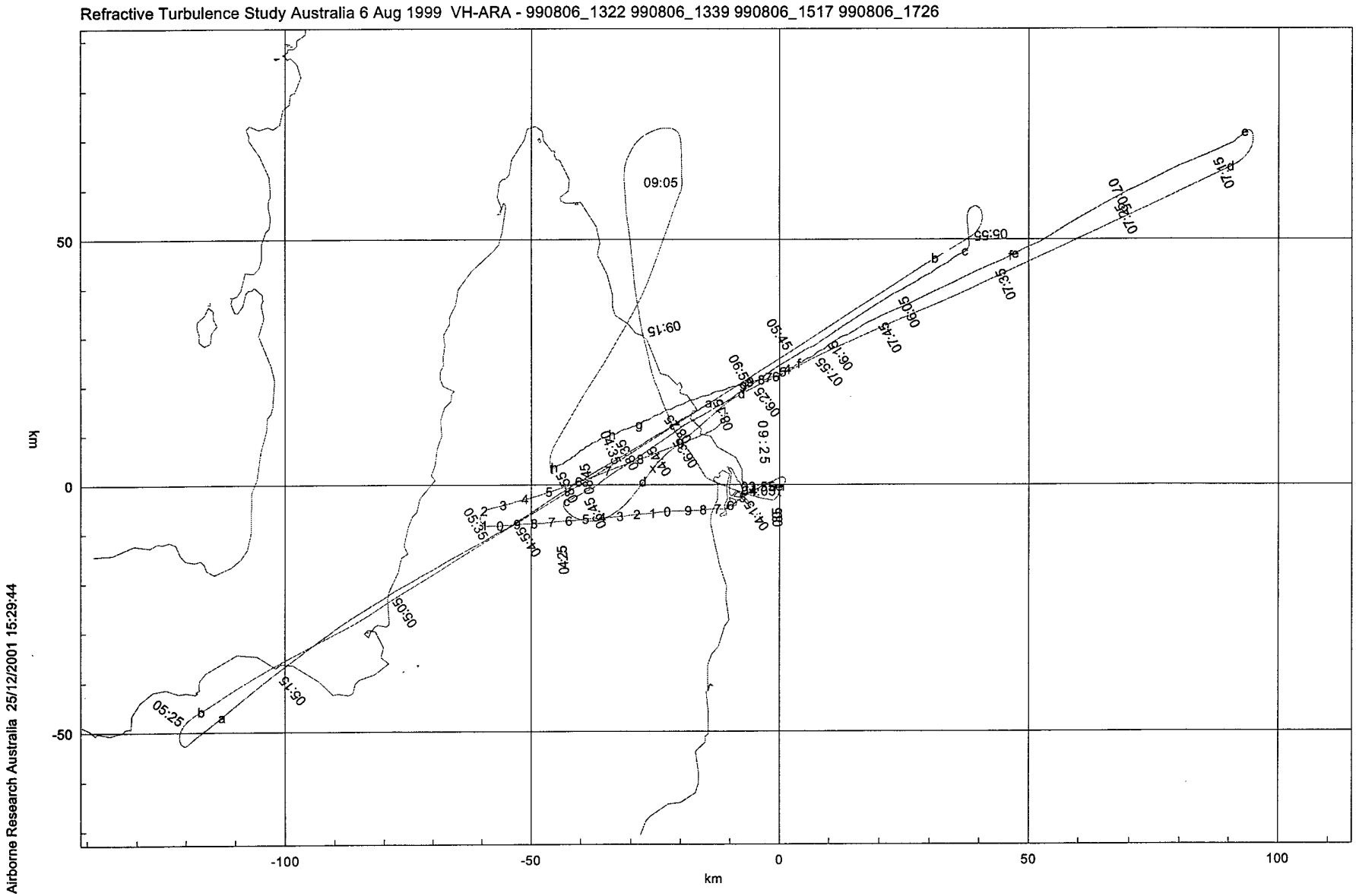
Refractive Turbulence Study Australia 6 Aug 1999 VH-ARA - 990806_1322 990806_1339 990806_1517 990806_1726
Airborne Research Australia 25/12/2001 15:29:44
km
50
0
-50
-100
-50
0
50
100
km
09:05
09:15
09:25
05:25
05:35
05:45
05:55
06:05
06:15
06:25
06:35
06:45
06:55
07:05
07:15
07:25
07:35
07:45
07:55
08:05
08:15
08:25
08:35
08:45
08:55
04:25
04:35
04:45
04:55

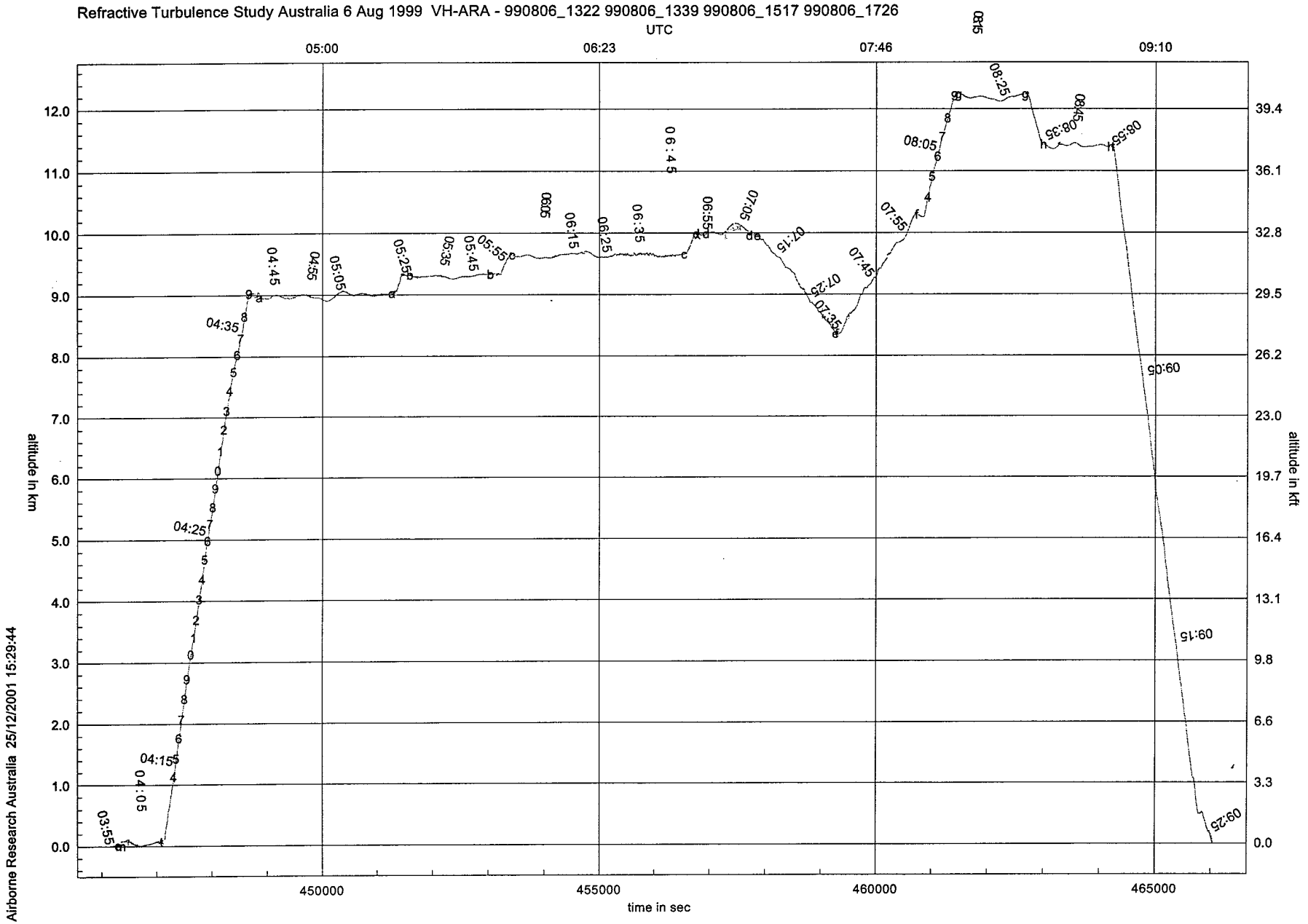
Refractive Turbulence Study Australia 6 Aug 1999 VH-ARA - 990806_1322 990806_1339 990806_1517 990806_1726
UTC
05:00
06:23
07:46
09:10
altitude in km
altitude in kft
time in sec
450000
455000
460000
465000
Airborne Research Australia 25/12/2001 15:29:44

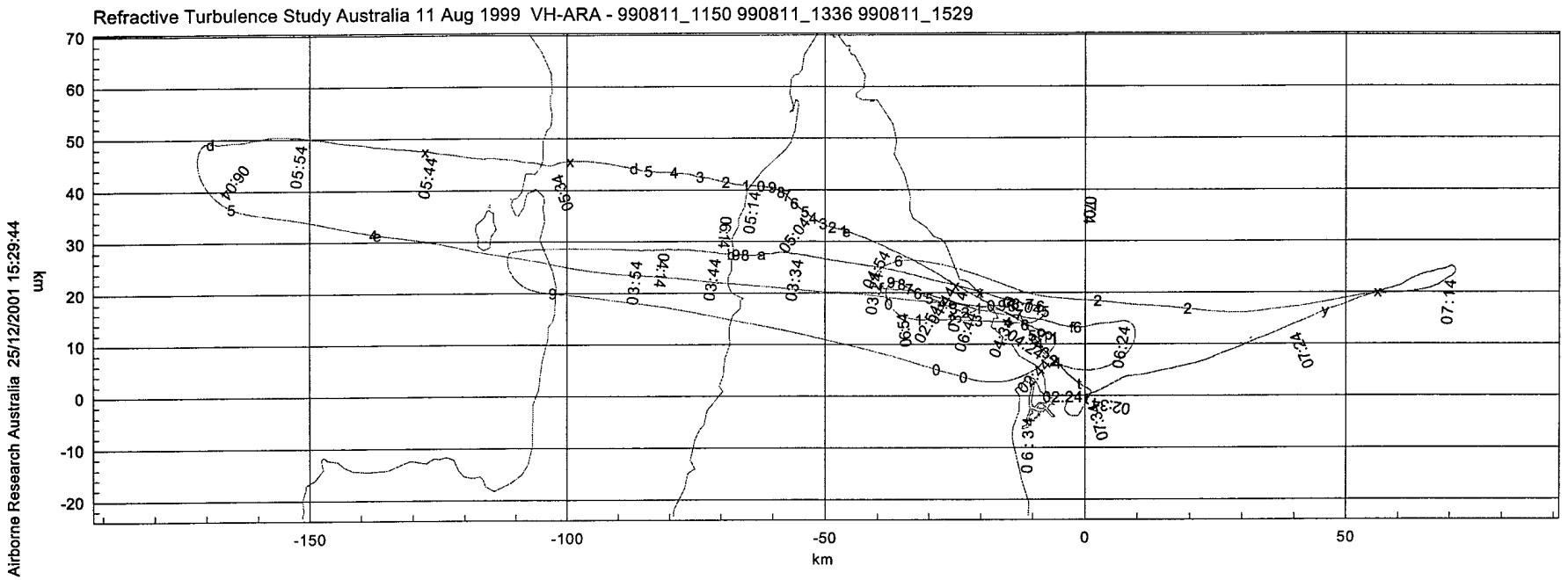
Refractive Turbulence Study Australia 11 Aug 1999 VH-ARA - 990811_1150 990811_1336 990811_1529
Airborne Research Australia 25/12/2001 15:29:44
km
70
60
50
40
30
20
10
0
-10
-20
-150
-100
-50
0
50
km

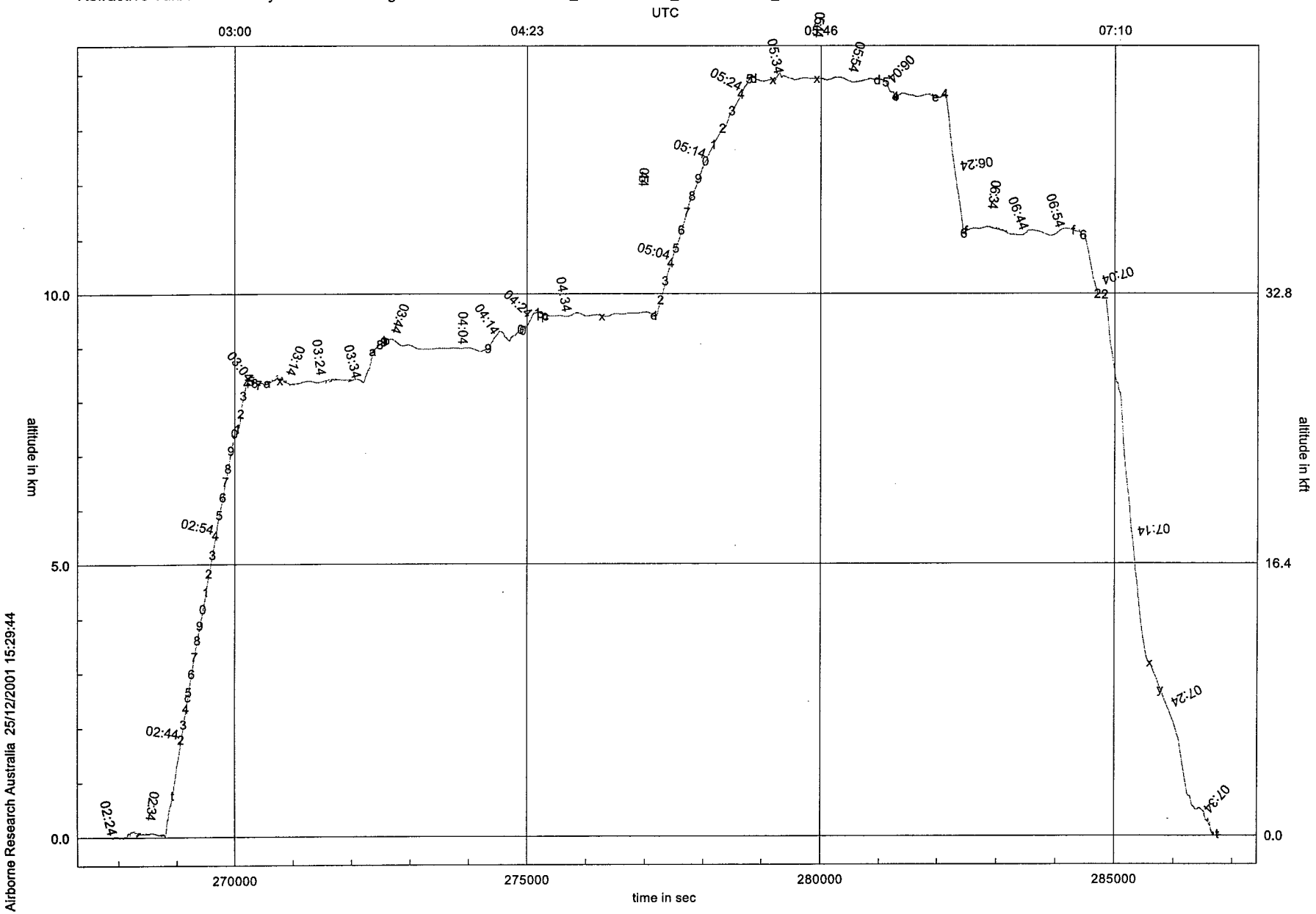
Refractive Turbulence Study Australia 11 Aug 1999 VH-ARA - 990811_1150 990811_1336 990811_1529
UTC
03:00
04:23
05:46
07:10
10.0
5.0
0.0
32.8
16.4
0.0
altitude in km
altitude in kft
270000
275000
280000
285000
time in sec
Airborne Research Australia 25/12/2001 15:29:44

Refractive Turbulence Study Australia 12 Aug 1999 VH-ARA - 990812_1327 990812_1535

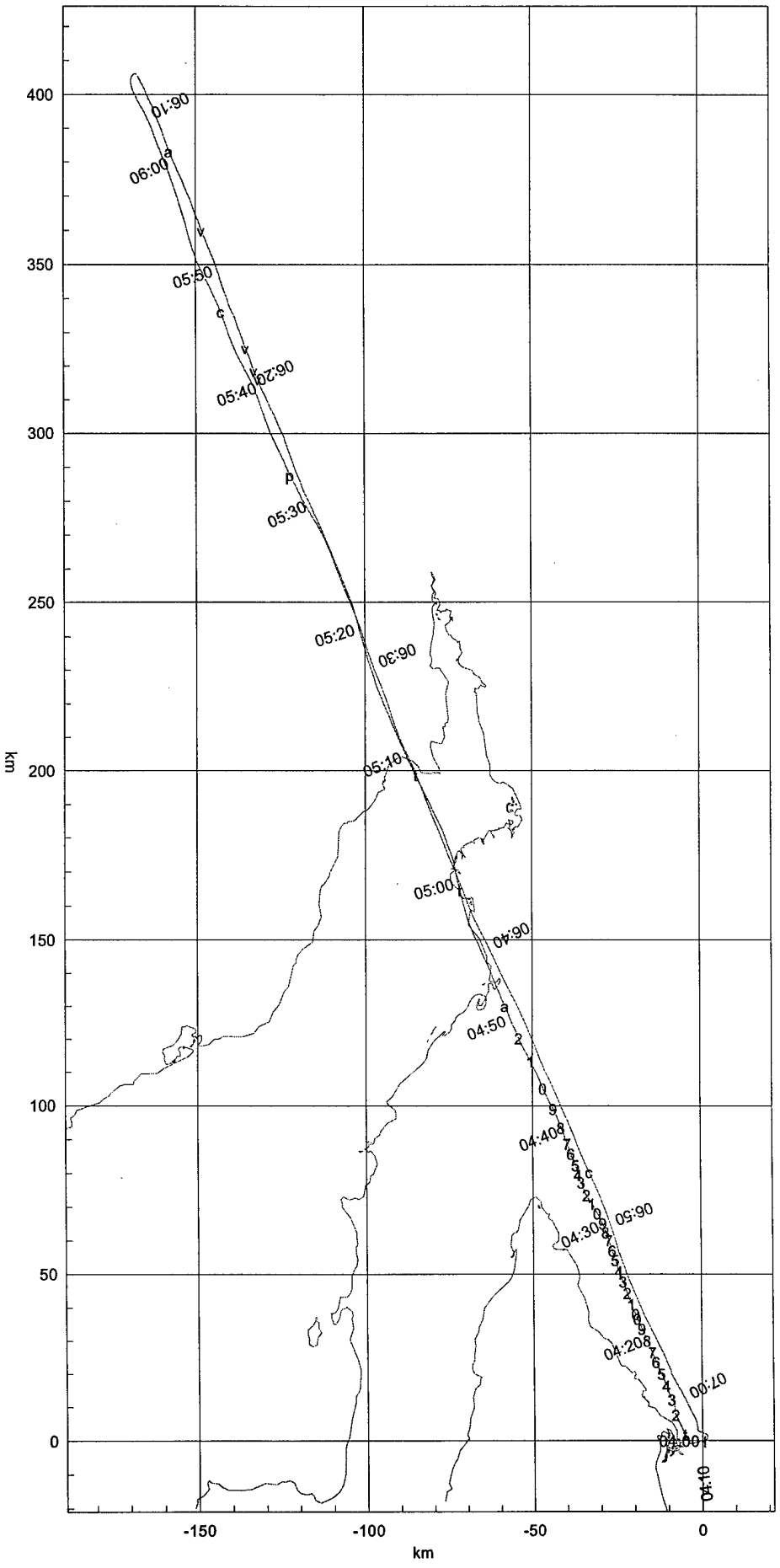

Airborne Research Australia 25/12/2001 15:29:44

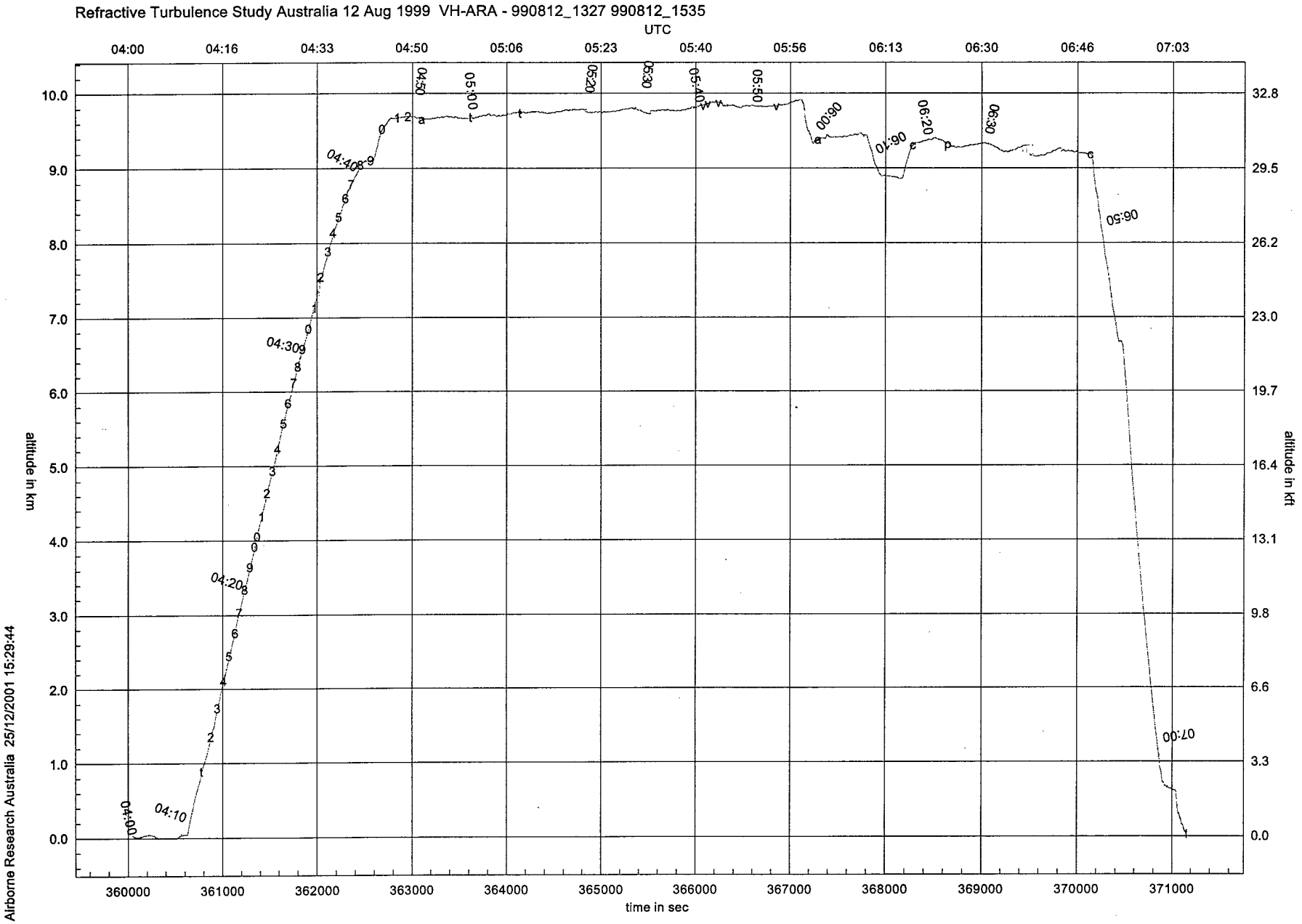
Refractive Turbulence Study Australia 12 Aug 1999 VH-ARA - 990812_1327 990812_1535
UTC
04:00
04:16
04:33
04:50
05:06
05:23
05:40
05:56
06:13
06:30
06:46
07:03
10.0
9.0
8.0
7.0
6.0
5:0
4.0
3.0
2.0
1.0
0.0
32.8
29.5
26.2
23.0
19.7
16.4
13.1
9.8
6.6
3.3
0.0
altitude in km
altitude in kft
04:10
04:20
04:30
04:40
04:50
05:00
05:20
05:30
05:40
05:50
06:00
06:10
06:20
06:30
06:50
07:00
360000
361000
362000
363000
364000
365000
366000
367000
368000
369000
370000
371000
time in sec
Airborne Research Australia 25/12/2001 15:29:44

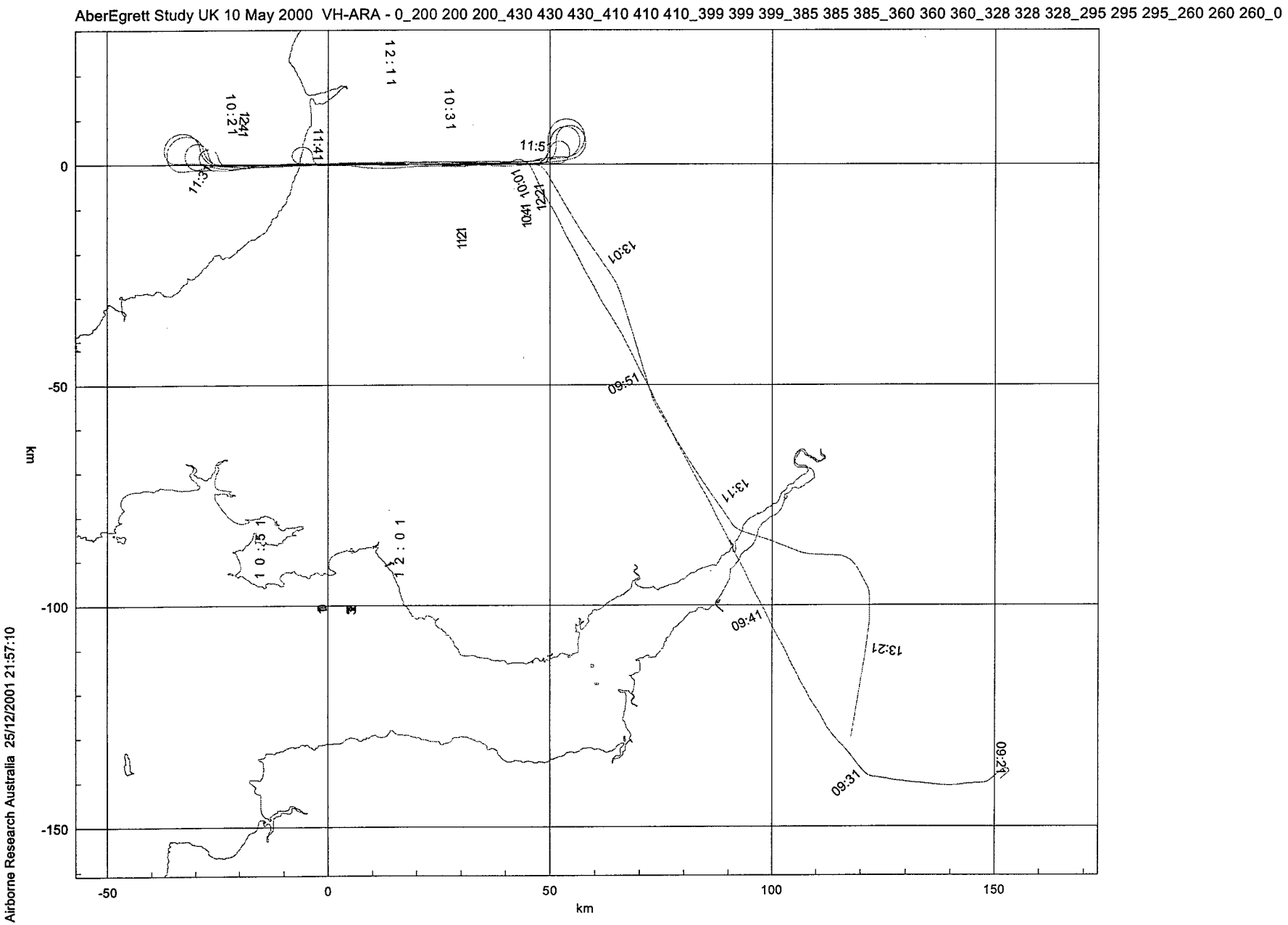
AberEgrett Study UK 10 May 2000 VH-ARA - 0_200 200 200_430 430 430_410 410 410_399 399 399_385 385 385_360 360 360_328 328 328_295 295 295_260 260 260_0
12:11
10:31
11:41
11:5
10:01
10:41
12:21
13:01
09:51
13:11
09:41
13:21
09:31
09:21
km
0
-50
-100
-150
-50
0
50
100
150
Airborne Research Australia 25/12/2001 21:57:10

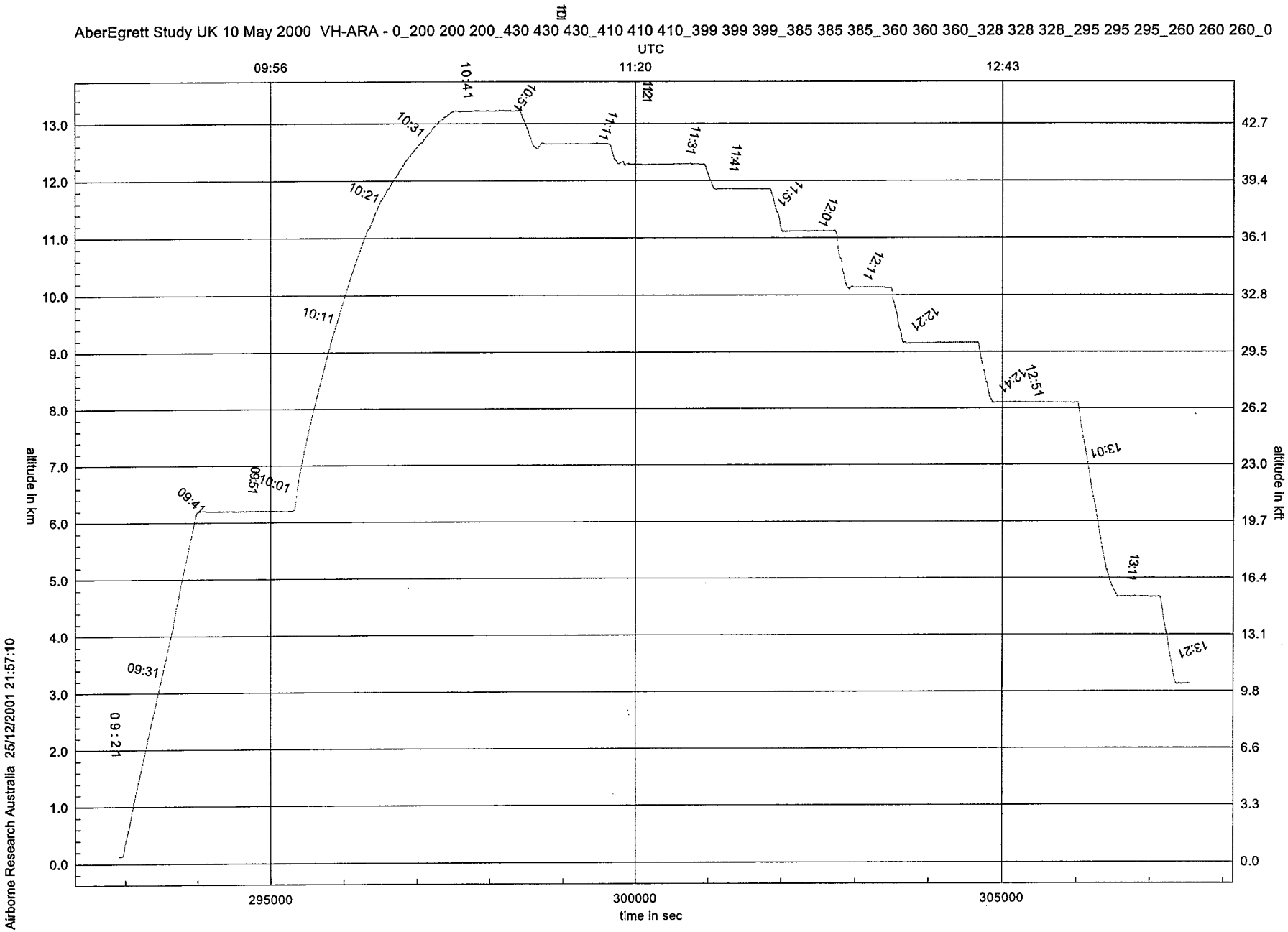
AberEgrett Study UK 10 May 2000 VH-ARA - 0_200 200 200_430 430 430_410 410 410_399 399 399_385 385 385_360 360 360_328 328 328_295 295 295_260 260 260_0
UTC
09:56
10:41
11:20
12:43
altitude in km
altitude in kft
time in sec
295000
300000
305000
Airborne Research Australia 25/12/2001 21:57:10

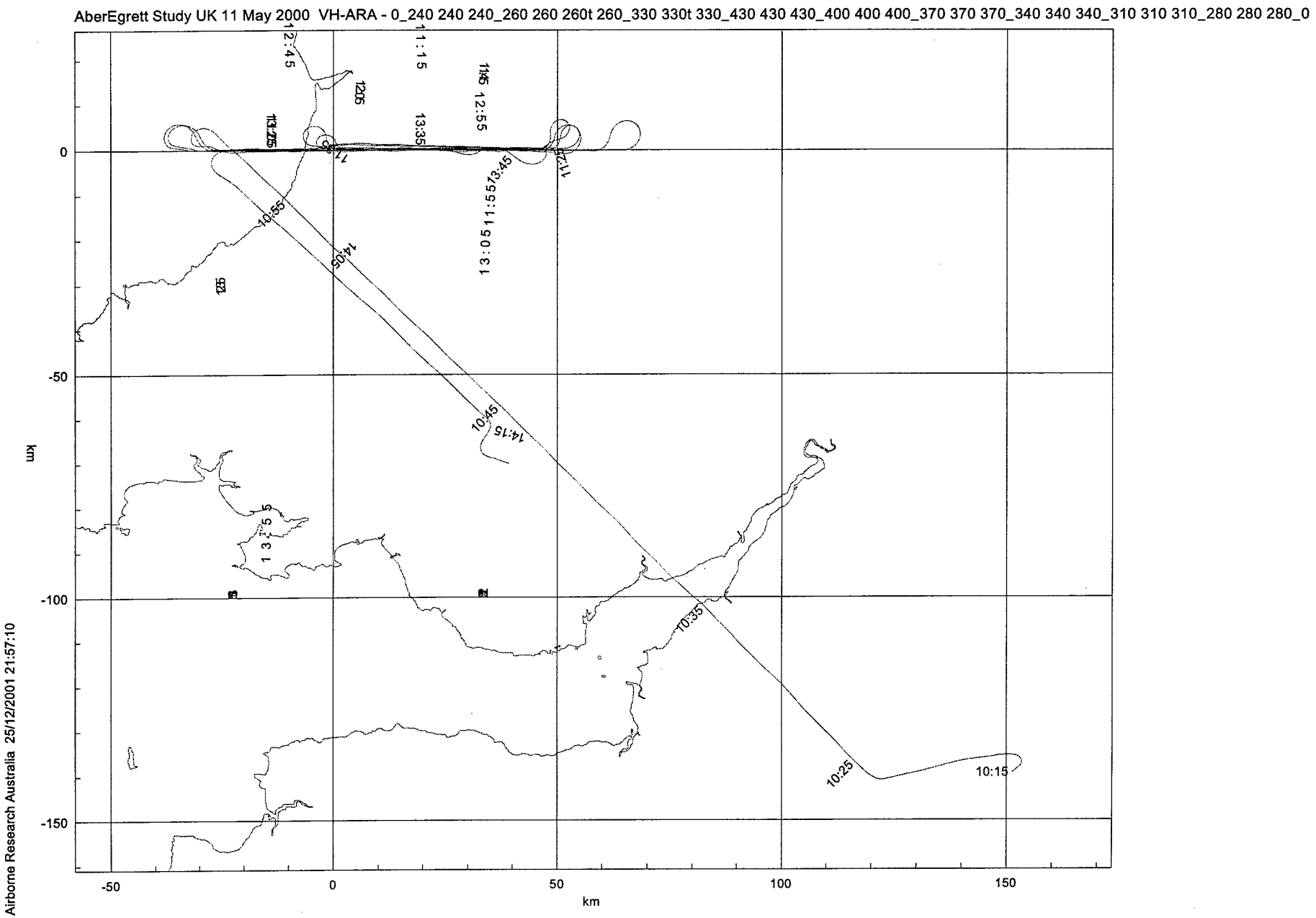
AberEgrett Study UK 11 May 2000 VH-ARA - 0_240 240 240_260 260 260t 260_330 330t 330_430 430 430_400 400 400_370 370 370_340 340 340_310 310 310_280 280 280_0
12:45
11:15
12:55
13:35
13:45
11:55
13:05
10:55
14:05
10:45
14:15
10:35
10:25
10:15
0
-50
-100
-150
km
-50
0
50
100
150
km
Airborne Research Australia 25/12/2001 21:57:10

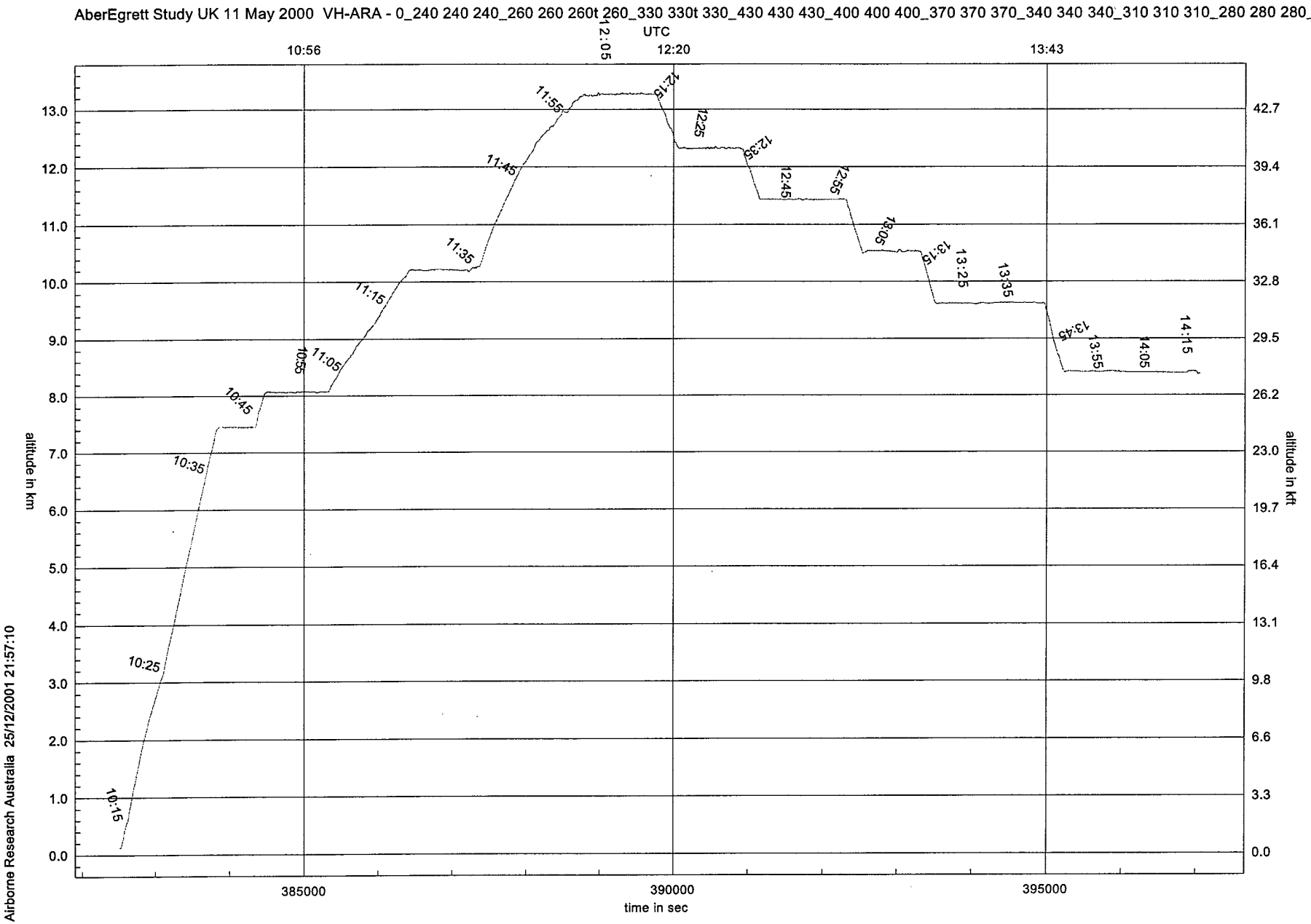
AberEgrett Study UK 11 May 2000 VH-ARA - 0_240 240 240_260 260 260t 260_330 330t 330_430 430 430_400 400 400_370 370 370_340 340 340_310 310 310_280 280 280_0
UTC
10:56
12:05
12:20
13:43
altitude in km
altitude in kft
time in sec
385000
390000
395000
Airborne Research Australia 25/12/2001 21:57:10

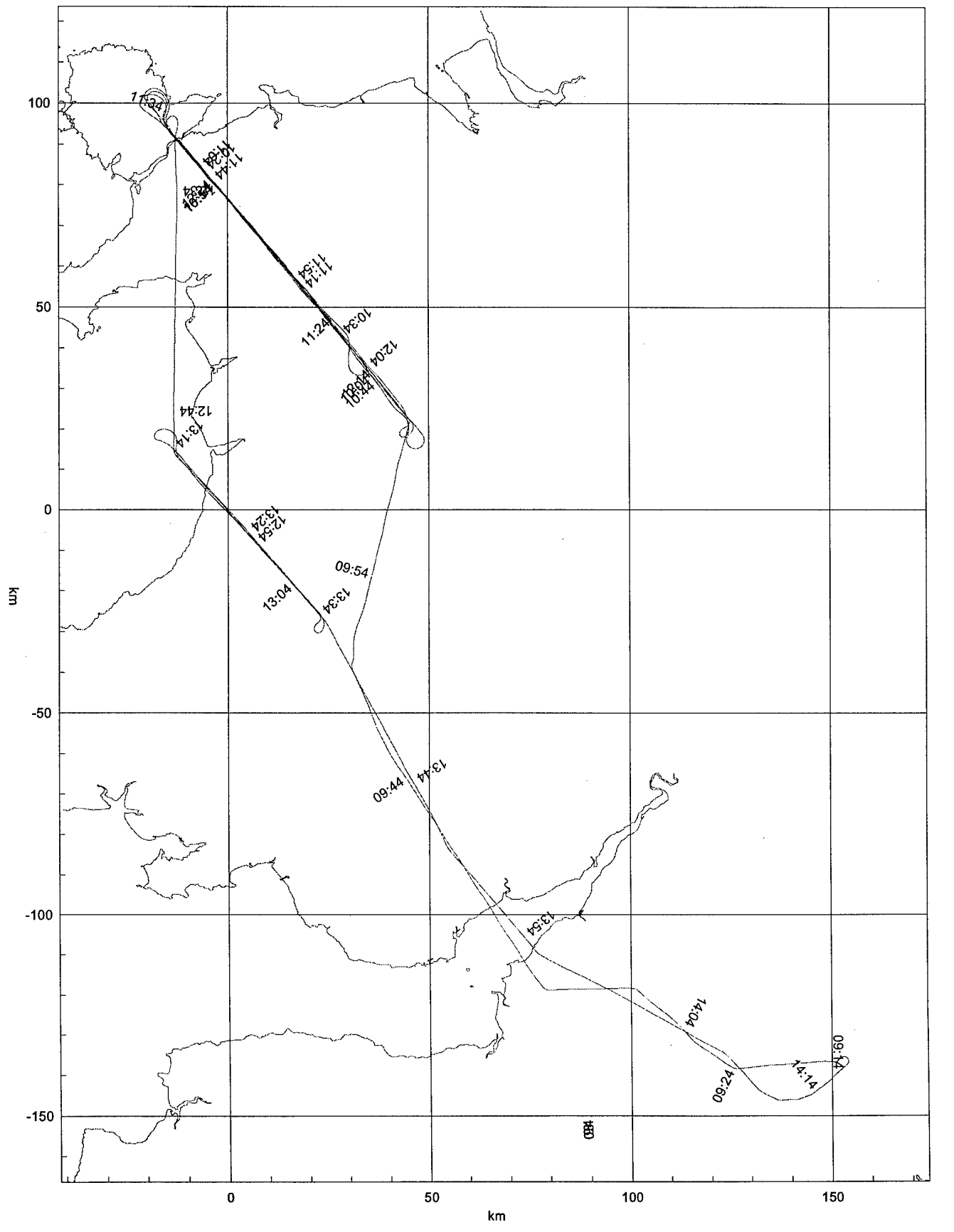
AberEgrett Study UK 12 May 2000 VH-ARA - 0_376 376_430 430 430t 430_400 400 400_370 370 370_360 360 360_331 33
100
50
0
-50
-100
-150
km
0
50
100
150
km
11:34
11:44
11:54
10:34
11:24
12:04
10:44
12:44
13:14
12:54
13:24
09:54
13:04
13:34
13:44
09:44
13:54
14:04
09:24
14:14
09:44
Airborne Research Australia 25/12/2001 21:57:10

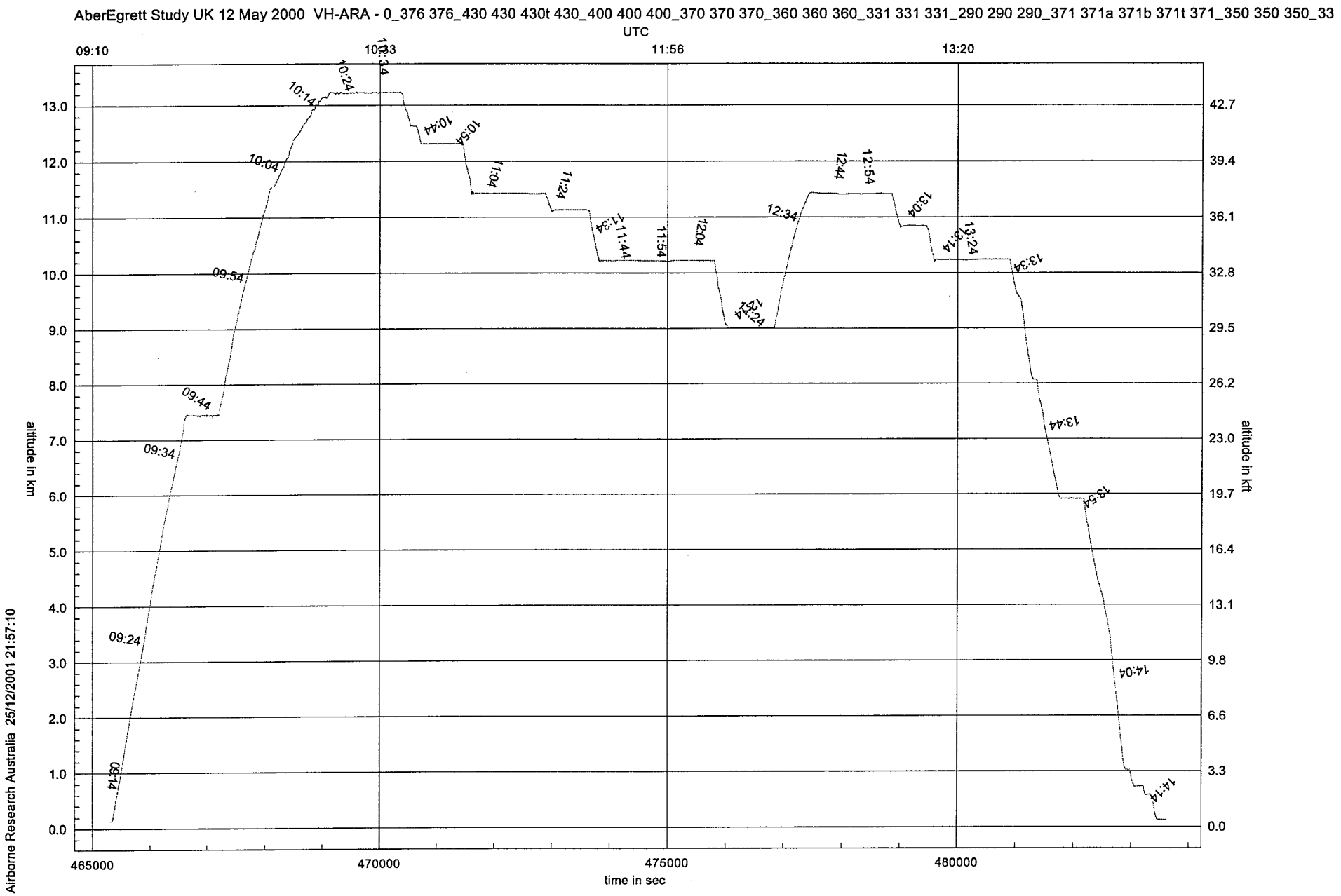
AberEgrett Study UK 12 May 2000 VH-ARA - 0_376 376_430 430 430t 430_400 400 400_370 370 370_360 360 360_331 331 331_290 290 290_371 371a 371b 371t 371_350 350 350_33
UTC
09:10
10:33
11:56
13:20
altitude in km
altitude in kft
time in sec
465000
470000
475000
480000
0.0
1.0
2.0
3.0
4.0
5.0
6.0
7.0
8.0
9.0
10.0
11.0
12.0
13.0
0.0
3.3
6.6
9.8
13.1
16.4
19.7
23.0
26.2
29.5
32.8
36.1
39.4
42.7
09:14
09:24
09:34
09:44
09:54
10:04
10:14
10:24
10:34
10:44
10:54
11:04
11:24
11:34
11:44
11:54
12:04
12:24
12:34
12:44
12:54
13:04
13:14
13:24
13:34
13:44
13:54
14:04
14:14
Airborne Research Australia 25/12/2001 21:57:10

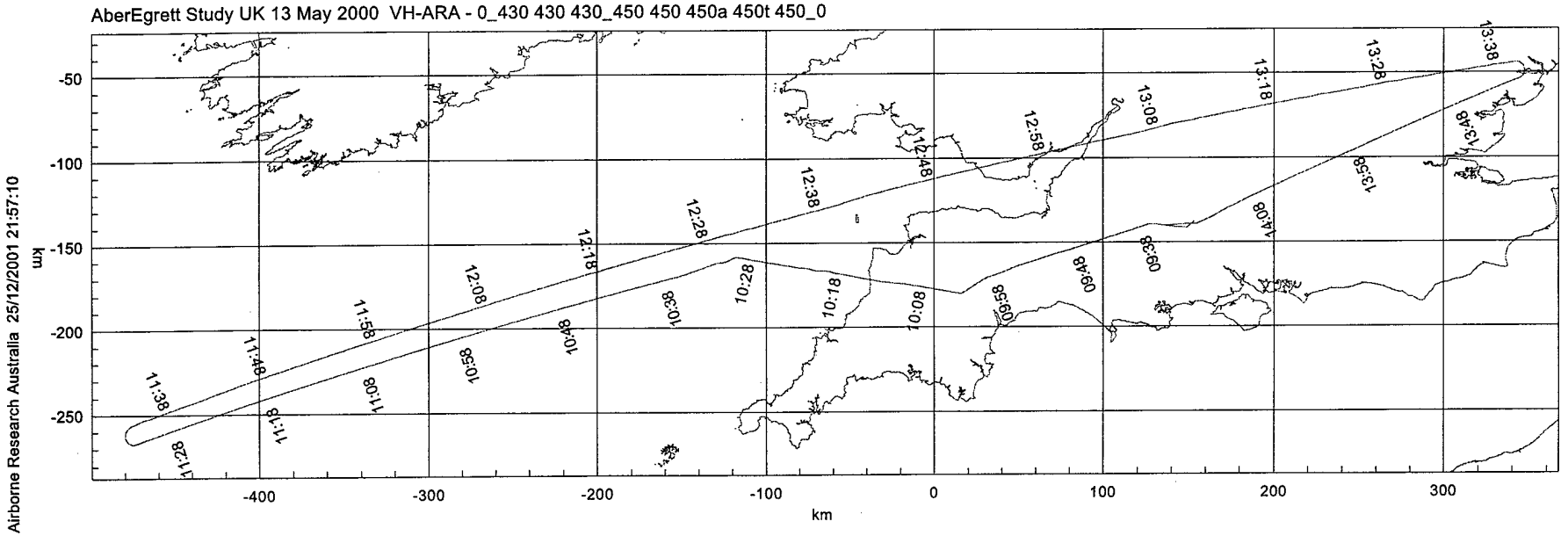
AberEgrett Study UK 13 May 2000 VH-ARA - 0_430 430 430_450 450 450a 450t 450_0
Airborne Research Australia 25/12/2001 21:57:10
km
-50
-100
-150
-200
-250
-400
-300
-200
-100
0
100
200
300
km
11:28
11:38
11:48
11:58
12:08
12:18
12:28
12:38
12:48
12:58
13:08
13:18
13:28
13:38
10:08
10:18
10:28
10:38
10:48
10:58
09:38
09:48
09:58
13:48
13:58
14:08

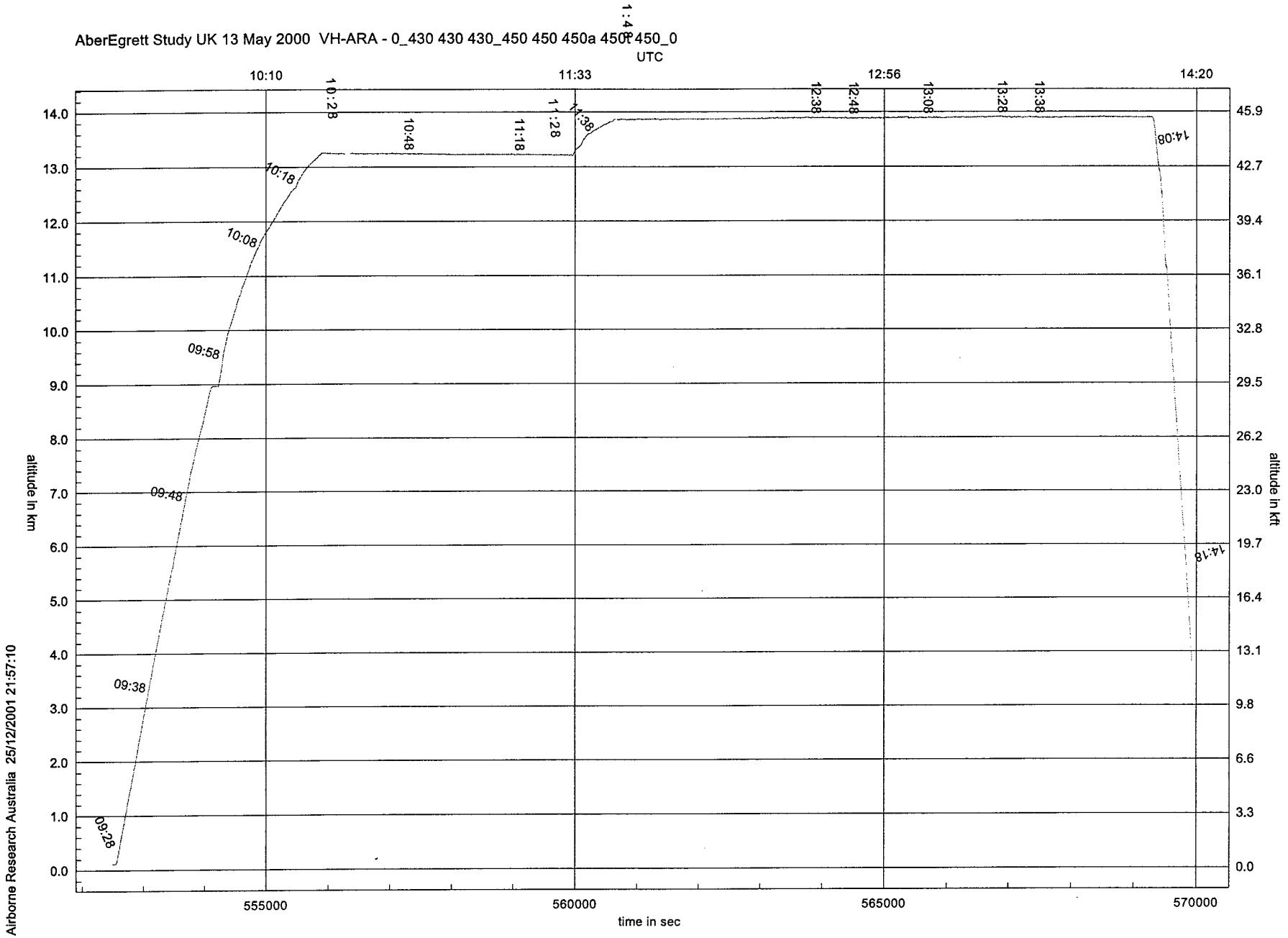
AberEgrett Study UK 13 May 2000 VH-ARA - 0_430 430 430_450 450 450a 450 450_0
UTC
10:10
11:33
12:56
14:20
10:28
10:48
11:18
11:28
11:38
12:38
12:48
13:08
13:28
13:38
14:08
14:18
10:18
10:08
09:58
09:48
09:38
09:28
14.0
13.0
12.0
11.0
10.0
9.0
8.0
7.0
6.0
5.0
4.0
3.0
2.0
1.0
0.0
45.9
42.7
39.4
36.1
32.8
29.5
26.2
23.0
19.7
16.4
13.1
9.8
6.6
3.3
0.0
altitude in km
altitude in kft
555000
560000
565000
570000
time in sec
Airborne Research Australia 25/12/2001 21:57:10

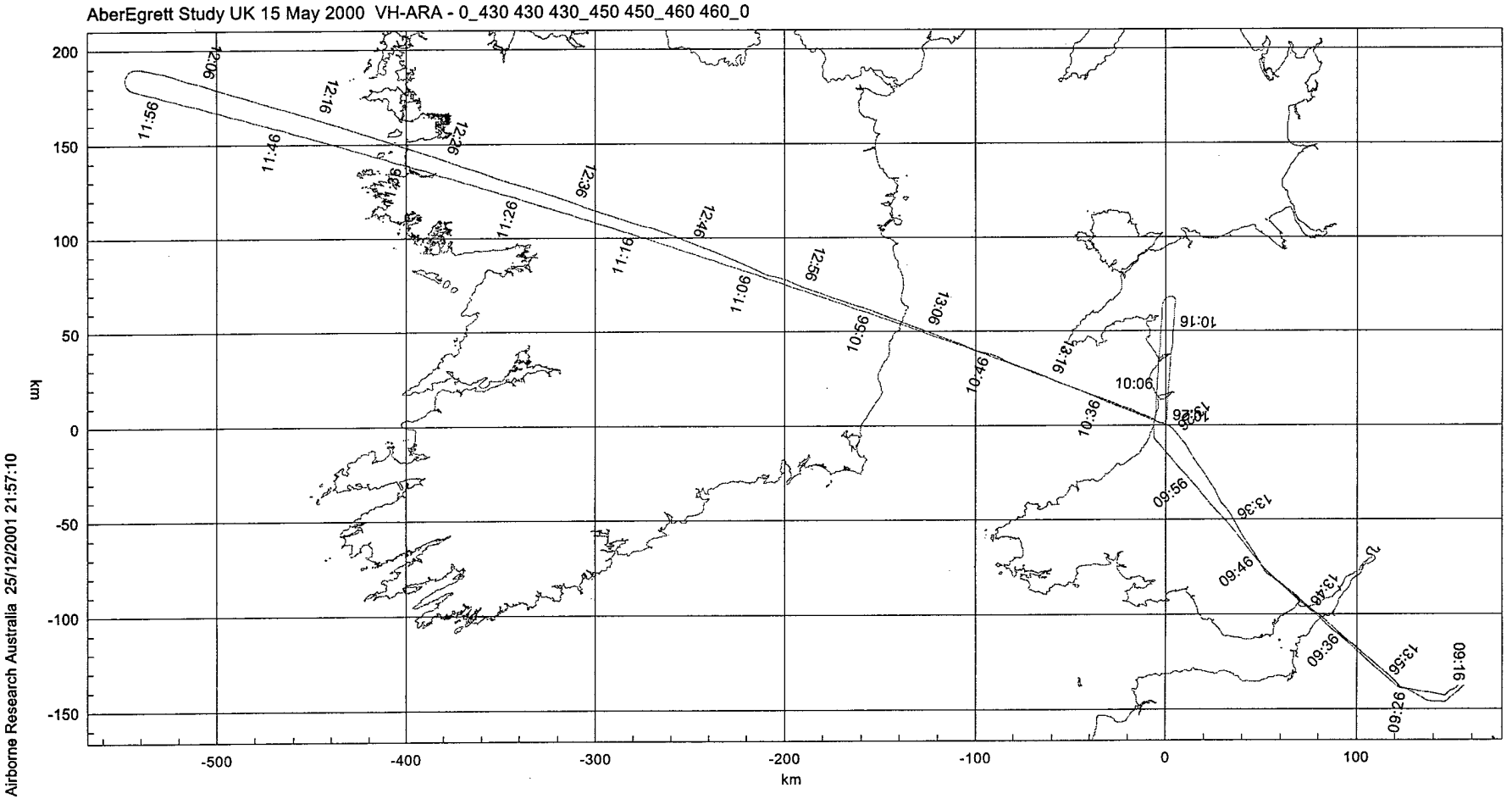
AberEgrett Study UK 15 May 2000 VH-ARA - 0_430 430 430_450 450_460 460_0
Airborne Research Australia 25/12/2001 21:57:10
km
km
200
150
100
50
0
-50
-100
-150
-500
-400
-300
-200
-100
0
100
11:56
12:06
12:16
11:46
12:26
12:36
11:26
12:46
11:16
12:56
11:06
13:06
10:56
13:16
10:46
10:16
10:06
10:36
13:36
13:46
13:56
14:06

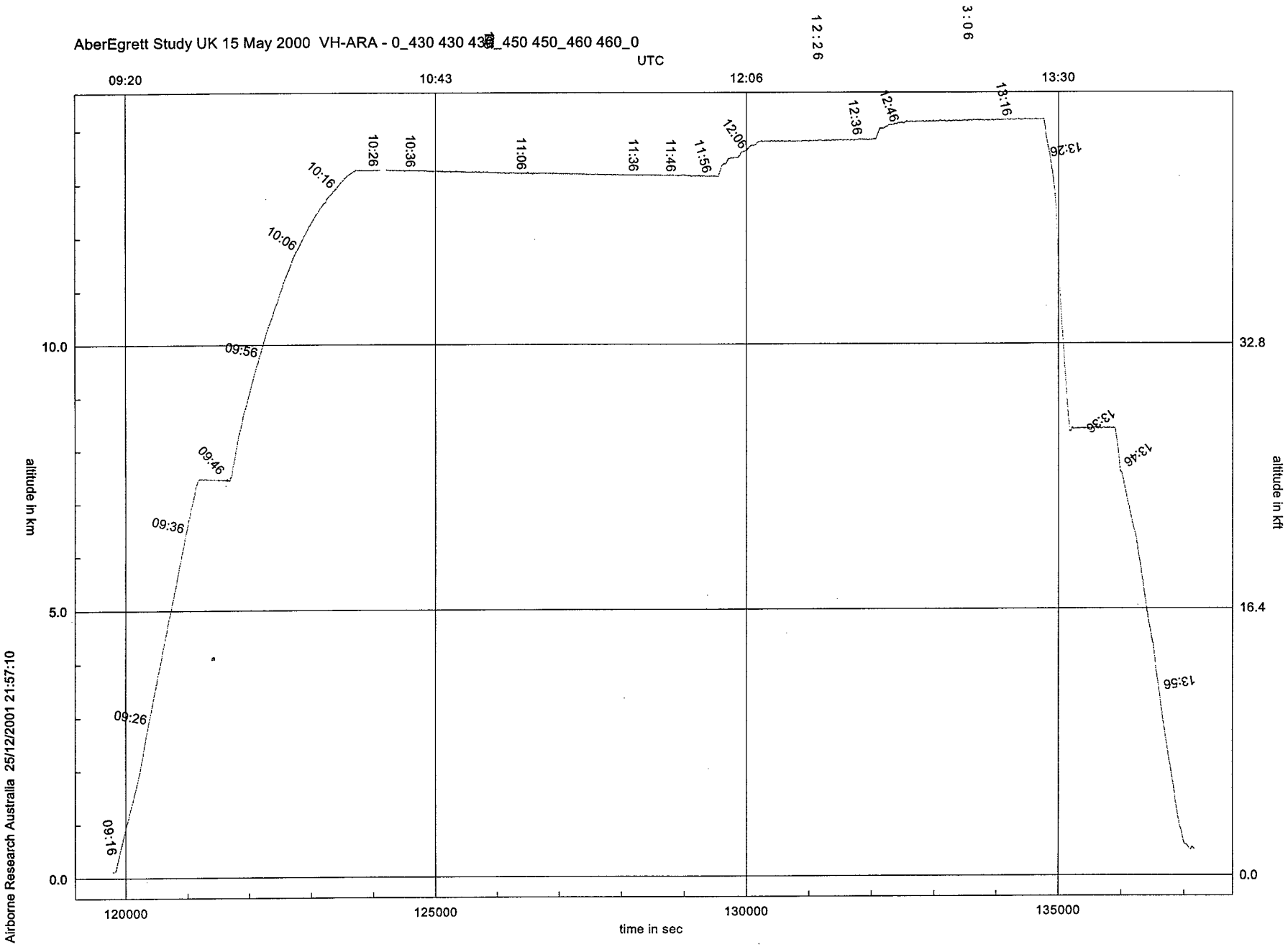
AberEgrett Study UK 15 May 2000 VH-ARA - 0_430 430 430_450 450_460 460_0
UTC
09:20
10:43
12:06
13:30
12:26
3:06
09:16
09:26
09:36
09:46
09:56
10:06
10:16
10:26
10:36
11:06
11:36
11:46
11:56
12:06
12:36
12:46
13:16
13:26
13:36
13:46
13:56
10.0
5.0
0.0
32.8
16.4
0.0
altitude in km
altitude in kft
120000
125000
130000
135000
time in sec
Airborne Research Australia 25/12/2001 21:57:10

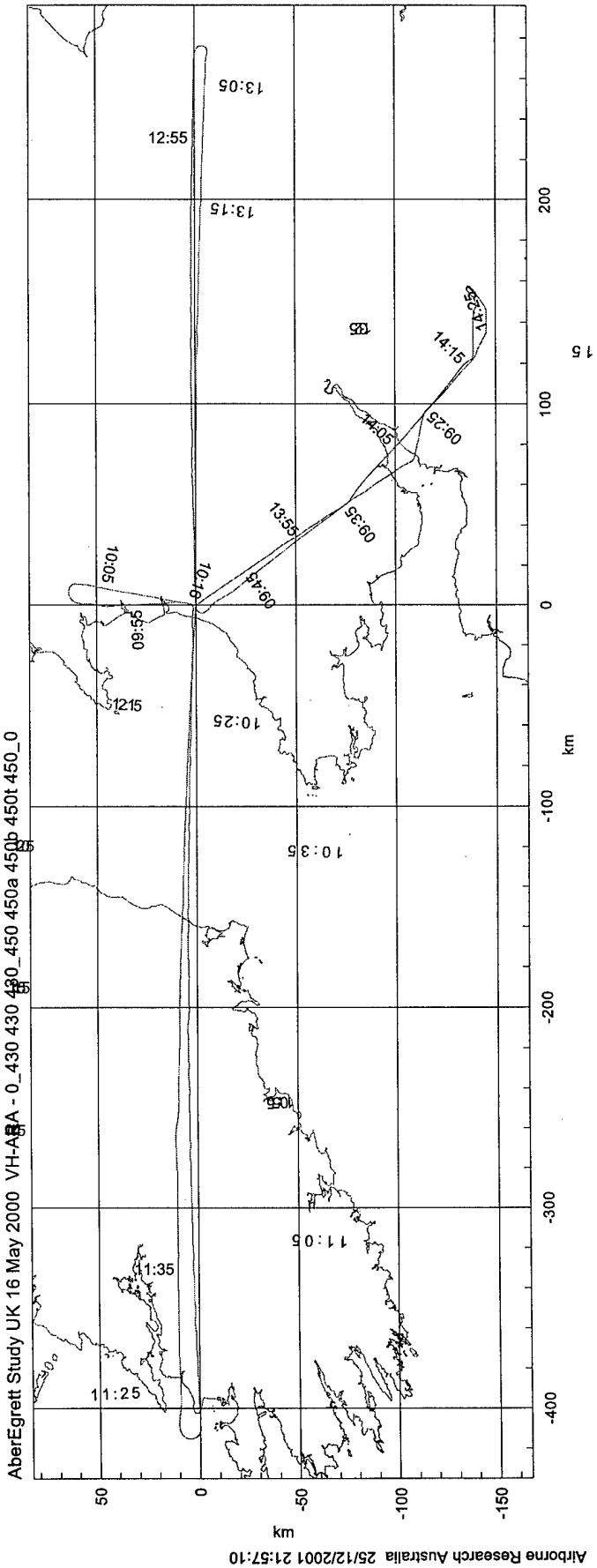

12:45

12:35

12:25

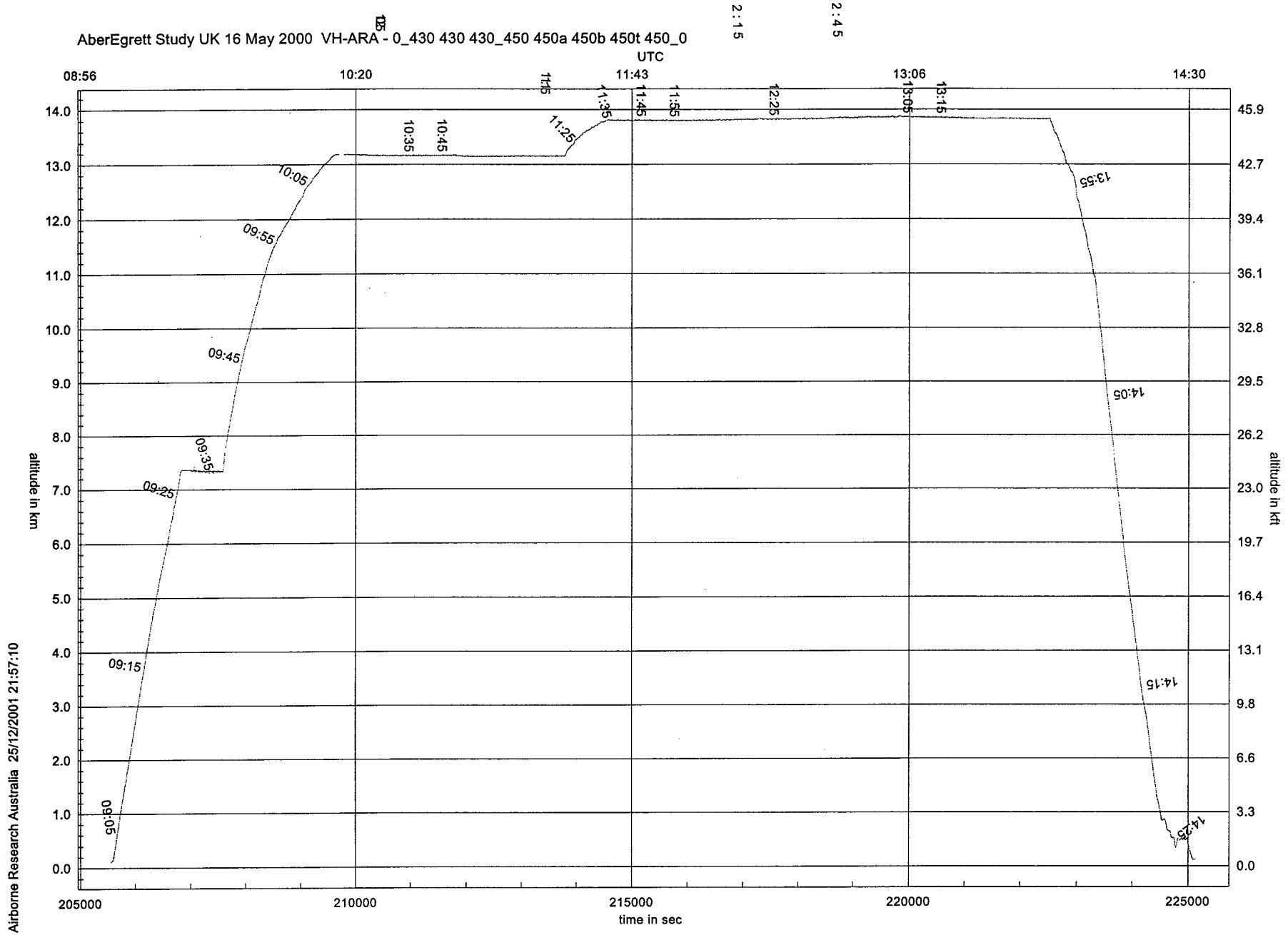
AberEgrett Study UK 16 May 2000 VH-ARA - 0_430 430 430_450 450a 450b 450t 450_0
UTC
08:56
10:20
11:43
13:06
14:30
2:15
2:45
10:35
10:45
11:25
11:35
11:45
11:55
12:25
13:05
13:15
09:05
09:15
09:25
09:35
09:45
09:55
10:05
13:55
14:05
14:15
14:25
altitude in km
14.0
13.0
12.0
11.0
10.0
9.0
8.0
7.0
6.0
5.0
4.0
3.0
2.0
1.0
0.0
altitude in kft
45.9
42.7
39.4
36.1
32.8
29.5
26.2
23.0
19.7
16.4
13.1
9.8
6.6
3.3
0.0
205000
210000
215000
220000
225000
time in sec
Airborne Research Australia 25/12/2001 21:57:10

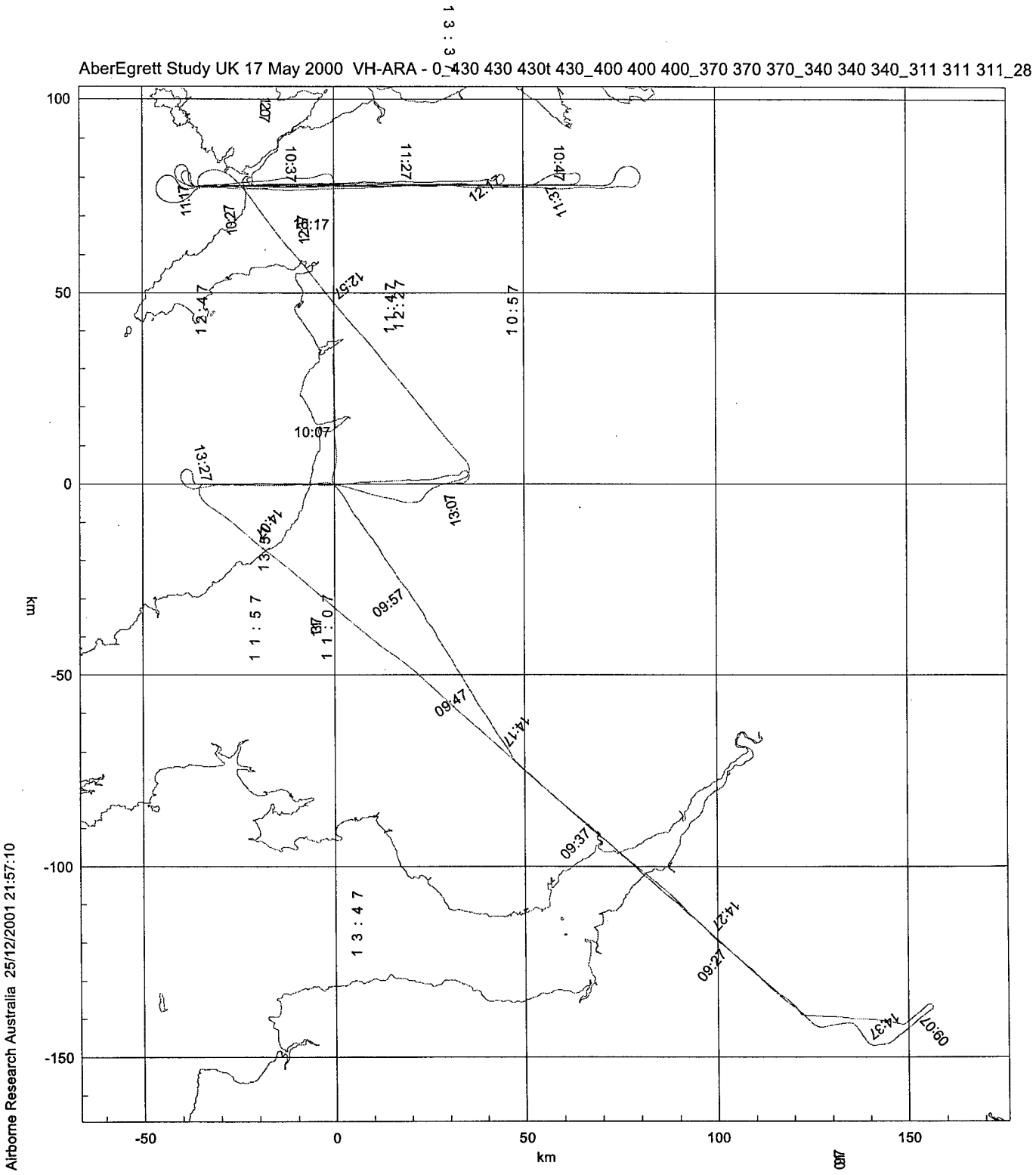
AberEgrett Study UK 17 May 2000 VH-ARA - 0_430 430 430t 430_400 400 400_370 370 370_340 340 340_311 311 311_28
100
50
0
-50
-100
-150
km
-50
0
50
100
150
km
10:07
13:07
09:57
09:47
14:17
09:37
14:27
09:27
14:37
09:07
10:57
11:47
12:37
13:27
Airborne Research Australia 25/12/2001 21:57:10